Title
Macular imaging with optical coherence tomography in glaucoma

Journal
Survey of Ophthalmology, 65(6)

ISSN
0039-6257

Authors
Mohammadzadeh, Vahid
Fatehi, Nima
Yarmohammadi, Adeleh
et al.

Publication Date
2020-11-01

DOI
10.1016/j.survophthal.2020.03.002

Peer reviewed

HHS Public Access

Author manuscript

Surv Ophthalmol. Author manuscript; available in PMC 2021 November 01.

Published in final edited form as:

Surv Ophthalmol. 2020 ; 65(6): 597–638. doi:10.1016/j.survophthal.2020.03.002.

Macular Imaging with Optical Coherence Tomography in Glaucoma

Vahid Mohammadzadeh, MD[1], **Nima Fatehi, MD**[1,2], **Adeleh Yarmohammadi, MD**[3], **Ji Woong Lee, MD**[4], **Farideh Sharifipour, MD**[5], **Ramin Daneshvar, MD**[6], **Joseph Caprioli, MD**[1], **Kouros Nouri-Mahdavi, MD, MSc**[1]

[1.]Glaucoma Division, Stein Eye Institute, David Geffen School of Medicine, University of California at Los Angeles, Los Angeles, California

[2.]Saint Mary Medical Center – Dignity health, Long Beach, CA

[3.]Shiley Eye Institute, University of California, San Diego, La Jolla, California, United States

[4.]Department of Ophthalmology, Pusan National University College of Medicine, Busan, Korea

[5.]Department of Ophthalmology, Shahid Beheshti university of Medical Sciences, Tehran, Iran

[6.]Eye Research Center, Mashhad University of Medical Sciences, Mashhad, Iran

Abstract

With the advent of spectral-domain optical coherence tomography (SD-OCT), imaging of the posterior segment of the eye can be carried out rapidly at multiple anatomical locations, including the optic nerve head (ONH), circumpapillary retinal nerve fiber layer (cp-RNFL), and macula. There is now ample evidence to support the role of SD-OCT imaging of the macula for detection of early glaucoma. Macular SD-OCT measurements demonstrate high reproducibility, and evidence on its utility for detection of glaucoma progression is accumulating. We present a comprehensive review of macular SD-OCT imaging emerging as an essential diagnostic tool in glaucoma.

Corresponding author: **Kouros Nouri-Mahdavi, MD, MSc, 100 Stein Plaza, Los Angeles, CA, 90095, USA**, Phone: 310-794-1487, Fax: 310-794-6616, nouri-mahdavi@jsei.ucla.edu.

Conflict of Interest
Kouros Nouri-Mahdavi has these financial disclosures
1: Heidelberg Engineering
2: Aerie
Joseph Caprioli has these financial disclosures
1: Aerie
2: Allergan
3: Novartis
4: Glaukos
Other authors:
None

Keywords

Optical coherence tomography; OCT; Glaucoma; Macula; Imaging; Detection; Structure-function; Variability; Progression

I. Background: history of macular imaging in glaucoma

1A. The early days: emergence of OCT as a new tool for ophthalmic diagnosis

Glaucoma is a leading cause of irreversible blindness worldwide.[316] The hallmark of glaucomatous neuropathy is loss of the retinal ganglion cells (RGC) and their axons that leads to characteristic changes in the optic disc with concomitant visual field damage.[317, 319] Early detection of glaucomatous damage and monitoring its progression are essential tasks in glaucoma management.[69, 398, 399] While structural damage in glaucoma can be assessed subjectively by clinical examination of the optic nerve head (ONH) and the retinal nerve fiber layer (RNFL),[318, 331, 351] sequential introduction of various ocular imaging modalities revolutionized structural assessment in glaucoma eyes.[86, 121]

Several imaging tools were explored over the last 3 decades and found to be potentially useful for the diagnosis and management of glaucoma.
[8, 9, 15, 38, 74, 127, 244, 254, 286, 340, 349, 363] Optical coherence tomography (OCT) has become the structural imaging technology of choice for glaucoma diagnostics due to the speed of acquisition, high resolution, and excellent reproducibility.[88, 342] It generates cross-sectional images of the posterior segment by measuring the echo time delay and the magnitude of backscattered light reflected off the retina or the ONH through the principle of low-coherence interferometry. Details of this technology have been well described.[175, 342] In brief, OCT uses a low-coherence infrared light source, which is directed through the ocular media onto the retina to produce an interference pattern. The interference pattern is then intercepted by a sensor and processed to create two-dimensional images of the retina that resembles cross-sectional histologic sections.

Objective and quantitative measurements of the ocular structures with high reproducibility have led to a new paradigm in glaucoma diagnostics.[341, 342] Optical coherence tomography has been widely adopted for detection and monitoring of structural damage from glaucoma.
[86, 122] The two-dimensional configuration of the ONH and the circumpapillary RNFL (cp-RNFL) thickness measurements were originally the primary OCT structural parameters of interest.[28, 121, 244] Several studies established the capability of cp-RNFL and ONH measurements to provide reproducible thickness measurements that could aid in glaucoma management.[46, 48, 119, 183, 343]

Although macular involvement in early glaucoma had long been reported in histological studies,[14, 294] it was only after the introduction of OCT that it became a focus of interest. Up to 50% of the total RGCs reside in a multilayered fashion in the macular region, and macular measurements demonstrate similar or lower inter-subject measurement variability compared to other OCT structural measurements.[21, 70, 368, 396] Also, evaluation of the macula targets the most crucial RGCs affected in glaucoma in the region of their highest concentration and

could allow early detection of RGC loss and its progression.[368, 409] This premise was further supported by animal studies that showed the susceptibility of macular RGCs to injury in experimental primate models of glaucoma.[84, 97, 115, 397, 413] Moreover, the number of RGCs correlated with visual function in histologic studies in both monkeys[131, 132] and humans with glaucoma.[189, 317] Zeimer and coworkers were the first to propose quantitative detection of glaucomatous damage in the posterior pole by mapping of the retinal thickness with the Retinal Thickness Analyzer (Talia Technology Ltd.). The device projected an oblique scanning laser slit beam onto the retina. A video camera recorded the reflected light and measured the thickness between the vitreoretinal and the chorioretinal interfaces as the retinal thickness.[426] Their finding of decreased macular thickness in glaucomatous eyes provided an impetus for subsequent work with OCT.[425]

1B. Early experience with time-domain OCT

After the introduction of time-domain OCT (TD-OCT), studies reported the utility of macular thickness parameters for glaucoma detection.
[29, 30, 112, 120, 124, 126, 141, 173, 182, 217, 237, 261, 302, 374, 407] Giovannini and coworkers[112] used an early version of the TD-OCT to measure the macular volume and found progressively lower macular volume as a function of glaucoma severity. These findings were confirmed by other studies that reported a significant correlation between macular measurements obtained by TD-OCT and severity of the disease in adult glaucoma patients,
[29, 30, 120, 124, 182, 261, 302, 406] as well as in children with glaucoma.[141] Greenfield and coworkers[120] and Wollstein and collaborators[407] showed that macular thickness measurements were correlated with RNFL thickness, a sign of concordance between loss of RGCs and their axons; however, cp-RNFL thickness measurements outperformed macular thickness measures as far as correlation with visual function was concerned.

Some studies with TD-OCT found that macular thickness measurements were capable of discriminating between healthy and glaucomatous eyes even in the early stages of the disease;[120, 124, 406, 407261, 302] however, the diagnostic accuracy of cp-RNFL[120, 124, 406;261, 302, 407] and ONH[261, 406] parameters were higher than macular thickness measurements. Leung and colleagues[237] evaluated the macular retinal nerve fiber layer (mRNFL), in addition to total macular thickness and cp-RNFL, in a group of normal subjects, glaucoma suspects, and glaucoma patients. They found a significant reduction in mRNFL thickness in glaucoma compared with normal eyes. However, similar to previous studies,[120, 124, 406;29, 261, 302, 407] cp-RNFL thickness outperformed both total macular and mRNFL thickness in terms of detection of glaucoma and correlation with visual function.

Overall, studies performed with TD-OCT provided proof of concept for the potential utility of macular thickness measurements in glaucoma; however, despite consistently lower macular thickness corresponding to severity of glaucomatous damage, the diagnostic accuracy of macular parameters was inferior to cp-RNFL thickness measurement.[368, 409] This could be, at least in part, explained by the limited resolution of TD-OCT technology. Most of these studies relied on total macular retinal thickness for the diagnosis of glaucoma as a surrogate for thickness of the ganglion cell layer (GCL).
[112, 120, 124, 217, 406;29, 30, 126, 141, 173, 182, 237, 261, 302, 374, 407] Glaucoma preferentially affects

the innermost retinal layers, consisting of the mRNFL, GCL, and the inner plexiform layer (IPL), the combination of which is collectively known as the macular ganglion cell complex (GCC).[188, 413] Given that the outer retinal layers, which are not affected by glaucoma, constitute 65–70% of the total retinal thickness,[409] it was proposed that use of macular GCC to the exclusion of outer layers might improve the diagnostic accuracy of macular OCT imaging in glaucoma.[374, 409]

Ishikawa and coworkers[173] and Tan and colleagues[374] used custom software algorithms that enabled automated segmentation of retinal layers on images acquired with TD-OCT. Ishikawa et al.[173] found that the diagnostic accuracy of macular inner retinal layers (called MIRL) was similar to cp-RNFL and better than the total macular thickness for differentiating glaucoma from healthy eyes. Tan and coworkers[374] were the first to demonstrate that thinning of the macular inner retinal layers could be detected before visual field changes occurred in a patients with glaucoma suspects and preperimetric glaucoma. The findings of these two studies emphasized that analysis of the inner retinal layers might improve the diagnostic ability of macular parameters; however, macular TD-OCT images were limited by inadequate scan quality and difficulties in segmenting retinal layers due to the low signal-to-noise ratio (SNR) and uneven tissue reflectivity across sampling lines within scans.[173, 374]

1C. The advent of spectral-domain OCT (SD-OCT) imaging makes measurement of the ganglion cell machinery possible: advantages of SD-OCT over TD-OCT for imaging of the posterior pole

The advent of SD-OCT sparked interest in the use of macular imaging in glaucoma because of its ability to rapidly acquire high-quality images of the retinal structures, facilitating assessment of individual retinal layers.[368, 409] The hardware and software developments of SD-OCT technology provided many potential advantages for glaucoma detection and monitoring. The older TD-OCT technology consisted of an interferometer with a low coherence and broad bandwidth light source. This technology was limited by relying on time-consuming movement of a reference mirror to relay a signal.[88, 234] The SD-OCTs similarly use a broadband light source, but the moveable reference mirror is replaced with a stationary mirror and the OCT signal is detected with a spectrometer. This technology relies on differences in the frequency spectrum of light reflected off different retinal layers where frequency information from all depth levels in one A-scan is converted into an intensity profile by Fourier transformation of the acquired signal. The implementation of a spectrometer allows significantly faster image acquisition and a higher SNR, lowering the prevalence of motion artifacts. The broadband light source of SD-OCT led a to significant improvement in the axial resolution, since axial resolution is dependent on the central wavelength and the half-maximum of the full length of the optical coherence system.[77, 88, 224, 293, 403, 404]

Compared to TD-OCT systems with an approximate scanning speed of 100–400 A-scans/second and axial resolution of 10 μm, SD-OCT systems are capable of obtaining images with approximate scanning speeds of 27,000–100,000 A-scans/second and an axial resolution approaching 3–5μm with diminished motion artifacts.[56] The enhancement in the

quality of SD-OCT scans is in part due to the higher spatial resolution of images, but mainly the result of significantly faster scan speeds that allows averaging of multiple images within one B-scan. Faster scan rates enable raster scan patterns that provide a more comprehensive coverage of the area of interest, and also reduce sampling errors and motion artifacts.[404] These improvements allow acquisition of three-dimensional data cubes around the ONH and in the macula with much less interpolation between adjacent points resulting in enhanced visualization of cp-RNFL or GCL defects within the 3D data set.[338, 404] Hence, SD-OCT allows visualization of spatial details not easily seen on images acquired with earlier TD-OCT devices.[341]

The combination of denser sampling and superior resolution led to a significantly higher precision of SD-OCT measurements. Several studies showed that measurements obtained with SD-OCT offered improved reproducibility over TD-OCT measurements.[98, 116, 263, 264] By minimizing test-retest measurement variability, SD-OCT technology has improved the ability to monitor glaucomatous change over time.[238] New post-acquisitional software algorithms provide automatic segmentation of multiple individual retinal layers. With significantly improved scanning speed, image resolution, and SNR, SD-OCTs not only allow for more information from the biological tissues to be rapidly acquired and visualized, but also provide an efficient platform to quantify individual retinal layers in the macular region that are particularly affected by glaucoma, specifically, the mRNFL, GCL, ganglion cell/inner plexiform layer (GCIPL) and GCC.

With increasing popularity of SD-OCTs, many studies investigated the utility of SD-OCT macular parameters in glaucoma. Some reports used the earlier TD-OCT devices as a benchmark for comparison. Early studies conducted with SD-OCT technology used algorithms that were developed to measure the GCC. Yang and coworkers[419] described a segmentation approach based on gradient information in dual scales that demonstrated high accuracy and reproducibility in normal subjects. Hood et al.[151] later reported very good intra- and inter-observer reproducibility in 10 normal and 10 glaucoma subjects. In a landmark study, Tan and coworkers[373] found similar diagnostic performance for macular GCC thickness measured with an early SD-OCT device compared with cp-RNFL measurements acquired with TD-OCT. Macular GCC measurements demonstrated high reproducibility similar to cp-RNFL thickness. De Moraes and coworkers[80] showed that variations in foveal shape and anatomy did not contribute to artifacts seen in RGC probability maps provided by SD-OCT.

II) Application of macular SD-OCT imaging for detection of glaucoma

2A. Factors influencing macular OCT measurements in normal subjects

Many factors can affect the macular thickness measurements in normal subjects. Understanding the impact of these factors on full macular or inner retinal thickness is essential in order to take into account the influence of such confounding factors on macular measurements.

Age—Numerous investigations have demonstrated age as a strong and consistent predictor of the macular thickness. Most studies showed a consistent reduction in cp-RNFL, full

macular, GCC and GCIPL thickness with aging; however, the majority of these studies were based on cross-sectional data.[82, 114, 167, 198, 208, 278, 303, 324, 385] Mwanza and associates[278] studied normal eyes from different ethnic groups with Cirrus high-definition OCT (HD-OCT) (Carl Zeiss Meditec, Dublin, CA, USA); they found that the GCIPL thickness was stable between 18 and 49 years and then decreased progressively by about 0.10% per year. They also demonstrated that the age-related GCIPL rate of thinning varied among macular sectors with the inferonasal and superonasal sectors showing the fastest rates of thinning. Mauschitz and coworkers[255] studied 1306 individuals ranging from 30 to 95 years with Spectralis OCT. They found that rates of thinning per decade were −2.98%, −1.17%, −0.14%, −0.91% and for the GCL, inner retina, outer retina, and total retina, respectively. The results suggested a significant nonlinear effect of age on GCL. The aging influence on the macular thickness was more prominent after the sixth decade. Girkin and coworkrs[114] reported a decrease of 0.1 μm/year in GCC in a large cross-sectional sample of patients (632 eyes of 350 patients). In contrast, other studies failed to find a significant correlation between age and GCC thickness; however, the enrolled subjects were mostly young adults in those reports.[177, 371, 436] More recently, Chauhan and colleagues investigated age-related loss of thickness in 6 individual macular layer (RNFL, GCL, IPL, inner nuclear layer, outer plexiform layer, and outer nuclear layer) and compared those with age-related loss of Bruch membrane-based minimum rim width (BMO-MRW) and cp-RNFL thickness.[59] Their study sample consisted of 246 white subjects with median age of 52.9 (age range: 19.8–87.3 years). The only factor that was significantly different among subjects of different ages was the axial length. They found that among the 6 layers studied, only GCL, IPL and inner nuclear layer displayed statistically significant thinning with advancing age at − 0.11 μm/year, − 0.07 μm/year, and − 0.03 μm/year, which corresponds to 2.8%, 2.1%, and 0.8% loss per decade, respectively. The age-related thinning of GCL was twice larger than that of BMO-MRW and cp-RNFL.

Two longitudinal studies explored the effect of aging on macular thickness parameters. Leung and coworkers[240] reported that the proportion of eyes showing progression based on GCIPL, inner retina (GCC), full macular thickness (FMT) and outer retina decreased after age-related changes were taken into account. The mean age-related loss for GCIPL and inner retina (GCC) were −0.31 μm/year and −0.24 μm/year, respectively, after adjusting for baseline macular thickness, spherical error, and signal strength. Zhang and colleagues[432] also reported on the age-related decline in GCC thickness ina cohort of normal subjects from the Advanced Glaucoma Imaging Study who were followed for 5 years. The rates of change were greater in younger subjects in this study; GCC thickness decreased by −0.31, −0.34 and −0.11 μm/year in subjects aged 40–55, 55–65 and >65 years, respectively. The average yearly rate of thinning for all age groups was −0.25 μm/year, which is consistent with Leung et al.'s findings.[240] A reduction in RGC count of 0.55% to 0.59% per year has been reported in histological studies.[42, 130, 136] The reduction in RGC density tends to be lower in the macular region at about 0.29% per year. This discrepancy between histological and OCT age-related rates of RGC decay may be related to limitations of measuring the GCL with OCT in the peripheral macula where it is reduced only to a single layer of cells as GCL thickness and RGC density demonstrate high correlation.[158]

Gender—Most reports regarding the influence of gender on macular thickness measurements found significant differences in FMT with women having thinner retinal thickness.[89, 187, 246, 391, 401, 408] The findings on between-gender differences in inner retinal thickness parameters are more controversial. Huo and coworkers[167] and Zhao and colleagues[436] found no significant differences in GCC thickness between men and women; however, Koh and coworkers[208] found significantly thinner GCIPL thickness in females. Mauschitz and coworkers[255] reported significantly lower GCL thickness, but similar IPL thickness measurements, in women compared to men. Ooto and coworkers[303] investigated the influence of gender on individual retinal layer thickness measurements and found that the inner nuclear layer and outer plexiform + outer nuclear layers were significantly thicker in men, whereas the mRNFL was thicker in women. Mwanza and associates[277] reported no significant differences in average GCIPL thickness between male and female subjects after adjusting for axial length and ethnicity; however, men had thicker superotemporal and inferotemporal GCIPL compared to women. In addition, male gender was a significant negative predictor of mean GCIPL thickness ($\beta = -1.62$) in multivariate regression analysis. Therefore, models incorporating inner retinal measurements for discrimination of glaucoma eyes from normal subjects may need to take gender into account, although mixed results suggest small differences that may not be clinically relevant.

Axial length—An inverse correlation between axial length (AL) and total macular thickness has been well documented.[242, 249, 255, 362, 408, 410] More recent studies showed the same trend for the inner retinal layers with thinning of the inner retina with longer AL or more myopic refractive error.[20, 194, 198, 277, 348, 371, 436] Tateyama and associates[371] evaluated the influence of axial length on GCC thickness in young adults with varying degrees of myopia. They found that GCC thickness ($r = -0.384$), outer retinal thickness ($r = -0.444$) and the total retinal thickness ($r = -0.493$) were all significantly correlated with AL. Lam et al.[213] evaluated the relationship between myopia and macular thickness at the fovea, the inner macular 1–3 mm ring and the outer 3–6 mm ring in 143 subjects with high myopia, low to moderate myopia and non-myopic eyes. The average foveal thickness had a significant positive correlation with AL ($r = 0.374$), i.e., longer AL was associated with thicker central fovea; in contrast, the macular thickness within the outer 3–6 mm ring demonstrated a significant negative association with AL ($r = -0.471$) and showed no correlation with AL at the inner 1–3 mm ring. Kim and coworkers[199] reported that mean GCC thickness decreased by approximately 1.6 μm for each millimeter increase in AL and by about 0.8 μm per 1 D of worsening myopia. Mwanza and colleagues[275] found AL to be inversely related to GCIPL thickness ($\beta = -0.87$ μm/mm), with a 1.1% reduction in average GCIPL thickness for every millimeter increase in AL as measured with Cirrus HD-OCT. Another study failed to find a significant association between inner retinal thickness parameters and AL or refractive error.[167]

The influence of AL or myopia has been attributed to both magnification error and true retinal thinning in elongated globes. The inner retina undergoes progressive thinning as a result of mechanical stretching of the sclera, although there is no clear histological evidence supporting degeneration of RGCs with an increase in AL. The reduction in measured inner retinal thickness parameters with longer AL could also be due to the effect of ocular

magnification on the measured area of interest, however, none of the available OCT device software fully correct for the magnification error. Higashide and coworkers[142] studied the effect of clinical factors and magnification correction on the total and inner macular thickness. A modified Littmann's formula (Bennett's formula), which takes only AL into account, was used to correct for ocular magnification. They reported that the significant correlation between inner retinal thickness and AL became non-significant after magnification correction.

Ethnicity—Most previous investigations found that African-American subjects had thinner total retinal thickness measurements in comparison to Caucasian[24, 113, 123, 185, 187, 391] and Hispanic subjects;[113, 185] however, there are few studies on the influence of ethnicity on inner retinal thickness measurements. Girkin and associates[113] reported that African-Americans had the thinnest GCC measurements compared to other ethnic groups including subjects of European descent or Hispanic ethnicity, Indians, and Japanese. The diagnostic ability of macular measurements for detection of glaucoma was, however, similar across ethnic groups in another study.[113]

Miscellaneous—The role of systemic factors such as body mass index, diabetes and systemic hypertension on macular parameters have been investigated with no significant relationship found in one report.[208] Another study evaluated the effect of diabetes and diabetic retinopathy (DR) on FMT and found that moderate to severe DR was associated with increased foveal and outer temporal macular thickness but there was no difference in macular thickness in eyes with mild DR and in diabetic patients without DR.[359] Presence of systemic hypertension has been associated with a reduction in central macular thickness over time.[219]

In summary, macular thickness measurements decrease with aging. Longer AL is also consistently associated with thinner macular measurements. Subjects of African descent tend to have thinner macular measurements compared to other ethnicities. Many studies reported thinner macular thickness in women while some others found no differences between genders.

2B. Review of macular imaging algorithms by various OCT software

Cirrus HD-OCT—The original time-domain OCT devices introduced by Carl Zeiss Meditec had slow scanning speed and low resolution. Stratus OCT, the fastest commercially available TD-OCT device, had a speed of 400 A-scans per second resulting in a resolution of 10 μm. Cirrus HD-OCT (Carl Zeiss Meditec, Dublin, CA, USA) is an SD-OCT with a speed of 68,000 scans per second in the latest version (Cirrus HD 6000). The faster speed enables higher resolution scan acquisition and less image artifact compared to TD-OCT. Cirrus HD-OCT provides the combined thickness of the GCL and IPL, called the GCIPL, in the Ganglion Cell Analysis printout. The Cirrus HD-OCT macular volume scan (Macular Cube 200×200) measures a 6×6×2 mm cube in an emmetropic eye and consist of 200×200 or 512×128 A-scans centered on the fovea. The FMT is represented as an ETDRS grid with thickness measurements in 8 sectors that cross the horizontal midline (Figure 1A). After segmentation of the inner layers, a Ganglion Cell Analysis (GCA) map is also provided

(Figure 1B). The GCIPL thickness is presented on the GCA printout within a horizontally oval 4.8×4.0 mm area after exclusion of a central perifoveal ellipse 1.2×1.0 mm in size. Global average GCIPL, minimum GCIPL (see below), and GCIPL thickness in 6 wedge-shaped sectors are provided (Figure 1B).

The normative database for Cirrus' macular OCT measurements is based on a multicenter (7 centers) prospective study. Two hundred eighty-two normal subjects (133 males and 149 females) with age ranging between 19–84 years (mean age: 46.5 years) were enrolled. Six age categories were defined based on decades. Since there were only 28 subjects aged 70–79 years and only 3 subjects above age 80, results in these age groups should be interpreted with caution. There is no normative database for subjects younger than 19 years. The ethnic composition of the enrolled subjects was as follows in numerical order: Caucasian, Asian, African American and Hispanic; however, the mean difference in average GCIPL thickness between any pairs of ethnicities was 6 μm or less. The refractive error of the normative group varies between −12 to +8 D. It must be noted that the results of Cirrus' macular measurements and printouts for individual subjects are adjusted only for age, not by ethnicity or any other clinical factors such as axial length, refraction, optic disc area, or signal strength.[1] Mwanza and coworkers evaluated the profile and predictors of GCIPL thickness in Cirrus' normative database. They found that thinner RNFL, older age, longer axial length, and male gender were independent factors associated with thinner GCIPL. They concluded that the effect of age, axial length and gender should be taken into account for interpretation of Cirrus HD-OCT's GCIPL thickness measurements.[275]

RTVue SD-OCT—The RTVue (Optovue Inc. Fremont, CA, USA) is an SD-OCT system with a speed of 26,000 A-scans per second and depth resolution of 5 μm (Figure 2). The newer SD-OCT device from Optovue (Avanti) has a speed of 70,000 A-scan/second and follows the same strategy for imaging the macula in glaucoma patients. A 3D scan of macular GCC over a 7-mm square centered 0.75 mm temporal to the fovea is provided. Tan and colleagues originally defined GCC as a new macular parameter on RTVue 1000 macular cube for detection of glaucoma.[372] They also introduced two new OCT parameters, the global loss volume (GLV) and the focal loss volume (FLV) to distinguish glaucoma from normal subjects. Global loss volume (GLV) is calculated by first measuring percent thickness loss in each pixel in relation to the normative database and then dividing the number of these pixels by the total number of pixels. Therefore, GLV represents the percentage of global GCC loss in the entire GCC map. Focal loss volume (FLV) creates a pattern map based on thickness values at each pixel and compares it to the normative database average pattern map; the difference between these is then calculated as a difference map. To calculate FLV percentage, the software divides pixels displaying a thickness measurement less than 1 percentile probability cutoff on the difference map by the total number of pixels. Therefore, FLV displays focal loss of GCC in the entire GCC map (Figure 2).

The RTVue device's normative database consists of 861 normal subjects enrolled at 15 centers. A major advantage of RTVue's normative database is that it allows users to choose a specific ethnic group for comparison. Additional factors adjusted for are age and optic disc size (for RNFL measurements). The age range of the database subjects varies from 19 to 82

(mean age: 50 years).[358] Girkin et al. evaluated the influence of race, age, disc size and disease severity on diagnostic ability of ONH, RNFL and macular OCT thickness measurements in group of 312 eyes of 167 normal subjects and 233 eyes of 163 glaucoma patients.[113] Subjects of African and European descent were included with a mean age of 47.4 and 54.8, respectively. The spherical equivalent for the enrolled eyes varied between −5 to +5 D. They found that RTVue OCT's diagnostic performance did not significantly improve when a race-specific normative dataset was used.

Topcon 3D-OCT—Topcon 3D-OCT (Topcon, Inc., Paramus, NJ, USA) has had multiple generations including 3D-OCT 1000 and 3D-OCT 2000 and a newer swept-source (SS) OCT (DRI OCT-1). Topcon 3D-OCT has the ability to acquire up to 50,000 A-scans per second. The typical scan area is 6×6 mm and 128 horizontal linear B-scans consisting of 512 A-scans in each B-scan are carried out resulting in a depth resolution of 5 μm. In contrast, DRI OCT-1 has the ability to acquire up to 100,000 A-scans per second and can acquire widefield scans measuring up to 12×9 mm with 256 horizontal linear scans each comprised 512 A-scans with a depth resolution of 8 μm. Macular RNFL, GCIPL and GCC are presented in a single 3D wide-field report.

The Topcon OCT device's normative database was collected at 6 centers in the United States. The age range varies between 19–84 years with a female to male ratio of 122/67. Most of the subjects were Caucasians (64 %) followed by African-American and Hispanic ethnicities. Based on the inclusion criteria, the axial length and spherical equivalent of the enrolled subjects were between 22 and 26 mm and −6 D and +3 D, respectively.[379]

Spectralis SD-OCT—The macular imaging algorithm of the Spectralis SD-OCT (Heidelberg Engineering GmbH), called the Posterior Pole Algorithm (PPA) or Posterior Pole Asymmetry Analysis (PPAA), consists of 61 horizontal B-scans, each comprised of 768 A-scans, which are acquired along the Bruch's membrane opening (BMO)-fovea axis. Each B-scan is repeated 9–11 times to decrease speckle noise (Automatic Real Time or ART =9–11). The data are then averaged and an 8×8 thickness grid (64 superpixels, 3° wide) for the layer of interest is created (Figure 3 A and B). The output provides direct thickness comparisons between corresponding superpixels of fellow eyes and between corresponding superior and inferior superpixels of the same eye. However, no comparison to normative data is available on the PPAA. The latest software (Glaucoma Module Premium Edition or GMPE) is able to segment all the individual retinal layers.

The characteristics of the normative database for Spectralis have not been formally published although some studies have reported data on small groups of normal subjects.[59, 123, 295, 296] Chauhan and coworkers[59] evaluated 254 normal white subjects with equal number of patients per decade up 90 years (median age: 52.9 years) to calculate age-related loss of 6 individual macular layers. A decline in GCL thickness with advancing age was reported.

2C. Detection of preperimetric and perimetric glaucoma with macular OCT imaging

A diagnosis of preperimetric glaucoma is made when there is evidence of glaucomatous optic disc changes or RNFL loss on clinical examination or structural tests while no

definitive sign of VF loss is present on standard automated perimetry (SAP); therefore, it should be considered a form of early glaucoma. On the other hand, in eyes with perimetric glaucoma, an established glaucomatous VF defect is observed on SAP. Assessment and comparison of various glaucoma diagnostic tests for detection of glaucoma has been frequently based on measuring the area under receiver operating characteristics (ROC) curves (AUC), sensitivity, and specificity; however, there are shortcomings to these approaches such as dependence of the results on the dataset, challenges with definition of glaucoma and normal eyes and results are often inflated by bootstrap techniques used to calculate the 95% confidence intervals.[171]

Studies on detection of glaucoma based on Stratus OCT mainly focused on total macular thickness measurements. The AUCs for discriminating between glaucoma patients and normal subjects with total macular thickness ranged from 0.53 to 0.64 for glaucoma suspects/preperimetric glaucoma eyes[124, 237] and 0.68–0.88 in perimetric glaucoma.[124, 237, 261, 406] The highest AUC was observed in the temporal outer macular region on the EDTRS grid.[261, 394] Ojima and coworkers[302] and Wollstein and colleagues[406] used the macular volume for this purpose and reported AUCs of 0.800 and 0.919, respectively, for the detection of perimetric glaucoma. Evaluation of inner retinal layers for detection of glaucoma was proposed for the first time by Tan and coworkers,[374] who reported an AUC of 0.8 for macular GCC with Stratus OCT measurements.

Utility of GCIPL thickness measurements from Cirrus HD-OCT for detecting glaucoma has been evaluated in many studies. The AUCs for the average GCIPL thickness ranged between 0.67 and 0.94 for early to moderate glaucoma[43, 60, 179, 194, 214, 279, 287, 300, 420, 437] and 0.730 to 0.953 for advanced glaucoma.[179, 420, 437] Mwanza and coworkers[279] introduced a new local thickness parameter known as minimum GCIPL thickness defined as the GCIPL thickness on the meridian showing the lowest average measurement.[279] The minimum GCIPL thickness was found to be the best GCIPL parameter for discriminating early glaucoma (perimetric and preperimetric) from normal eyes by some investigators (AUCs 0.860–0.962).[43, 179, 214, 276, 279, 300, 420] Among sectoral GCIPL thickness parameters, the inferotemporal and inferior macular sectors perform best for distinguishing between normal subjects and early glaucoma patients (AUC of 0.79–0.96 and 0.77–0.94, respectively).[43, 179, 214, 276, 279, 287, 300, 322, 420] Hwang and coworkers showed that absence of a macular GCIPL defect on the Ganglion Cell Analysis in eyes with glaucoma was associated with increased angular distance of the peripapillary RNFL defect from the temporal region on the TSNIT curve.[169]

Kim and coworkers demonstrated that a GCIPL hemifield test with Cirrus HD-OCT had an AUC of 0.967 (sensitivity 94.9% and specificity of 98.5%) for differentiating preperimetric glaucoma eyes from normal controls in Korean patients.[204] The corresponding numbers for early perimetric glaucoma were an AUC of 0.962 with a sensitivity of 94.0% and specificity of 96.6%. In both comparisons, the AUCs for the GCIPL hemifield test were higher than that of the best macular parameter, i.e., minimum GCIPL thickness ($p = 0.09$). The GCIPL hemifield test performed better than cp-RNFL thickness parameters in this study ($p \leq 0.01$). It must be noted that results in Asian patients with a high prevalence of normal-tension

glaucoma may not be generalizable to other populations, given the sometimes localized nature of the glaucomatous damage in such eyes.

Although more recent platforms, such as the Avanti OCT, are available from Optovue, most studies used older versions of Optovue devices to assess its performance in glaucoma detection. The reported AUCs for the average GCC thickness measurements for detection of glaucoma in preperimetric and early perimetric glaucoma range between 0.72–0.795,[21, 245, 321, 332] and 0.79–0.977,[21,145, 205, 273, 326, 339, 346] respectively. The RTVue 100 software provides superior and inferior macular hemiretinal thickness measurements; in most studies, the inferior macular GCC thickness demonstrated a higher AUC (0.75–0.98 for all levels of glaucoma severity) compared to the superior GCC.
[21, 145, 245, 273, 321, 326, 332, 339, 346] Also, global loss volume (GLV) performed better than focal loss volume (FLV) with AUCs of 0.59–0.76 and 0.78–0.92 for preperimetric and perimetric glaucoma, respectively.[21, 245, 321, 326, 332, 339, 372] Some investigators reported GLV to be the best GCC parameter to detect preperimetric and early glaucoma;
[21, 332, 339, 373, 395] two other studies, however, reported that the average and inferior macular GCC thickness performed better.[245, 321]

Huang and coworkers assessed the ability of inner macular parameters for detecting perimetric glaucoma from glaucoma suspects and compared it to cp-RNFL parameters.[165] The average cp-RNFL thickness and inferior GCC thickness had the best performance (AUC = 0.919 and 0.871, respectively). They used stepwise linear discriminant analysis to formulate a discriminant function for improving diagnostic capability by combining various OCT parameters. The AUC for the final linear discriminant function was 0.970, which was significantly larger than the best single RTVue OCT parameter (p =0.002).

There are relatively few studies reporting the performance of Topcon 3D-OCT inner retinal layer measurements for detection of glaucoma. Nakatani and associates explored FMT measurements to discriminate early glaucoma patients (including preperimetric eyes) from normal subjects.[292] The global FMT had an AUC of 0.53 with 16% sensitivity at 91% specificity. The best regional thickness measurements were outer temporal, outer inferior and inner inferior macular areas based on the EDTRS grid. Yoshida et al. investigated GCIPL measurements derived from the Topcon 3D-OCT device for the same task.[421] The global GCIPL thickness had an AUC of 0.894, while the superior and inferior hemiretinal GCIPL thickness measures demonstrated AUCs of 0.794 and 0.918, respectively. Kotera and coworkers evaluated Topcon 3D-OCT's ability to differentiate eyes with suspected or preperimetric glaucoma from normal eyes. The inferior temporal outer sector had the largest AUC (0.86 ± 0.05) compared to other parameters. The AUC for this parameter was also significantly larger than the best cp-RNFL parameters, namely RNFL thickness in the 6 o'clock sector and inferior quadrant (p =0.001 and 0.009, respectively). Most of the patients in this cohort had evidence of glaucoma damage in the inferior optic disc region and therefore, the findings might be a reflection of the characteristics of the selected sample.

Recent studies based on DRI OCT-1 are encouraging. Yang and coworkers[420] evaluated the diagnostic ability of GCC and GCIPL for early glaucoma with DRI OCT-1 and compared the results to Cirrus HD-OCT. The AUCs for the average and sectoral macular GCIPL and

macular GCC varied between 0.65 and 0.81 and 0.71–0.84, respectively, for differentiating between healthy and glaucomatous eyes. The diagnostic accuracy of OCT parameters was generally similar between the two OCT modalities, as shown in two other studies.[232, 233] In another study by Lee and associates[232], inferior and inferotemporal macular ganglion cell measures (GCIPL with or without mRNFL) showed the largest AUC for detection of preperimetric and early perimetric glaucoma. Hood and colleagues recently showed that a single, wide-field scan from DRI OCT-1 could detect glaucoma with very high sensitivity and specificity when the judgment of two glaucoma specialists who had access to 24–2 and 10–2 VFs, fundus photos, patient chart information, and Hood's single-page report was used as the external reference.[152] Hong and coworkers compared the ability of wide field swept-source OCT scans providing macular and cp-RNFL data for discriminating glaucoma to standard macular and RNFL scans and found no significant difference, although the former has the advantage of providing data ina single image.[147]

Sullivan-Mee and associates[366] used FMT measurements from Spectralis PPA to detect early glaucoma. The inferior macular thickness displayed the highest sensitivity: 65% and 48% at 80% and 95% specificities. Among the inter-eye macular asymmetry parameters, the AUC was largest for the inter-eye macular thickness difference (0.913). Several other studies using the same algorithm found similar results.[75, 76, 344, 416]

The diagnostic ability of individual or combined layer measurements derived from Spectralis OCT has been explored in recent investigations. The GCL[31, 65, 90, 243, 253, 295], GCC,[65, 192] and mRNFL[68] thickness were found to be the single best parameter for detection of glaucoma in different studies; however, no consistent difference has been observed between macular outcomes of interest. Inner macular thickness measurements on larger grids[65] or outer sectors[31, 68, 243, 295] have displayed better diagnostic capability for early and preperimetric glaucoma. Also, temporal[31, 295] or temporal and inferior[68, 90] macular sectors have generally performed better for this task. Segmental macular analysis also showed good diagnostic performance for detection of normal tension glaucoma and congenital glaucoma.[68, 90, 243, 272]

Zha and colleagues[427] evaluated FMT measurements derived from PPA in primary angle closure suspects; they reported thinner measurements and larger asymmetry in primary angle closure suspects compared to normal eyes. Alluwimi and coworkers[10] explored the FMT and GCL thickness asymmetry for detection of glaucoma and found that variability in asymmetry was lower than thickness measurements and, therefore, asymmetry measures were superior for identifying early to moderate disease (average sample MD = −5.1 dB). It should be noted that such asymmetry measures could miss glaucoma with symmetrical damage, which is not uncommon.[149] They also found that GCL asymmetry tended to perform better than FMT asymmetry for the same purpose. Vercellin and associates[389] developed a custom-built software to calculate GCC and total macular thickness and volume with Spectralis OCT. They found that GCC volume within a ring extending from 3 to 4 mm from the fovea had the best diagnostic performance among 3-D parameters.

In summary, inner retinal thickness measurements of the central macula perform well for detection of glaucoma, including early/preperimetric stage. The best-performing parameters

among different devices include the minimum GCIPL thickness and GCIPL hemifield test (Cirrus HD-OCT), and the inferior hemiretina GCC thickness and the GLV index (RTVue OCT). Inter-eye asymmetry of full and inner macular thickness measurements with Spectralis OCT have also been reported to have good discrimination ability.

2D. Comparison of macular parameters to ONH/RNFL measures for detection of glaucoma

Diagnostic performance of any given parameter depends on many factors in a stud,y including the inclusion and exclusion criteria, the mix of glaucoma severity, the ethnic profile of patients, and the prevalence of myopia in the sample. Overall, cp-RNFL parameters have been shown to have higher AUC and sensitivities/specificities for detection of glaucoma than FMT parameters.[237, 257, 261, 287, 302, 406] In contrast, when inner macular layer parameters were compared to cp-RNFL measures for this purpose, most of the available reports found no significant differences between the two types of measures.[60, 90, 147, 194, 232, 233, 243, 300, 321, 332, 339, 366, 374, 420] A few studies reported that macular parameters performed better than those of cp-RNFL.[71, 179, 205, 256, 273, 387] A meta-analysis by Kansal and associates of 150 studies that evaluated 16,104 glaucomatous and 11,543 normal eyes compared the ability of cp-RNFL and macular parameters for detection of glaucoma.[184] For preperimetric and mild glaucoma, the AUC of the average cp-RNFL (0.831 and 0.912, respectively) was higher than the average macular GCC (0.797 and 0.861, respectively). In more advanced stages of glaucoma and in myopic eyes, the performance of the cp-RNFL and macular parameters were comparable. Results of a pooled AUC analysis also revealed that the difference in diagnostic performance among various devices was not significant. Morreno and colleagues[273] found that the average and superior macular inner layer thickness had significantly larger AUCs than average and superior cp-RNFL thickness, respectively. Kita and coworkers[205] reported that the global average GCC to FMT ratio performed better than mean cp-RNFL thickness and average FMT for discrimination between normal and early glaucoma patients. In a study by Mayama and co-investigators[256], the most sensitive mRNFL and GCC parameters demonstrated superior performance compared to the best cp-RNFL parameter. A recent longitudinal study reported that the macular GCIPL deviation map was superior to cp-RNFL for earlier detection of change in glaucoma.[202] This was attributed to early involvement of the macular vulnerability zone (see below). This is in contradiction to histological studies that indicated that death of the RGC soma occurs after axonal degeneration.[428] This finding may be related to the differences in the respective layer thickness measurements in the macula and the peripapillary area.[202] An earlier study showed that although both cp-RNFL and macular GCL were thinned in glaucoma, the GCL was substantially thinner, especially in eyes with parafoveal VF loss.[204, 279, 415] Furthermore, the GCL thickness overlap for normal and glaucomatous eyes was minimal.[279, 414] A few other studies, however, found that cp-RNFL thickness performed better than macular parameters for detecting early and preperimetric glaucoma.[37, 245, 265, 268, 309]

The diagnostic ability of inner macular thickness measurements has been reported to be the same as, or superior to, ONH parameters for the detection of perimetric glaucoma.[279, 339] A recent population-based study in China showed that the best Cirrus HD-OCT ONH

parameter (vertical cup to disc ratio) had a higher AUC than the best GCIPL parameter (minimum GCIPL thickness). However, this study included patients with a wide range of severity with an average MD of −8.9 dB.[207] Inner macular thickness OCT measurements also performed better than OCT angiography parameters (macular vessel density) for detection of glaucoma in other studies.[306, 392]

Inner macular thickness measures may perform better than cp-RNFL thickness in highly myopic patients.[291, 355, 356, 395, 435] Akashi and coworkers found that cp-RNFL thickness parameters performed significantly worse for detection of glaucoma in highly myopic eyes compared to non-highly myopic eyes whereas GCC's performance was not significantly different.[6] The topographic distribution of cp-RNFL thickness is altered in myopia. In addition, optic disc tilt and peripapillary atrophy, frequent findings in myopic eyes, may affect the cp-RNFL thickness measurements. Reproducibility of macular OCT measurements is good in myopic eyes. Lee and colleagues evaluated reproducibility of GCIPL thickness with two macular SD-OCT images ≥1 year apart in 99 eyes of 99 patients with high myopia without glaucoma and found that GCIPL thickness measurements were highly reproducible in highly myopic eyes; however, chorioretinal atrophy and posterior staphyloma affected measurement repreoduciblity.[223] Similar to studies reporting on sectoral and regional macular OCT parameters (see section 2G; factors affecting the SF relationship), studies in myopic patients have reported that the inferotemporal GCIPL was the best discriminator between normal and glaucomatous eyes, especially for detection of preperimetric glaucoma in highly myopia glaucoma patients.[66, 166, 345]

The topographic pattern of glaucoma damage also influences the diagnostic ability of OCT imaging. Seong and coworkers demonstrated that GCC thickness performed as well as cp-RNFL in eyes with normal tension glaucoma and early involvement of the central 10 degrees of the VF.[346] Shin and associates showed higher diagnostic performance for minimum GCIPL thickness in comparison with the average cp-RNFL thickness in eyes with parafoveal VF loss. Kim and colleagues[197] evaluated the influence of the profile of localized RNFL defects on diagnostic performance of cp-RNFL and GCIPL thickness measures. The inner directional angle of the RNFL defects rather than the angular width, affected diagnostic sensitivity of macular GCIPL; sensitivity of the GCIPL measures was higher in eyes with an inner directional angle of less than 30° (i.e., those closer to the temporal quadrant) compared to those with a directional angle of 30°−59.9° or greater than 60°.

Hood and colleagues[158] introduced the concept of the 'macular zone of vulnerability' (MZV), referring to a region extending from the inferior portion of the temporal quadrant of the macula to the temporal portion of the inferior quadrant of the disc (Figure 4). The inferior region of the macula (the MZV), mostly projects to the inferior pole of the disc, a region that is particularly susceptible to glaucomatous damage. Kim and coworkers[203] showed that all glaucoma patients with cp-RNFL defect in the MZV also showed inferior macular GCIPL loss, but the reverse was not true; there were several eyes with inferior macular GCIPL loss that did not display cp-RNFL defects in the MZV. A longitudinal investigation by the same group further confirmed this finding;[202] twenty percent of eyes with initially inferior macular GCIPL loss without cp-RNFL defect in the MZV subsequently showed an RNFL defect during a 3-year follow-up interval. Meanwhile, only

2% of eyes without preexisting inferior macular GCIPL loss developed a cp-RNFL defect in the MZV in the same period ($p < 0.001$).

In summary, inner macular thickness measurements demonstrate similar diagnostic ability for detection of glaucoma compared to cp-RNFL thickness; the former also perform as well as or better than ONH parameters for this purpose; in addition, macular measurements may be the best parameters for detection of glaucoma in myopic eyes.

2E. Combining various OCT parameters for detection of glaucoma

Several studies have investigated whether a combination of structural parameters (including ONH, cp-RNFL, macular, and OCT angiography parameters) could perform better than any individual measure. A variety of algorithms and statistical models, mainly based on logistic regression[248, 276, 300, 339,214, 281] or machine learning techniques,[22, 306, 421] have been used for this purpose. With some exceptions, combined parameters generally performed better than any individual parameter for detection of glaucoma.

Schulze and colleagues[339] proposed a model combining the best ONH, cp-RNFL, and macular OCT parameters (cup-to-disc ratio, average cp-RNFL thickness, GCC global loss volume) along with age. The resulting model was better than any of the individual parameters for discriminating early glaucoma patients from healthy subjects. This model did not discriminate well, however, ocular hypertensive patients from healthy subjects. Nouri-Mahdavi and coworkers found that a combination of the best macular parameter (minimum GCIPL) and the best cp-RNFL parameter (inferior quadrant cp-RNFL thickness) performed better than either modality for separating perimetric glaucoma eyes from normal subjects.[300] The combined model had a higher AUC than either parameter (Figure 5). Mwanza and collaborators introduced and validated the University of North Carolina Optical Coherence Tomography (UNC OCT) index, which combines the ONH, cp-RNFL, and GCIPL parameters.[281, 283] These investigators showed that the AUC for the UNC OCT index was larger than any single parameter for detecting glaucoma eyes with early VF loss. Another study by the same group explored a combination of the best GCIPL with the best cp-RNFL or ONH parameters using a binary *or*-logic, which requires at least one of the parameters in consideration to be abnormal, and an *and*-logic, which requires all parameters in the model to be abnormal for glaucoma to be considered to be present. The *or*-logic approach combining the minimum GCIPL thickness and average cp-RNFL thickness showed the best diagnostic ability for detecting early perimetric glaucoma.[276] Wu and colleagues[411] reported that qualitative assessment of all the information provided by 3D OCT-2000 had superior ability for detection of glaucoma compared to global cp-RNFL thickness evaluation (sensitivity of 95.5% vs 86.5% at 95% specificity, respectively, $9 < 0.001$).

Loewen and associates[248] introduced a similar concept defining the glaucoma structural diagnosis index (GSDI); it includes the composite overall thickness (NFL+GCC), composite FLV (NFL+GCC) and vertical cup-to-disc ratio. The GSDI has a range of zero to one with 75% of glaucoma eyes demonstrating a GSDI of ≥0.8. The AUC for GSDI was 0.922 for detecting perimetric glaucoma, and it performed better at high specificities when compared to the single best OCT variables ($p = 0.047$). The 99% specificity cut-off point for GSDI was 0.81 and GSDI showed 69% sensitivity at this specificity. The GSDI had better sensitivity

than the best single macular OCT parameter at both cut-off points while maintaining high specificity.

Larrosa and coworkers[214] developed and validated a multivariate predictive model to detect glaucoma with a combination of cp-RNFL, ONH and GCIPL parameters. A combination of qualitative and quantitative data displayed the highest AUC (0.937), which was significantly higher than other individual parameters for both early and advanced glaucoma. Choi and coworkers found that a linear discriminant function (LDF) combining macular and cp-RNFL parameters performed better than the single best OCT parameter, i.e., inferior cp-RNFL thickness.[67]

There is a growing interest in a diagnostic tool development based on supervised machine learning techniques to detect early glaucoma based on a combination of imaging data. These algorithms split of datasets into training/validation and testing subsets. The model is then trained to discriminate between normal and glaucomatous eyes, and its accuracy is evaluated with the testing dataset. The most commonly used machine learning techniques include linear discriminant analysis, support vector machines, and decision and classification trees (random forest).

Yoshida and coworkers[421] explored a random forest method to distinguish between glaucoma and normal eyes with OCT measurements including cp-RNFL, mRNFL and macular GCIPL. They found that the AUC of the Random Forest method (0.985) was significantly larger than the AUC of any single parameter. Diagnostic performance of a combination of GCIPL thickness and macular vessel density, based on an artificial neural network, was evaluated by Park et al.[306] The estimated combined parameter showed significantly enhanced diagnostic performance to detect early glaucoma than either macular vessel density or GCIPL thickness alone. Asaoka and colleagues[22] developed a deep learning approach that combined macular GCC and macular RNFL thickness data. Deep learning methods are similar to artificial neural networks, but have many more hidden layers. They used a transfer learning method for training model's hyperparameters and achieved an AUC of 0.937, which was significantly larger than the random forests model.

In summary, combining various OCT parameters derived from the ONH, cp-RNFL, and macula can help achieve higher diagnostic ability to discriminate glaucomatous from healthy eyes. Deep learning approaches seem to be promising.

2F. Alternative macular outcome measures: Vertical macular asymmetry and microcystic macular edema

Glaucoma is typically a bilateral disease; however, both inter- and intra-eye asymmetry are commonly observed and have long been used for glaucoma detection. Inter-eye asymmetry in cup/disc ratio,[94] intraocular pressure,[55, 241] or central corneal thickness (CCT)[170, 365] can help with glaucoma diagnosis. The asymmetry between threshold sensitivities of the superior and inferior hemifields on SAP is the basis for the Glaucoma Hemifield Test (GHT) used for detection of early glaucomatous field loss.[360] The central macula (central 16° or the area within 4.5 mm of the foveal center) contains up to 50% of the RGC complement of the eye.[70] Early macular thinning in glaucoma is usually greater on one side of the temporal

horizontal meridian, or the horizontal raphe, with preferential early inferior loss being most frequent;[158] hence, macular thickness asymmetry across the temporal raphe or horizontal meridian as measured with SD-OCT has been a topic of interest. As mentioned above, GCIPL and GCC thickness measurements can detect glaucoma better than FMT measures.[326, 373] Their diagnostic ability is close or equal to that of cp-RNFL thickness in early glaucoma.[200, 210, 279, 332, 373] It has been proposed that vertical macular asymmetry measures may provide additional diagnostic information in early glaucoma.[61]

Several studies have reported on presence of an afferent pupillary defect (APD) in asymmetric glaucoma.[40, 57, 64, 220, 297, 337, 376, 423] Some studies investigated the correlation between macular OCT findings and presence of APD.[40, 64, 220, 297, 376, 423] Besada and coworkers[40] evaluated the inter-eye difference for cp-RNFL thickness, GCC thickness, GLV and FLV in a group of 43 patients, of which 33 had glaucoma and 8 were diagnosed with non-glaucomatous optic neuropathies. They found that there was a significant correlation between presence of APD and the difference in cp-RNFL and GCC thickness measurements for all measures of interest. There was a significant correlation between APD and FLV percent difference when FLV fell below normal limits in one eye according to RTVue's normative database. The mean percentage loss difference for average cp-RNFL thickness, average GCC thickness, GLV and FLV was 23%, 15%, 12% and 6% at a 0.6 log unit APD, respectively.

Zeimer and colleagues were the first to show that retinal thickness asymmetry in glaucoma as measured with Retinal Thickness Analyzer was significantly correlated with asymmetry in visual sensitivity loss.[425] Using a similar approach, Salgarello and coworkers showed that relative and absolute vertical (superior/inferior) and horizontal (nasal/temporal) retinal thickness asymmetry (thickness difference) was increased in open-angle glaucoma (OAG) and ocular hypertension (OHT).[335] In OAG eyes, thickness asymmetry was associated with corresponding threshold asymmetry. Bagga and coworkers reported that macular asymmetry measurements with TD-OCT may help glaucoma detection.[30] Utility of vertical macular asymmetry for glaucoma detection has been the subject of a number of studies since then.[7, 25, 72, 76, 168, 186, 191, 226, 227, 344, 366, 386, 414, 416, 418] However, differences in study design including sample size, type of glaucoma, refractive error, ethnicity, disease stage, layer(s) of interest and method of asymmetry analysis should be considered when comparing the results of these studies. Most current SD-OCT devices are able to measure GCC, GCIPL, mRNFL, and FMT that could be used for hemispheric intra-eye or inter-eye asymmetry comparisons.

Studies in normal individuals have shown that the inferior macula is on average thinner than the superior macula[186] and that retinal thickness asymmetry is influenced by older age,[7, 174] gender (male more than female),[72, 174] and increasing distance from the center of fovea especially on the nasal side of the fovea where temporal vascular arcades cause physiologic asymmetry.[11, 266, 416] The influence of age and gender, however, should be interpreted with caution because of the small number of studies and the small samples.[72, 174] These findings need to be considered when diagnosis of early glaucoma is attempted based on the retinal thickness asymmetry. Additionally, sectoral retinal thickness is influenced by axial length, which may affect the relationship between the superior and inferior retinal thickness.[226, 417]

Young first- and second-degree relatives of POAG patients show asymmetry patterns similar to controls.[311]

Most studies have revealed that inner retinal layer (GCIPL or GCC) asymmetry measures perform better than FMT asymmetry for glaucoma detection.[210, 227, 414] Additionally, within-eye asymmetry in mRNFL thickness has been reported to perform both worse[414] or better[227] than vertical GCIPL or GCC asymmetry for glaucoma detection. An explanation for worse performance is that part of the mRNFL is derived from peripheral RGCs, while GCIPL thickness measurement only include macular RGCs.

Studies exploring vertical macular asymmetry in glaucoma have shown that it is more prominent in mild and moderate glaucoma and less pronounced in advanced glaucoma where generalized loss of RGCs decreases the magnitude of asymmetry.[168, 414] This is analogous to the visual field pattern standard deviation, which decreases in advanced glaucoma and pseudo-normality of GHT and pattern deviation plot in end-stage glaucoma.[45] Therefore, although asymmetry measures remain abnormal throughout most of the glaucoma severity spectrum, its utility to detect progression in advanced disease would seem limited. This is in contrast to thickness measurements, which diminish as glaucoma progresses and demonstrate significant correlations with VF thresholds.

Various methods have been used to estimate vertical asymmetry along the temporal raphe or horizontal midline, including thickness difference,
[25, 76, 168, 186, 191, 227, 333, 335, 344, 366, 386, 416] inferior to superior retinal thickness ratio,
[30, 186] and the absolute value of the logarithm of superior/inferior retinal thickness.[168, 414]

Spectralis SD-OCT (Heidelberg Engineering, Germany) was the first OCT device to incorporate a macular asymmetry analysis within its macular imaging algorithm (PPA) (Figure 6). The PPA shows the absolute difference in total macular thickness for each pair of an 8×8 grid centered on the fovea and aligned along the fovea-disc axis (or fovea-BMO axis in the newer software). Intra-eye and inter-eye superpixel-to-superpixel comparisons are made with a cutoff value of equal to or greater than 30 μm for the black color and the difference is presented as a gray-scale grid. The number of black squares has been used to determine sensitivity and specificity in different studies. This strategy was initially reported by Asrani et al.[25] and later used in a number of studies.[76, 191, 206, 332, 344, 366, 416] Reproducibility of PPA has been reported to exceed that of RNFL measurements.[206] Um et al. used total macular thickness differences between 5 corresponding superior and inferior zones similar to the GHT sectors of the Humphrey Field Analyzer. This macular Hemifield Test had higher sensitivity and similar specificity compared to average cp-RNFL thickness in early glaucoma but showed sensitivities and specificities that were comparable to sectoral cp-RNFL thickness measurements in glaucoma suspects and advanced glaucoma.[386] Two studies divided the PPA map into corresponding superior and inferior zones and showed that the central zone had higher diagnostic performance compared to the peripheral zones or the entire posterior pole map.[163, 434] Kawaguchi et al. reported that macular full thickness differences between the superior and inferior zones and between corresponding zones of both eye were significantly higher in preperimetric glaucoma eyes than normal eyes. They

used the ratio of the macular thickness in the inferior zone to that in the superior zone (x 100) for estimating vertical asymmetry.[186]

Yamada and coworkers introduced a global asymmetry index (AI) using 10 vertically oriented B-scans on Spectralis SD-OCT according to the following formula (Figure 7):[414]

$$\text{Asymmetry Index} = \left|\log_{10}(\text{lower hemiretinal thickness/upper hemiretinal thickness})\right|.$$

They calculated the AI for the mRNFL, GCL, GCC, and FMT and showed that the macular hemifield GCL thickness asymmetry had excellent diagnostic performance for all stages of glaucoma including early glaucoma compared to FMT or GCC in Japanese patients. Interestingly, the performance of this asymmetry index did not change with severity of glaucoma. They also showed that a GCL-based asymmetry index yielded a better diagnostic capability as compared to the one based on GCIPL thickness especially in preperimetric and early glaucoma. While the thickness of all macular layers correlated well with visual field mean deviation (MD) values, no or only weak correlations were observed between asymmetry indices and MD. This may indicate that the asymmetry index may not be a useful tool for detection of glaucoma progression. Additionally, since glaucomatous damage usually starts as localized tissue loss, averaging thickness measurements or asymmetry measures may actually hide localized changes.

Hwang and coworkers investigated macular asymmetry with a method similar to Yamada and coworkers based on GCIPL thickness parameters and observed that asymmetry parameters provided the highest AUC in early and moderate glaucoma and lower AUCs in preperimetric and advanced glaucoma.[168] Glaucoma diagnostic ability of the Asymmetry Index based on GCIPL was better than GCIPL thickness parameters only in early stage of glaucoma while in other stages, these parameters had worse diagnostic ability than GCIPL thickness parameters. Interestingly, for all stages of glaucoma, the reported AUCs for the Asymmetry Index were higher than those for thickness difference, which indicates that the Asymmetry Index may be a better measure of asymmetry than thickness difference. In a study comparing different asymmetry methods, Sharifipour and colleagues observed that Yamada and coworker's asymmetry method displayed a better performance than the absolute difference in all stages of glaucoma.[350]

Other studies found that local asymmetry measures may have a better diagnostic performance as they can detect localized damage early in the course of the disease. Kim and coworkers reported that a local asymmetry method called GCIPL Hemifield Test using differences in GCIPL thickness within 10 pixels above and below the temporal horizontal raphe with a cutoff value of 5 μm; this GCIPL Hemifield Test performed better than sectoral GCIPL and cp-RNFL thickness for detection of early glaucoma in Korean patients.[204] Sharifipour and coworkers showed that local asymmetry measures along the temporal horizontal meridian performed significantly better than a global asymmetry index based on Yamada and coworker's approach for glaucoma detection in a diverse group of patients in a tertiary referral center in the United states indicating that averaging may hide local changes characteristic of early glaucoma (Figure 8).[350] A local asymmetry index, however, still performed worse than GCIPL thickness measurements for this purpose. Horizontal macular

asymmetry, i.e., temporal to nasal (TNM) thickness ratio, was found helpful for detection of early glaucoma in eyes manifesting early paracentral VF defects in one study.[304]

Variations in alignment of the horizontal raphe with regard to the horizontal meridian have been well documented.[35, 36, 58, 164] Bedggood and associates introduced methods for measuring disc-fovea-raphe angle and found that with each algorithm, the least error was found when vertical scans on en face OCT were used.[36] The same group found that a substantial amount of the variation in the temporal nerve fiber raphe orientation in normal and glaucoma subjects could not be predicted despite considering age, axial length, optic disc and foveal anatomy and data from the contralateral eye.[35] The angle between the axis connecting the centroid of the BMO to the foveal center and the horizontal axis of the SD-OCT image is called the fovea-BMO (FoBMO) angle, which reflects anatomic variations between the fovea and BMO locations. The FoBMO angle is currently used by the Spectralis SD-OCT to adjust the cp-RNFL and the imaging tilt direction for the macular cube. Ghassabi and coworkers[110] showed that GCIPL symmetry across the horizontal meridian was influenced by the FoBMO angle; a more (negatively) tilted FoBMO angle was associated with relatively thinner inferior GCIPL thickness compared with the superior region along the horizontal raphe (Figure 10).

Different cutoff values for intra-eye and inter-eye thickness differences and the asymmetry index have been found for glaucoma detection. The reported cutoff values have been in the range of 9 μm,[366] 3.1–23.2 (up to 30 μm in nasal-peripheral macular area),[416] and 30 μm[30, 172, 344] for intra-eye macular asymmetry, and 5 μm,[366], 8 μm[72], and 23 μm[12] for inter-eye macular thickness asymmetry. A cutoff value of 0.09 for GCIPL Asymmetry Index yielded a sensitivity of ≥90% at a specificity of 100% in one study.[414]

The diagnostic ability of asymmetry analysis has been compared to those for cp-RNFL thickness and macular layer thickness measurements. Some reports indicate that intra-eye asymmetry between superior and inferior total macular or inner layer thickness measurements has equal or greater diagnostic ability than cp-RNFL[204, 344, 386] or GCIPL measurements for detection of early glaucoma,[204, 414] while other studies reported that intra-eye macular thickness asymmetry had worse performance for glaucoma detection.[76, 168, 191, 366]

Although the PPA is commercially available, it has some limitations and some modifications could improve its glaucoma diagnostic ability. It evaluates retinal asymmetry by measuring the full retinal thickness; thus, retinal layers other than inner layers could bias the results. In order to overcome this shortcoming, some recent investigations applied PPA to inner macular thickness measurement.[10, 110] The peripheral cells or superpixels of the grid especially on the nasal side, where vascular arcades confound measurements, have shown weak correlations with VF sensitivities compared to central superpixels and hence, have a lower utility for glaucoma detection. No comparison to a normative database is currently carried out for the total macular thickness measurements on the Spectralis SD-OCT;[125] however, a new software update will soon address this issue.

Vertical asymmetry could also help discriminate between glaucomatous and non-glaucomatous optic neuropathies. A step-like configuration near the temporal raphe on the Cirrus GCA Analysis report, the so-called temporal raphe sign, was shown to be potentially useful for detection of glaucomatous optic neuropathy in a study by Lee and coworkers, especially in the absence of a relative afferent pupillary defect.[22063, 297] They reported an AUC of 0.811 for the temporal raphe sign in distinguishing glaucomatous from non-glaucomatous optic neuropathy.

Microcystic macular edema (MME) has been associated with various optic neuropathies, including glaucoma.[2, 50, 51, 54, 95, 108, 118, 137, 190, 274, 400, 402, 405] It is defined by presence of hyporeflective cystic and lacunar areas (vacuoles) within the inner nuclear layer on macular OCT images; a confirmation on 2 adjacent B-scans and 2 separate tests is required and speckle noise needs to be excluded as the differential diagnosis (Figure 9).[108] Several mechanisms have been proposed for development of MME, such as vitreous traction or anterior mechanical force from the internal limiting membrane in setting of inner retinal atrophy[34, 41], trans-synaptic (retrograde) degeneration of bipolar cells secondary to RGC loss,[108, 111, 357, 405] and most importantly, dysfunction of Müller cells that are crucial for retinal homeostasis.[209, 330] Although MME is not a pathognomonic feature of glaucoma, it has been associated with the more advanced stages and progressing disease.[50, 51, 95, 108, 118, 137, 190] Murata and coworkers[274] evaluated 636 eyes of 341 glaucoma patients and found that MME was observed in 1.6% of the eyes. Visual field MD and PSD and visual acuity was significantly worse in eyes demonstrating MME. Hasegawa and coworkers[137] investigated the association between MME and other structural and functional factors in a group of eyes with POAG, preperimetric glaucoma, and normal subjects. Microcystic macular edema was only observed in the POAG group (13 out of 217 eyes; 6%). Eyes with MME demonstrated a significantly higher proportion of advanced glaucoma compared to POAG eyes without MME. In the majority of eyes (76.9%), the hemi-macula with MME corresponded to the hemifield showing more severe visual field loss. The MD rates of change were significantly greater for eyes with MME compared to those without. The authors also found significantly thinner GCIPL measurements in the hemi-macula demonstrating MME.

In summary, vertical asymmetry of inner macular layers across the temporal raphe is a valuable diagnostic tool to detect glaucoma especially in mild to moderate stages although it may not outperform cp-RNFL and/or GCIPL thickness measurements. It may also be helpful for discriminating glaucomatous from non-glaucomatous optic neuropathies. However, its utility may be limited for detection of glaucoma progression. Microcystic macular edema is an infrequent finding on macular OCT images in glaucoma patients and tends to occur more commonly in with eyes with more advanced glaucoma.

2G. Macular Structure-function relationships and comparison to cp-RNFL

Understanding the linking of structure and function with various structural and functional parameters can shed light on the nature of damage in glaucoma and assist with detecting or confirming presence or progression of glaucomatous damage.[23, 83, 150, 153, 158, 178, 181, 200, 201, 221, 267, 285, 312] Functional loss is usually measured based

on VF assessment, although other functional tests such as electrophysiological responses, visual acuity, and contrast sensitivity have also been explored. The primary structural measures of interest at this point in time are OCT-derived measurements of the cp-RNFL, neuroretinal rim, and macular thickness. Measurement of the cp-RNFL may not provide a thorough picture of the central (macular) structure-function (SF) relationships since the cp-RNFL is relatively thin in the temporal region of the disc and demonstrates a high degree of variability even in healthy individuals.[158]

Correlations between mean macular thickness measurements derived from TD-OCT and visual field sensitivity were first reported by Greenfield and associates.[120] Wang and coworkers[393] later demonstrated the feasibility of manually segmenting the inner retinal layers and confirmed correspondence of macular thickness measures with visual field sensitivity.

Hood and associate's body of work has elegantly described the correspondence of early central structural and functional damage in glaucoma and their topographic relationship.[154, 156–159] Macular damage has been demonstrated to be more frequent in the inferior macula, in an area that projects to a localized region of the inferotemporal ONH. This 'Macular Zone of Vulnerability' (MZV) is most likely to demonstrate the earliest signs of glaucomatous damage (Figure 4). The MZV corresponds and projects to a roughly 23°-wide sector of the inferotemporal ONH, which is the thickest ONH sector in healthy subjects; this sector is commonly associated with occurrence of disc hemorrhages.[157–159] This is consistent with the finding that central VF defects are more frequent in the superior hemifield.[307, 308, 381] While RGC loss in the MZV and corresponding VF defects tend to be deep and localized and closer to fixation on 10–2 VFs, glaucomatous structural loss in the superior macula is shallower and more diffuse with consistent corresponding inferior functional damage.[160, 307, 308, 381]

Hood and associates[159] also introduced the concept of overlaying 10–2 VF test locations onto macular OCT images to establish correspondence of structural and functional findings in individual eyes.[159] Hood and Raza[156] proposed combining central structural and functional data by aligning the RNFL and macular images based on blood vessels and adjusting the location of central test locations accounting for the RGC displacement from the fovea.[87] Structural glaucoma damage is displayed as continuous probability maps. This approach facilitates matching of central visual fields to macular OCT thickness maps and may improve detection of early central glaucoma damage (Figure 11).[156]

Mohammadzadeh and coworkers[269] recently investigated longitudinal SF relationships between macular OCT parameters (FMT, GCC, GCIPL and GCL) and central 10–2 VF in a cohort of 116 eyes with advanced or central glaucomatous damage at baseline. Macular 3°×3° superpixels were matched to 68 locations of the central 10–2 VF after adjusting for RGC displacement. Structure-function relationships were investigated at 3.4°, 5.6° and 6.8° eccentricities from the fovea and within inferior and superior hemiregions. Weak to fair correlations between various longitudinal measures of structural and functional change were observed; the highest correlation coefficient (0.41) was found at 3.4° eccentricity from the fovea for all the inner retina layers (GCL, GCIPL and GCC). The magnitude of correlation

was not statistically different between different inner retinal layers. This study concluded that GCC demonstrated overall the highest correlation coefficients with functional measures; the authors proposed that given GCC's higher average thickness measurements, it is less affected by segmentation artifacts and therefore, it might be the macular outcome measure of choice for monitoring glaucoma through advanced stages.

Some important considerations need to be considered for better understanding of macular SF relationship: First, macular functional damage does occur in early glaucoma; however, because of the sparsity and topography of the test locations on the 24–2 VF test, central functional loss is underestimated and frequently missed with this testing strategy.[78, 176] The test points of the 24–2 strategy are 6° apart along the horizontal and vertical meridians; therefore, the region of greatest central RGC loss could extend inside of or between the central 4 points and go undetected. Second, Hood and Kardon[154] have argued against the traditional concept that structural damage (e.g., loss of RGCs) precedes functional damage (i.e., VF sensitivity loss). They attributed earlier detection of structural loss to lower variability of structural measures in comparison to functional measures. The same team of researchers recently proposed enhancing the 24–2 strategy with 8 additional points from the 10–2 grid that were found to be frequently involved in early glaucoma (see below).[91] Finally, Qiu and coworkers reported that, the greater the fovea-disc, the higher percentage of false positive classification of normal subjects which will affect misclassification of glaucomatous eyes and therefore SF relationships in glaucoma.[315]

SF relationship models—Models for the SF relationship between various imaging and functional modalities have been described.[103, 104, 218, 270, 369] Hood introduced a linear model for correlating cp-RNFL thickness measurement with VF sensitivities.[148, 150, 154] Local relationships between individual or groups of superpixels or arbitrarily defined areas of the macula and VF test locations or sectors have been a topic of significant interest. The premise is that the direct one-to-one SF relationships in the macula could demonstrate the true and possibly higher correlation of macular thickness with functional measurements in the central retina. Most studies have found the pattern of macular SF relationships to be consistent with the broken-stick or the simple linear model as described by Hood and colleagues.[150, 154, 158, 267] Harwerth and coworkers[132, 135] described a non-linear SF model (NLM) based on the previously reported relationship between VF sensitivities and RGC density in experimental glaucoma. The proposed NLM describes the relationship between structure and function in both normal eyes and eyes with various degrees of glaucoma before advanced stages of glaucoma.

Displacement of RGC bodies from their receptive fields in the central macula may affect local SF correlations. In the central macula, RGCs are displaced from their receptive fields, mainly due to the length of the laterally connecting Henle fibers and to a smaller extent, to the oblique pathway through the bipolar cells.[87] Drasdo and coworkrs[87] estimated the magnitude of the RGC displacement in a histological study; the results of this investigation have been applied in most studies evaluating local macular SF relationship.[156, 216, 221, 267, 328] This model does not consider the individual variations in RGC displacement.

Raza and coworkers[328] described the correlation of the central GCIPL thickness measurements with VF sensitivities on the 10–2 VF after adjusting for RGC displacement (Figure 12). They found that the simple linear model as previously described for the cp-RNFL also applied to GCIPL thickness (see appendix). Regions of GCIPL thickness and VF loss were matched after accounting for the RGC displacement; SF relationships increased after this correction.

Lee and colleagues[221] reported that the correction for RGC displacement had the highest influence on the paracentral test locations closest to fixation although the improvements were not statistically significant. Turpin and associates[382] proposed that the RGC displacement from the receptors is related to local RGC thickness and is shorter than average in subjects with thicker inner retinal layers. They used macular SD-OCT images to customize RGC displacement in individual eyes by accounting for macular shape parameters and to determine the possible influence of individual anatomical differences on SF mapping in the central visual field. Individualizing macular displacement of RGCs based on OCT data resulted in a small difference on average but spatial shifts of up to 1–2° were observed in individual eyes especially in the inferior macula. The largest displacements were observed between 1° and 3° from the foveal center near the four oblique meridians. This adjustment for individual differences in RGC displacement does not seem to have significant practical implications at this point.[149]

There is marked variability in foveal shape among normal individuals.[24, 378, 391] The influence of foveal features on SF relationships have been investigated. Sepulveda and colleagues[347] quantitively evaluated variations of the foveal shape by calculating the central foveal thickness, maximum perifoveal thickness, and the distance between these points (the ‘radius’) in a group of 30 normal subjects. Variations in foveal shape and related parameters were observed among the study subjects. One of the goals of the study was to customize SF maps in each individual and estimate superior or inferior meridian parameters from the other; the maximum thickness was highly correlated between meridians but there was more variability in the radius measurements. Hood and coworkers[155] reported improved alignment of the central SF loss by scaling and rotating the structural and functional maps so that the centers of the fovea and disc corresponded to those in individual eyes. However, the customized model did not perform better than the standard model. Previous investigations with cp-RNFL thickness measurements also confirmed this finding.[13, 280]

Montesano and coworkers[270] introduced a novel SF model by matching the fundus image provided by Compass perimetry (CenterVue, Padua, Italy) to that from Spectralis SD-OCT. The Compass perimeter is equipped with a scanning laser ophthalmoscopy (SLO) tracking system that allows to accurately determine the retinal location where the threshold sensitivity is measured. Ganglion cell layer thickness maps were transformed to estimate ganglion cell density (GCD) centered on each VF test location after adjusting for RGC displacement. The first model included 31 glaucoma eyes with mean MD of −13.9 and 20 normal subjects; standard prior distributions previously described for the ZEST strategy were used.[383] The investigators created a multivariate logistic model with a binary response (see vs. not see) as the dependent variable and age, local $\log_{10}$(GCD), and eccentricity as the predictors. The logistic curves from this model was interpreted as estimated structural

probability of seeing curves. Subsequently, they repeated the model including the structural probability of seeing curves as structural prior distribution and introduced structural macular ZEST (MacS-ZEST) strategy to predict threshold sensitivity. The advantage of this strategy is to use different thresholds as prior distribution based on GCD. To gauge the accuracy of the model, these models were tested on 20 glaucoma eyes that underwent perimetry multiple times to obtain the 'true' threshold sensitivities. They found that in patients with reliable exams, there was no difference in mean absolute error between the standard ZEST and MacS-ZEST strategies; however, in patients with non-reliable VF exams, mean absolute errors were lower for MacS-ZEST. The number of presentations and testing time also were lower for MacS-ZEST strategy.

Ledolter and Kardon[218] explored random effect trend models to compare average baseline RNFL and GCIPL thickness values (intercepts), their slopes of change, and inter-subject variability in slopes and intercepts in two cohorts of 105 glaucoma patients and 55 normal subjects. Random effects models are a subtype of repeated-measure or mixed linear regression models and can detect differences in trends and baseline values between groups and more importantly variability of slopes and baseline measurements. Baseline structural measurements were significantly lower in the glaucoma group; although significant negative trends for both RNFL and GCIPL measurements were observed over time in both groups, the difference between the two groups was not statistically significant for either GCIPL or RNFL rates. However, there was larger inter-subject variability in structural slopes for glaucoma patients.

Factors affecting SF relationships—The strength of the correlation between VF sensitivity and structural thickness measurements varies among the macular sectors. Shin and coworkers[352] found that, among the six GCIPL sectors from Cirrus HD-OCT, the strongest association was observed between the inferotemporal GCIPL thickness and the corresponding superonasal central mean sensitivity. Kim and co-investigators[201] found that the strength of SF associations was significantly greater in the temporal parafoveal sector in each hemimacula compared to central and nasal sectors. They also reported that the strength of the SF relationships was significantly greater in the inferior hemimacula than in the superior hemimacula. Another study[269] also reported that the magnitude of SF correlation was higher for inferior hemimacula compared to superior hemimacula for all macular outcomes (FMT, GCC, GCIPL and GCL). Other studies have confirmed these findings.[285, 301, 325] Inferior and inferotemporal macular sectors are the most vulnerable areas to glaucoma damage and therefore, have a wider range of thickness measurements, which could explain the strength of SF correlations in these areas. On the other hand, the nasal macular sector corresponding to the papillomacular RNFL bundles demonstrate lower correlations than other macular regions.

One important issue is that SF relationships need to be explored as a function of distance from the foveola. Given the varying thickness within the central macula, this approach could reduce variability of SF relationships by averaging macular layer thickness and functional measurements at predefined eccentricities. Raza and coworkers evaluated SF relationship of GCIPL and 10–2 VF in 5 eccentricities ranging from 3.4° to 9.7° from the foveal center.[327] Ganglion cell/inner plexiform thickness at 7.2° eccentricity showed the highest correlation

with VF sensitivities among all eccentricities. The main reason for decreased correlation at outer eccentricities (i.e., farther from the fovea) seems to be thinner macular measurements. Miraftabi and colleagues investigated SF relationship at 3.4°, 5.6° and 6.8° from the fovea and found that measurements at 5.6° eccentricity displayed the highest SF correlations with 10–2 VF total deviation measurements.[267] Nouri-Mahdavi and coworkers recently reported that longitudinal SF relationships varied as a function of distance from the fovea.[298] Mohammadzadeh and colleagues[269]evaluated longitudinal SF relationships between macular OCT parameters (FMT, GCC, GCIPL and GCL) and central VF measurements at 3.4°, 5.6° and 6.8° eccentricities from the fovea and reported the highest SF correlations at 3.4° and 5.6° eccentricities.

Glaucoma severity influences the magnitude and pattern of SF relationships when cp-RNFL is used as the structural measure.[5, 117, 252] Glaucoma severity also affects the relationship between inner macular layer thickness and visual field sensitivity. No correlation between structure and function has been observed in macular regions with normal visual field sensitivity.[200] Structural changes may be more effectively detected than functional changes in early glaucoma due to lower inter-individual variability compared to VFs. Substantial RGC loss may occur before reduced SAP sensitivity on standard 24–2 VF can be identified (see ‘enhancing the SF relationship’ below). Araie and coworkers[18] showed that the correlation between GCC or GCIPL thickness and VF sensitivity (unlogged value) was greater in eyes with more advanced glaucoma (average MD = −9.8; ×2.7 for GCC and ×2 for GCIPL) than in those with mild damage (average MD = −3.0 dB). Kim et al. evaluated SF relationships between GCIPL thickness and VF means sensitivity (MS) for a range of glaucoma severity and compared the results to those for cp-RNFL.[195] In preperimetric glaucoma, neither GCIPL nor cp-RNFL demonstrated a significant correlation with MS. With increasing glaucoma severity, the SF relationships became stronger. The correlation between cp-RNFL thickness and MS was significant in early and moderate glaucoma but not in advanced glaucoma. The severity of glaucoma can affect the topography of SF relationships. Lee et al.[221] reported that in early to moderate glaucoma, the highest correlation was observed between the inferotemporal GCIPL and corresponding VF region, whereas in advanced glaucoma, the superotemporal GCIPL displayed the highest correlation with VF measurements. Other studies have found similar results.[195, 301]

In more advanced stages of glaucoma, macular thickness may reach its measurement floor. The residual thickness represents glial tissue and blood vessels along with possibly resistant or melanopsin RGCs and other RGC types, which have been reported to constitute up to 50% to 65% of average GCC in normal eyes.[212] The estimated measurement floor may be influenced by the study sample, the area imaged, the OCT device used, and the statistical models applied. The measurement floor and ceiling determine the dynamic range of measurements and dictate the utility of macular measures for detection of glaucoma deterioration (see section IV).[3, 195, 216, 384] As macular thickness measurements reach their measurement floor, detection of change becomes more challenging and beyond the measurement floor, such OCT measurement lose all utility for detection of progression. Miraftabi and coworkers[267] reported that all macular measures, including FMT, GCC, GCIPL, and GCL, reached their measurement floor at about −8 dB of sensitivity loss (Figure

13). The dynamic range of macular measures was directly related to their average thickness in normal subjects.

Enhancing macular SF relationships—As mentioned above, several investigations have shown that the 24–2 testing pattern might underestimate or entirely miss early central VF defects. Retinal ganglion cell loss in the MZV can be associated with VF loss that largely falls between or inside the central four points of the 24–2 test pattern. Therefore, adding additional points to the standard 24–2 VF has been proposed. Hood and coworkers[155] originally suggested that two points located at x = ±1°, y = 5° coordinates be added within the central 10° of the standard 24–2 VF. This hypothesis was explored by Chen and coworkers[62] using the Medmont M700 perimeter, which includes more densely packed test locations in the macula than the 24–2 pattern of the Humphrey Field Analyzer. They evaluated all possible pairs of Medmont locations that had not been used to derive the 24–2 pattern and found that adding a pair of locations to the superior macular region of the 24–2 pattern increased the number of abnormal locations identified in individuals with glaucoma; however, they did not find a significant difference in performance between various pairs of test locations and the proposed pair of test locations by Hood and associates. Lee and coworkers[221] evaluated the correlation between GCIPL thickness and 10–2 VF locations and found that 11 out of 34 superior locations and 10 out of 34 inferior locations demonstrated significant associations with the corresponding GCIPL sectors. Of those, 2 superior test points and one inferior test location are also tested on the 24–2 pattern as well (Figure 14A and 13B). Finally, Ehrlich and colleagues[91] investigated 3 modified 24–2 visual fields by adding 4 points (24–2 + 4) or 16 points (24–2 + 16 Even and 24–2 + 16 Empirical) to the 24–2 test pattern; in the former, the 16 added points of the 10–2 VF test were evenly distributed while for the latter, the 16 points followed an empirical pattern. The AUC for these 3 VF patterns were significantly greater than the conventional 24–2 test pattern for detection of early glaucomatous defects in the central 10°. Adding 16 points from the 10–2 VF to 24–2 VF resulted in only slightly better results compared to adding 4 points.

The G pattern testing strategy of the Octopus perimeter (Haag-Streit AG, formerly Interzeag AG, Schlieren, Switzerland) consists of 59 test locations within central 30° with 5 central points located within foveal region and 17 test locations within the macula. Test locations are distributed along RNFL bundles to enhance detection of glaucomatous VF loss.[320] More recently a new testing pattern called 24–2c was introduced for the HFA (Carl Zeiss Meditec® Inc., Dublin, California), which combines all points from the 24–2 VF testing pattern with 10 points from the 10–2 VF found to be most susceptible to glaucomatous damage. This test strategy is more likely to detect early macular damage.
78, 139, 155, 158, 160, 381

The influence of the stimulus size on SF relationships was explored in a recent study. Yoshioka et al.[422] investigated the correlation between differential light sensitivity measured with Goldmann stimulus sizes I to V (GI to GV) on the 10–2 VF and the RGC count per stimulus area derived from Spectralis macular OCT measurements. The sensitivity derived from smaller stimulus sizes (GI–GII) showed higher correlations with GCL thickness compared to larger stimulus sizes (GIII–GV) in both normal and early glaucoma patients. It has been proposed that the nonlinearity in SF relationship is a result of incomplete spatial

summation due to use of a fairly large stimulus size (size III) exceeding Ricco's area centrally and linearity could be attained by correcting for this.[102] In the other words, the size III target exceeds the spatial summation area, particularly for the central test locations; this could potentially explain the improved SF relationships with the smaller stimulus sizes.

Prediction of function from structure—Considering the theoretical and methodological challenges, there have been few attempts to derive or predict visual field thresholds from OCT data. Since a retinal region near the optic disc receives axons from an arcuate area, any RGC damage along this path could affect the RNFL thickness near the ONH. Technically speaking, cp-RNFL thickness is a one-dimensional datapoint and could not predict a 2-dimential set of VF data. The ability to measure the inner retinal layers in the macular region mitigates some of the challenges encountered in prediction of VF from cp-RNFL thickness.[430]

Zhang and coworkers[430] used multiple linear regression to predict VF thresholds from GCIPL and mRNFL thickness and found a median agreement of 90% when abnormal points on the predicted and measured fields were used to assess agreement. Bogunovic and associates[47] predicted individual 24–2 VF thresholds from a nine-field array of cp-NFL and GCIPL thickness measurements using their proposed RGC-axonal complex model. The correlation between the predicted and observed VFs was 0.80 for the superior hemifield and 0.84 for the inferior hemifield. These findings are promising as one may be able to complement VF data with predicted functional data from OCT measurements, which are objective and have different sources of noise. However, perfect prediction of VF would not be expected.

Relationship of macular parameters and other functional measures—A few studies evaluated the relationship between visual acuity or contrast sensitivity and macular parameters. Kim et al.[193] reported that the relationship between the best-corrected visual acuity (BCVA) and SD-OCT parameters such as cp-RNFL and macular GCC were curvilinear with significant correlations noted only in eyes with severe glaucoma. The global average cp-RNFL thickness showed a higher correlation with BCVA compared to GCC parameters. Fatehi and colleagues found that contrast sensitivity at 6 cycles per degree demonstrated the highest correlation with FMT in the superior macular region in preference to GCIPL thickness.[93]

Retinal electrophysiological measurements have also been correlated to macular structural parameters in humans and experimental animals. Kanadani and coworkers[182] investigated the correlation between macular OCT measurements and defects on 10–2 VF and macular multifocal visual evoked potential (mfVEP) in a group of 55 eyes with OAG. The macular OCT was in agreement with the 10–2 VF and mfVEP findings in 85–89% of eyes. Luo et al.[250] found that on hexagon-by-hexagon analysis, various multifocal electroretinography (mfERG) measures were correlated with GCIPL thickness in a nonhuman primate model of experimental glaucoma in rhesus monkeys. The mfERG functional measures demonstrated greater and more extensive losses than corresponding OCT structural measures. Interestingly, the investigators found that the correlation between mfERG measures and GCIPL thickness was strongest in normal subjects and was highest centrally and decreased

with distance from fovea. The weaker relationship in glaucoma patients was seemingly driven by the lower range of GCIPL measurements and the already depressed mfERG measurements.

Pattern ERG (PERG) is an objective functional measure of the central retina.[106] It has been shown that PERG is generated mostly from the inner layers of the retina as compared to flash ERG.[19] Thus, use of PERG has been proposed for evaluating SF relationship in some recent studies. Kreuz and coworkers[211] reported a significant correlation between the steady-state latency and P50 peak time on PERG and macular RNFL thickness. This finding was confirmed by Park and coworkers[305] who showed that a linear regression model ($r^2 = 0.22$) best fitted the relationship between N95 amplitude on PERG and GCIPL thickness. Given the high level of variability, the applicability of PERG measurements in glaucoma remains questionable.[161]

Prager and coworkers assessed the correlation between macular thickness measurements and vision-related quality of life using the 25-item National Eye Institute Visual Function Questionnaire (NEI VFQ-25).[314] On univariate analyses, patients with diffuse macular GCIPL loss achieved significantly lower mean overall NEI VFQ-25 scores than patients with focal damage. The difference remained significant after controlling for mean GCIPL thickness. An association between early glaucomatous macular damage and decreased vision-related quality of life was also observed in a study by Garg and coworkers.[101]

The relationship between threshold sensitivities derived from microperimetry, Heidelberg Edge Perimeter (HEP), or Octopus perimeter and macular GCIPL thickness was recently investigated by Rao et al.[323] The investigators showed that threshold sensitivity measurements from 10–2 SAP VFs and those from microperimetry demonstrated a similar relationship with macular GCIPL measurements in glaucoma patients. In another study, the highest SF correlation was observed between the superotemporal mean sensitivity on microperimetry and the inferotemporal GCIPL thickness.[336] Kawaguchi and coworkers[186] found that indices of macular symmetry were significantly correlated with perimetric sensitivities and the asymmetry in threshold sensitivity measurements derived from 10–2 SAP and microperimetry in eyes with perimetric glaucoma.

In summary, there is moderate to good correlation between inner macular OCT thickness measurements and central VF sensitivities or other markers of central function. Anatomical considerations such as RGC displacement and foveal shape significantly affect such SF relationships.

2H. Predicting RGC counts from macular GCL thickness

Estimation of RGCs count based on VF sensitivity was explored by Kerrigan-Baumrind et al.[189] and Garway-Heath and co-authors.[105] Harwerth and associates[132–136] used cp-RNFL measurements from TD-OCT to estimate RGC counts. Harwerth and associates' model uses SAP and RGC histology and quantifies the RGC density in a defined area of the retina from the corresponding SAP sensitivity. Their proposed methods can be summarized as follows:

$$s\_loss = 10\text{^}[(s - 40)/10]$$
$$gc = log(s\_loss * k) * 10$$

Where: *s_loss* is the reciprocal of the SAP stimulus intensity, *s* is the SAP sensitivity in dB units, *k* is a constant of proportionality (175,534) to scale the data for a linear relationship at 4.2° eccentricity, and *gc* is the predicted RGC density (dB).

This model has been applied to quantify glaucomatous damage by Medeiros et al.[259, 262] based on 24–2 SAP fields and Cirrus HD-OCT cp-RNFL thickness measurements. They reported that glaucomatous eyes had an average RGC loss of 28% (range: 6%−57%), at the time the earliest visual field defect could be detected on SAP.[262] Distante and associates[85] estimated RGC counts using Medeiros et al.'s empirical models based on both RNFL and GCC parameters. Good correlations (r ≥0.61) were observed between RGC counts and mean deviation, Visual Field Index, and pattern standard deviation. The assumptions of Harwerth's model have been questioned by some authors.[329] Estimates of the number of RGCs derived from their model for healthy humans are substantially greater than those found by histological data; these estimates took into account eccentricity and included adjustments for the difference in axial length between monkey and human eyes.[329]

Raza and Hood[329] proposed a novel model for estimation of RGC count relying only GCL thickness acquired by swept-source OCT and compared the estimated counts with previous published histological data and Harwerth's model. They estimated an average of 381,000 RGCs to be present in the macula. Their estimates align well with histological data and seem less variable than the Harwerth's model. Comparison of the estimated RGC count to averaged absolute sensitivities showed weak to fair correlations for both global and corresponding hemifield/hemiretina pairs (Spearman ρ =0.26–0.47).

Estimation of RGC counts based on both cp-RNFL and macular inner retinal thickness measurements seems to be more accurate and correlates better with VF sensitivities than macular inner retinal measurements alone.

2I. Prediction of glaucoma progression

Glaucomatous damage is generally irreversible and early intervention is necessary to prevent further damage and potential blindness.[52, 140] Therefore, timely detection of glaucoma progression is essential. However, glaucoma treatment is not without side effects and can be a financial burden to the patient and society. Prediction of glaucoma progression and its rate can help with planning appropriate and timely treatment; it can also enhance the cost-effectiveness of treatment. Hence, clinicians are in need of algorithms that can assist them with predicting the rate of future glaucoma progression. Based on the results of multiple randomized clinical trials and retrospective cohort studies, a number of clinical risk factors have been proposed for forecasting future progression of glaucoma. These include older age, thinner central corneal thickness, disc hemorrhages, presence of larger beta-zone peripapillary atrophy, level of intraocular pressure (mean, peak, or fluctuation), magnitude or fluctuation of ocular perfusion pressure, and a diagnosis of pseudoexfoliation glaucoma.[53, 79, 100, 180, 235, 236, 251, 258, 260, 299, 367] Prognostic models using some or all of the above

risk factors to estimate the probability of subsequent progression have been previously proposed;[79] However, it is conceivable that adding quantitative structural or functional data that can be easily obtained could improve this task. Substantial loss of RGCs and subsequent structural changes on OCT can occur before early VF loss can be detected.[4, 131, 318, 361] Different structural parameters have been used in various models for prediction of future progression.[262, 334, 424] While macular OCT thickness parameters have been used to detect glaucoma progression in several studies,[222, 271, 289] there is a paucity of published evidence on the use of macular GCC or GCIPL thickness for prediction of subsequent disease progression.

Anraku and colleagues investigated the role of baseline OCT parameters for prediction of future visual field progression in 56 POAG patients who were followed for at least 2 years.[16] The cohort was mainly composed of eyes with early stage glaucoma and was divided into fast and slow progressors based on MD slope above or below −0.4 dB/year. Among various baseline parameters explored, including VF MD, PSD and macular, cp-RNFL and neuroretinal rim OCT thickness, only thinner macular GCC at baseline was a significant predictor of fast progression. Moreover, GLV and FLV were significantly higher in those with fast progression. On multivariate analysis, only macular GCC thickness in the inferior hemimacula was associated with disease progression.

Zhang and colleagues investigated baseline SD-OCT measurements for prediction of VF conversion in glaucoma suspects and patients with preperimetric glaucoma.[433] Over an average (±SD) follow-up period of 41 (±23) months, 55 out of 513 eyes (11%) demonstrated VF conversion. The GCC FLV was the best single predictor of subsequent conversion (AUC =0.753). Eyes with an abnormal or borderline GCC-FLV had a 4-fold increase in the risk of conversion over a 6-year period. The authors proposed a Glaucoma Composite Conversion Index (GCCI) based on the GCC-FLV, inferior cp-RNFL thickness, age, and VF PSD to predict conversion to glaucoma (AUC =0.783). At a cutoff value of 0.84, GCCI had a sensitivity, specificity and overall accuracy of 60%, 83% and 81%, respectively, with a negative predictive value of 95%. In another study, Zhang and coworkers explored predictors of VF progression in 277 eyes with established glaucoma with an average (±SD) follow up of 3.7 (±2.1) years.[431] Visual field progression was detected in 83 eyes (30%). The best performing single predictor for VF progression was GCC-FLV. Presence of an abnormal GCC-FLV at baseline increased the risk of VF progression by 3 times. A proposed Glaucoma Composite Progression Index (GCPI) based on age, CCT and GCC-FLV had an AUC of 0.653 for predicting subsequent VF progression over time and performed better than any single variable. Lee and colleagues[230] compared rates of GCIPL and cp-RNFL change in a group of eyes in which progression was established based on 24–2 VFs and disc and RNFL photographs. They found that global and sectoral GCIPL in the affected hemiretina demonstrated significantly faster rates of thinning compared to nonprogressing eyes. The best GCIPL parameters, according to trend-based analyses, for discriminating between progressors and nonprogressors were rates of thinning for global GCIPL (AUC =0.791), minimum GCIPL (AUC =0.755), and inferior hemifield GCIPL (AUC =0.708). Daneshvar et al.[73]compared baseline cp-RNFL and macular OCT parameters to qualitative review of optic disc photographs for prediction of subsequent VF progression in a cohort of eyes with mostly established glaucoma. They found that thinner cp-RNFL and average GCIPL at

baseline were significant predictors of VF progression, defined by both pointwise event and global trend-based analysis (based on VFI); none of the semi-quantitative disc variables had any predictive value.

A shortcoming common to all of the above studies is that the enrolled glaucoma eyes were highly homogenous and had mainly mild damage. Moreover, although some statistical models such as leave-one-out cross validation were used, the prediction models have yet to be validated on independent samples of patients. An important limitation to using structural tests is that the pace of technological innovations is faster than the required period for carrying out reliable longitudinal studies and it is difficult, if not impossible, to have evidence-based confirmation of the utility of the state-of-the-art technology. Finally, it should be stressed that all study designs have strict inclusion and exclusion criteria and extrapolation of their result to every day clinical practice should be done with great caution.

In summary, baseline inner macular thickness measurements are good predictors of subsequent glaucoma progression. Combining multiple structural and functional modalities along with clinical information could provide the best approach to forecasting glaucoma progression.

III) Variability and reproducibility of macular SD-OCT thickness measurements and application to detection of glaucoma progression

With any diagnostic method, it is important to establish how reliable and reproducible the data are. Validity and accuracy of the acquired data depend on the underlying method of data acquisition by the device and are expected to be similar between devices when the same approach and technology are used. However, data reproducibility and repeatability can vary among different devices and even software iterations of the same device.[144]

With rapid changes in SD-OCT hardware and upgrades in the software, clinicians frequently use devices for which limited data are available on repeatability and reproducibility.[310] Estimation of test-retest variability and reproducibility allows for definition of ‘clinically significant’ change so that true change can be differentiated from noise or fluctuation; also, one of the important factors influencing the required optimal frequency of a test to detect true change is the ratio of rates of change to noise.[17, 390] This is especially relevant for monitoring disease progression.

The human retina contains more than one million RGCs on average, but there is significant variability in the number of RGCs among individuals. Nearly 50% of the RGCs in humans are located in the macula.[70] Curcio and Allen found lower variability in the number of RGCs in the macula in contrast to the entire retina.[70] Therefore, macular RGC parameters may demonstrate less variability than cp-RNFL or neuroretinal rim measurements.[282] Several studies have demonstrated that macular RGC metrics have better or similar test-retest repeatability and reproducibility compared to cp-RNFL outcomes.[32, 33, 310, 390] This could be explained, at least partly, by the presence of more non-neural elements, such as large blood vessels, in and around the optic nerve head in contrast to the relatively hypovascular macula.[266] The macular region has also a less complex topography making it less

challenging for automated segmentation. Correct measurement of the cp-RNFL thickness depends on detection of the center of Bruch's membrane opening, which is a challenging task to automate and commonly requires manual adjustment. Centering macular cube measurements is facilitated through fixation by the subject being imaged. Software algorithms can also detect the foveal pit by finding the thinnest part of the retina on macular cube measurements.[310] All the aforementioned factors likely contribute to the high reproducibility of macular thickness measurements.

Studies to date have demonstrated high repeatability and reproducibility of FMT and inner retinal parameters in healthy and glaucoma subjects. With improved image resolution and better segmentation algorithms, it has become possible to measure the thickness of individual retinal layers, in addition to the FMT or inner retinal layers although the superiority of measuring individual layers, specifically the GCL, is yet to be established.[267, 290] Measuring 'targeted layers' such as the GCL or IPL, corresponding to the RGC soma and dendrites, respectively, or the GCC (consisting of GCIPL combined with the mRNFL), have improved diagnostic performance of macular measurements at minimal cost to variability.[26, 32, 81, 96, 98, 109, 196, 225, 247, 266, 282, 303, 310, 370, 390] Several inner macular thickness parameters have been reported to have equal or better repeatability and reproducibility compared to cp-RNFL and ONH measures and it has been suggested that inner macular thickness measurements may be more suitable for monitoring disease progression.[225, 282, 390] Based on the available evidence, a change in the average GCIPL thickness of more than 2 to 4 μm could represent clinically significant glaucoma progression.[196, 310, 390] In a study by Tan et al., global GCC and FMT measurements were highly reproducible with intra-class correlation coefficients ≥0.98 for all measures.[374] Francoz and associates reported that the average GCIPL displayed the highest intraclass correlation coefficient (ICC) and lowest variability among GCIPL parameters, whereas minimum GCIPL thickness demonstrated the lowest ICC and highest variability. Among sectors, the highest ICC and lowest variability was observed in the superotemporal sector.[96] In a longitudinal study, Kim and colleagues reported the superior GCIPL sector to have the highest reproducibility while the inferior sector had the lowest reproducibility.[196] Different OCT devices provide significantly different thickness measurements and their results may be not interchangeable.[225, 284] Miraftabi and coworkers reported variability of macular thickness measurements with Spectralis SD-OCT in a cohort of 102 glaucomatous and 21 healthy eyes.[266] The Posterior Pole Algorithm provides an 8×8 array of 64 superpixels (3°×3° squares) centered on the fovea and aligned to the FoBMO axis. Except for the most nasal and superior rows of superpixels, the remaining superpixels had very high reproducibility for all thickness parameters; the magnitude of the variability did not exceed 3 μm after exclusion of a small percentage of outliers. Age, axial length and image quality did not affect variability; however, poor quality images were excluded from the study and the segmentation was manually corrected.

Hirasawa and colleagues reported on the reproducibility of inner macular layer thickness measurement and the possible influence of different degrees of cyclotorsion.[143] Generally, the reproducibility of mRNFL, GCIPL and GCC measurements was high and GCIPL and GCC had better reproducibility compared to mRNFL; coefficients of variation were less than 1% for all regional and global GCIPL and GCC measures. Ocular cyclotorsion had

minimal effect on the reproducibility of measurements both in healthy and glaucomatous eyes. The authors attributed this finding to the minimal degree of ocular rotation between the 2 sessions of the study. One could anticipate more significant variability with severe cyclotorsion or when the glaucomatous defect is deep and highly localized.

Nouri-Mahdavi and coworkers[298] recently investigated the contribution of within-session variability in macular thickness measurements to total variability and compared longitudinal within-eye variability of central SF relationships to between-individual variability. The investigators demonstrated that that within-session variability contributed most to the total variability of macular thickness measurements (89–92% for GCL, GCIPL, and GCC). In their longitudinal cohort of eyes with severe glaucoma or central damage at baseline, between-individual variability for central macular structural and functional measurements was larger than within-eye variability; the investigators proposed that studying longitudinal within-eye SF relationships could be used to optimize detection of glaucoma progression.

3A. Predictors of variability

Various ocular and operator- or device-related factors could potentially affect macular measurement variability. Variability of GCIPL thickness measurements has been found to be mostly independent of GCIPL thickness, RNFL thickness, visual field defect severity, patient's age, patient's previous training with the test or examiner experience.[96, 196, 266, 310] These findings are in contrast to those related to visual field variability[44, 138, 196] and have significant implications with regard to applicability of macular measurements to monitoring disease progression. Macular thickness measurements were found to have higher repeatability than cp-RNFL thickness in normal children (and adults) and those with glaucoma.[109] There is also evidence that most of the total longitudinal variability of macular thickness measurements (about 89–92%) can be explained by intra-visit variability.[298]

3B. Device- and operator-related sources of variability

Higher image resolution and greater scan density have been shown to improve measurement repeatability.[107, 109, 247, 282] Higher scanning speed, real-time averaging of multiple images and eye tracking technology can reduce the artifacts introduced by eye movement, blinking, poor fixation and off-targeting by the operator and hence, reduce variability.[96, 129, 239, 390] Using the internal fixation target of OCT devices provides higher reproducibility than external fixation targets.[313, 343] Image registration has been an important addition to OCT devices as it can significantly reduce test-retest variability of follow-up exams.[129]

Worsening cataract and cataract surgery can affect reproducibility of macular thickness measurements. Bambo and coworkers found that this effect could be device dependent.[32] The investigators found that the macular thickness increased after cataract surgery when measured with Cirrus HD-OCT, while the change was not significant with Spectralis SD-OCT. The variability of macular thickness measurements improved after cataract surgery with both devices. The superior inner macula demonstrated the least variability before and after surgery.[32] Cataract can significantly reduce the quality and signal strength of OCT images and affect macular thickness measurements; this adverse effect is especially remarkable with cortical and posterior subcapsular cataracts.[92, 288, 388] In another study,

cataract surgery had a similar positive effect on macular measurements in diabetic patients without diabetic retinopathy.[99]

In summary, repeatability and reproducibility of macular OCT thickness measurements are high and are similar or superior to those for ONH and cp-RNFL thickness. Higher image resolution, greater scan density, using the OCT device's internal fixation and removal of cataract improve reproducibility of macular OCT measurements.

IV) Performance of macular OCT imaging for detecting glaucoma progression

Evidence for utility of macular thickness measurements for monitoring glaucoma is slowly accruing but is still sparse.[222, 364, 368, 380] Macular thickness measures demonstrate a strong correlation with visual field sensitivities comparable to that of the cp-RNFL thickness.[301, 352] Also, a strong correlation has been reported between the macular GCIPL layer thickness and estimates of RGC counts.[375, 429] There is evidence suggesting stronger SF relationships between GCIPL with VF sensitivity compared to cp-RNFL in eyes with advanced glaucoma.[195] A caveat for many studies is that they do not consider a ground truth for evaluation of glaucoma progression. Beyond considering functional outcomes as the ground truth for structural measures, which is suboptimal, a ground truth does not exist. Cutoff points for change from tightly controlled studies may not be suitable for detection of glaucoma progression clinically, considering the expected increase in variability and noise for most structural measures under clinical circumstances.[377]

Reproducibility of a given outcome measure is important with regard to its performance for monitoring the disease of interest, since a higher SNR (i.e., less noisy measurements) would provide superior ability for detection of change over time. Reproducibility of various macular thickness parameters has been shown to be high.[143, 198, 282, 374] Both within-session and inter-session reproducibility of SD-OCT parameters are important as far as detection of glaucoma worsening is concerned.[143, 282, 298, 374] In a group of 109 clinically stable glaucoma eyes, Kim and colleagues[196] reported very low inter-session variability for sectoral GCIPL thickness measurements.

Several studies have evaluated the rates of change of inner macular thickness measurements in glaucoma. Rates of GCIPL thinning (Cirrus HD-OCT) have been reported between −0.28 to −0.92 μm/year when all levels of glaucoma damage are considered.[128, 228, 230, 353] Lee et al. investigated rates of GCIPL thinning after an average follow-up of 3 years; the mean rates of change were −0.31 μm/year in normal eyes, −0.49 μm/year in POAG eyes and −1.46 μm/year in eyes with pseudoexfoliation glaucoma.[228] Suda et al. reported an average rate of change of −0.47 μm/year for GCC as measured with RTVue OCT in a longitudinal cohort of glaucoma patients with disease severity ranging from mild to severe (see below).[364] Mohammadzadeh and coworkers[269] investigated longitudinal rates of change for FMT, GCC, GCIPL and GCL in a cohort of glaucoma eyes with central or advanced damage at baseline. Mean rates of change at 5.6° were proportional to average thickness for various macular outcomes of interest (−1.32, −0.76, −0.54, and −0.32 μm/year for FMT, GCC, GCIPL and GCL, respectively). When the proportion of significant negative rates of change

(slope <0 and p <0.05) were compared for structural and functional measures over time, structural changes (GCC) were more likely to be detected over time compared to functional changes (supplemental Figure 1). In another study, Holló and Zhou evaluated rates of change of GCC measured in healthy eyes, treated ocular hypertension and glaucoma patients and reported average rates of −0.53 μm/year, −0.54 μm/year and −0.80 μm/year, respectively.[146] Differences in the macular outcome used, study population, glaucoma severity, type of treatment if any, and length of follow-up could explain differences in the magnitude of the rates of change observed among the different studies.

Progressive macular thinning has been shown to be related to VF progression (see section 2G).[16, 431] Several studies have compared progressive cp-RNFL thinning and FMT or GCIPL thinning for detection of glaucoma progression. Lee and colleagues[222] explored event analysis to detect progression based on average or quadrant RNFL thickness compared to sectoral FMT measurements in a group of mostly normal-tension glaucoma eyes with an average MD of −4.6 dB (range: −1.5 to −8 dB). The main finding was that FMT measurements had higher sensitivity for detection of change at both 95% and 80% specificities regardless of whether the average or quadrant-based cp-RNFL thickness measurements were used. Na and colleagues[380] found that ONH, cp-RNFL, and macular SD-OCT measures all showed faster rates of progression in glaucomatous eyes deteriorating based on VF and ONH findings; the average mean deviation was −4.3 dB in the progressing group as opposed to −0.8 dB in the stable group. Suda and coworkers[364]evaluated longitudinal changes in GCC and cp-RNFL measurements derived from OCT, neuroretinal rim thickness based on Heidelberg Retina Tomography (HRT) and VF indices in 125 eyes with moderately advanced glaucoma (baseline mean MD = −6.2 dB). All measures except HRT parameters showed significant negative trends over time; however, there was poor correlation between VF and structural outcome measures and between structural measures themselves.

Software for detection of glaucoma progression is now commercially available on some OCT devices such as Cirrus HD-OCT's Guided Progression Analysis (GPA). Cirrus' GPA provides event- and trend-based analyses for detection of progressive thinning of the cp-RNFL and macular GCIPL. Event-based analysis seeks differences in GCIPL thickness between follow-up macular images and the 2 baseline images. Performance of GPA to detect progressive GCIPL thinning has been evaluated in a few studies.[162, 353] Shin et al.[353] compared rates of GCIPL and cp-RNFL progression in a group of eyes with a wide range of glaucoma severity. They reported a higher number of progressing eyes based on GCIPL (39%) compared to cp-RNFL (22%) or VFs (25%). The GCIPL rates of progression in eyes deteriorating based on VFs was significantly higher than nonprogressors for eyes with mild (MD ≥−6 dB) or moderate to severe glaucoma (MD <−6 dB), whereas rates of progression for average cp-RNFL were significantly higher in the progressing group only in eyes with mild glaucoma. Hou et al.[162] evaluated serial GCIPL and cp-RNFL thickness maps to detect structural thinning in POAG and normal eyes followed for more than 5 years. The specificity of GCIPL and cp-RNFL GPA was 95.5% and 91.0%, respectively, whereas the agreement between GCIPL and cp-RNFL measures for presence of progressive thinning was only moderate (κ =0.41).

Macular GCIPL and cp-RNFL maps have been integrated to detect glaucoma progression in some studies.[162, 229, 231] Lee et al.[229] compared the performance of integrated cp-RNFL and GCIPL maps from Cirrus HD-OCT (PanoMap) with cp-RNFL and GCIPL GPA to detect glaucoma progression. They found that the wide-field OCT deviation map showed the best sensitivity (83%) and specificity (96%) to detect early glaucomatous structural progression. The topographic pattern of structural progression using PanoMap was evaluated by Lee and colleagues.[231] The location of progression was classified based on Hood et al.'s proposed scheme[158] as within the superior vulnerability zone (SVZ), papillomacular bundle (PMB), macular zone of vulnerability (MZV), and inferoinferior region. They found that when progression was located in the SVZ and inferoinferior areas, only progressive cp-RNFL thinning was evident on Panomap, whereas if progression was detected in the PMB or MZV, concurrent involvement of GCIPL and cp-RNFL was the most common pattern. Shin et al.[354] studied the pattern of progressive GCIPL thinning, evaluating 292 eyes with POAG with a mean follow-up of 6 years. Progressive GCIPL thinning was detected most frequently (25.0%) inferotemporally (average distance of 2.08 mm from the foveal center) and it extended in an arcuate pattern towards the fovea and the optic disc. Widening of GCIPL defects (58.3%) was the most common pattern of progressive GCIPL thinning, followed by deepening of defects (26.4%) and development of new GCIPL defects (20.8%)(Figure 15).

Recent studies have used new strategies to analyze macular OCT images for detecting glaucoma progression. Wu and associates[412] evaluated a 'region-of-interest' (ROI) approach to detect glaucoma progression using Spectralis OCT. Comparison of contiguous regions of GCC thickness that fell below the 1% lower normative limit were used for the automated ROI approach. For the manual ROI approach, they compared changes in manually outlined regions where glaucoma damage was observed or suspected. Both approaches were compared with global GCC thickness changes. Longitudinal SNRs were calculated for progressive changes detected by each of these methods using individualized estimates of test-retest variability and age-related changes. The manual ROI approach performed best for detection of progressive macular GCC changes. Fortune[95] recently proposed that structural changes detected on SD-OCT imaging such as paravascular defects, peripapillary retinoschisis, and pseudo-cysts of the inner nuclear layer are associated with severe and rapid progressing glaucoma.

In summary, rates of change of inner retinal thickness measurements have been shown to be helpful in monitoring glaucoma progression, especially in more severe and advanced glaucoma. There is fair correlation between progressive inner macula thinning and VF progression.

V) Role of macular SD-OCT imaging in advanced glaucoma

The strong correlation of macular SD-OCT thickness measurements with VF sensitivity measures, the high reproducibility of global and regional macular SD-OCT thickness measures, and the preliminary data on their ability to detect disease progression provide proof of concept that macular SD-OCT data may be used to monitor glaucoma especially in advanced stages. Asrani et al. first proposed the potential utility of macular OCT imaging in advanced glaucoma.[25] A few studies have demonstrated that the variability of macular

outcome measures does not significantly increase with worsening glaucoma damage.[266, 310] In the study by Miraftabi and coworkers,[266] the percentage of outliers for GCIPL, a proxy for measurement variability, increased only at very low thickness measurements suggesting a possible confounding effect from segmentation errors near the GCIPL measurement floor.

Detection of structural progression in advanced glaucoma could be challenging due to the floor effect,. The measurement floor or the lowest level macular measurements could reach represents the residual non-neural tissues. Several studies evaluated the performance of different structural measures to detect disease progression in advanced glaucoma. Sung et al.[368] showed that rates of progression for FMT measurements were significantly higher than cp-RNFL rates of changes in progressing eyes with advanced glaucoma; the average baseline mean deviation (MD) was −14 dB in this group. Bowd et al.[49] defined regions of interest for BMO-MRW, GCIPL and cp-RNFL parameters in a group of eyes with moderate to advanced disease (MD equal or worse than −8 dB) based on the variability and measurement floor for each measure. The GCIPL displayed the highest percentage of remaining region of interest (39%) above the measurement floor at baseline compared to BMO-MRW (19%) and cp-RNFL (14%). They concluded that GCIPL thickness might be the most likely structural measure to demonstrate change over time in advanced glaucoma. Belghith and colleagues[39] compared rates of structural progression in 35 eyes (35 patients) with very advanced glaucoma (MD worse than −21 dB) for cp-RNFL, BMO-MRW, and GCIPL thickness to those observed in 46 healthy eyes (30 subjects). Only GCIPL global rates of progression reached statistical significance in eyes with advanced glaucoma. The number of progressing eyes defined as eyes with a rate of change worse than the 5 percentiles of the healthy eyes was 31% for GCIPL, 11% for RNFL, and 6% for BMO-MRW. In a more recent study, Lavinsky and coworkers[215] studied the structural rates of change in 44 eyes with advanced glaucoma, a median MD of −10.2 dB, and an average follow-up of 4 years. In contrast to average cp-RNFL rates of change (0.009 μm/year), average GCIPL (−0.57 μm/year) and average rim area (−0.01 mm^2/year) demonstrated significant changes during the follow-up period. Hammel and colleagues[128] compared global and sectoral rates of cp-RNFL and GCIPL change in a group of normal and glaucoma eyes with varying levels of glaucoma damage. Global cp-RNFL rates of worsening tended to be larger compared to GCIPL rates in early glaucoma. However, in eyes with severe glaucoma (MD <−12 dB), the average normalized GCIPL rates of changes were higher (−1.8%/year) compared to the average RNFL rate of change (−1.1%/year). Miraftabi and coworkers[267] demonstrated that the dynamic range of all macular SD-OCT parameters did not exceed 8–10 dB of total deviation loss. Therefore, the utility of macular parameters lies in the fact that significant macular damage tends to occur relatively later compared to cp-RNFL or neuroretinal rim loss rather than a higher dynamic range. Given the more challenging nature of segmentation of the individual retinal layers in the more advanced stages of glaucoma, it is possible that GCC or FMT measurements would be the preferred outcome measures for detecting progression in the more advanced cases.[230]

In summary, the advantages of macular OCT imaging in advanced glaucoma include higher rates of change compared to other structural modalities, reaching measurement floor later during the course of glaucoma, no significant increase in variability with worsening glaucoma until the end stage, and good correlation with VF sensitivities.

VI) Limitations of Macular OCT imaging

There are limitations for using macular OCT measures for diagnostic purposes in glaucoma. Concurrent retinal diseases could affect the macular structure and inner layers thickness measurements. The influence of co-existing macular pathology needs to be considered. In clinical practice, patients with glaucoma commonly have age-related macular pathologies, which can affect automated segmentation of macular layers. Several published studies manually corrected segmentation, which could have led to underestimation of variability. However, this is not usually practical in clinical setting and real-life data are likely noisier with higher variability. Most repeatability studies were carried out on the same day or over a short period of time and did not truly measure long-term variability;[196] however, a recent study by Nouri-Mahdavi and coworkers found that within-session variability explained most of long-term variability.[298] Another limitation is that all relevant studies excluded poor quality images and those with low signal strength; such images are not uncommon in clinical practice. In a recent study, a total 6% of scans were excluded due to acquisition errors, segmentation artifacts or co-morbid macular pathology.[27] With continuing software updates and hardware upgrades of OCT devices, sufficient data on the variability of measurements made by the most recent technology may not be available;[144, 310] however, reproducibility of OCT devices is only expected to improve as newer technologies provides us with faster and higher resolution image acquisition algorithms. In comparison to cp-RNFL measurements, which sample the entire ganglion cell axonal complement of the eye, at most the central 50% of the RGCs residing in the macula can be evaluated with macular OCT imaging.

VII) Conclusions

Macular OCT imaging is an important diagnostic tool for detection of glaucoma or monitoring the disease and is now widely available worldwide. It focuses on the most important area of the human retina. The central RGCs are the last ones to disappear; hence, given the low variability of macular OCT images and the residual dynamic range, macular OCT imaging may be used in all stages of glaucoma for detection of glaucoma progression including the advanced stages.

VIII) Method of literature search

PubMed and Google Scholar websites were used to search articles with the following keywords and MESH headings: OCT, macula, structure-function, detection, variability, reproducibility, or progression combined with the term ‘glaucoma’ with an ‘and’ logic. The primary search was based only on English articles. In our initial search, we reviewed all the studies up to January 2018. Abstracts were reviewed by the senior author of the study (KNM) and 341 articles were selected for full review. These articles generally covered background history and evolution of macular OCT, factors influencing macular OCT especially axial length and myopia, comparison of OCT devices, glaucoma detection and comparison to other imaging modalities, structure-function relationship in glaucoma, vertical asymmetry, variability and reproducibility of macular OCT, and detection of glaucoma progression. A second search was done for studies published from January 2018

up to July 31, 2019; based on the same methodology, 41 additional articles were selected for further review.

Supplementary Material

Refer to Web version on PubMed Central for supplementary material.

Appendix

The broken stick equation used by Raza et al. is as follows:

$$R = (s_0 - b)T + b \text{ for } T \leq 1.0 \text{ and } R = s_0 \text{ for } T > 1.0,$$

Where,

s_0 is the median of GCIPL thickness in normal subjects at a particular eccentricity,

T is the relative sensitivity, defined as $10^{0.1D}$, and

D is the TD value compared to age-matched controls in dB.

The variable b was estimated as the median of the GCIPL thickness values at locations where the SAP sensitivity was less than −15 dB as previously described and represents measurement floor.

Glossary of all abbreviations

APD	afferent pupillary defect
AUC	area under receiver operating characteristics (ROC) curves
AL	axial length
BCVA	best-corrected visual acuity
BMO	Bruch’s membrane opening
BMO-MRW	Bruch’s membrane opening-minimum rim width
CCT	central corneal thickness
cp-RNFL	circumpapillary retinal nerve fiber layer
DR	diabetic retinopathy
ETDRS	Early Treatment of Diabetic Retinopathy Study
FLV	focal loss volume
FMT	full macular thickness
GCA	Ganglion Cell Analysis

GCL	ganglion cell layer
GCC	ganglion cell complex
GCIPL	ganglion cell/inner plexiform layer
GCCI	Glaucoma Composite Conversion Index
GHT	Glaucoma Hemifield Test
GSDI	glaucoma structural diagnosis index
GMPE	Glaucoma Module Premium Edition
GLV	global loss volume
GPA	Guided Progression Analysis
HRT	Heidelberg Retina Tomograph
IPL	inner plexiform layer
LDF	linear discriminant function
MIRL	macular inner retinal layer
mRNFL	macular retinal nerve fiber layer
MZV	macular zone of vulnerability
MD	mean deviation
mfERG	multifocal electroretinography
mfVEP	multifocal visual evoked potential
OHT	ocular hypertension
OAG	open-angle glaucoma
OCT	optical coherence tomography
ONH	optic nerve head
PERG	pattern electroretinography
PMB	papillomacular bundle
PPA	Posterior Pole Algorithm
PPAA	Posterior Pole Asymmetry Analysis
ROI	region-of-interest
RGC	retinal ganglion cell
RNFL	retinal nerve fiber layer

SNR	signal-to-noise ratio
SD-OCT	spectral-domain optical coherence tomography
SF	structure-function
TD-OCT	time-domain optical coherence tomography
TD	total deviation
VF	visual field
VFI	Visual Field Index
SVZ	superior vulnerability zone

References

1. Cirrus HD-OCT User Manual, 2660021162665 Rev. A. 2016–04:Appendix D1–9.
2. Abegg M, Dysli M, Wolf S, Kowal J, Dufour P, Zinkernagel M. Microcystic macular edema: retrograde maculopathy caused by optic neuropathy. Ophthalmology. 2014;121(1):142–9. [PubMed: 24139122]
3. Aggarwal D, Tan O, Huang D, Sadun AA. Patterns of ganglion cell complex and nerve fiber layer loss in nonarteritic ischemic optic neuropathy by Fourier-domain optical coherence tomography. Invest Ophthalmol Vis Sci. 2012;53(8):4539–45. [PubMed: 22678499]
4. Airaksinen PJ, Drance SM, Douglas GR, Mawson DK, Nieminen H. Diffuse and localized nerve fiber loss in glaucoma. Am J Ophthalmol. 1984;98(5):566–71. [PubMed: 6496612]
5. Ajtony C, Balla Z, Somoskeoy S, Kovacs B. Relationship between visual field sensitivity and retinal nerve fiber layer thickness as measured by optical coherence tomography. Invest Ophthalmol Vis Sci. 2007;48(1):258–63. [PubMed: 17197541]
6. Akashi A, Kanamori A, Ueda K, Inoue Y, Yamada Y, Nakamura M. The Ability of SD-OCT to Differentiate Early Glaucoma With High Myopia From Highly Myopic Controls and Nonhighly Myopic Controls. Invest Ophthalmol Vis Sci. 2015;56(11):6573–80. [PubMed: 26567476]
7. Al-Haddad C, Antonios R, Tamim H, Noureddin B. Interocular symmetry in retinal and optic nerve parameters in children as measured by spectral domain optical coherence tomography. Br J Ophthalmol. 2014;98(4):502–6. [PubMed: 24393664]
8. Alencar LM, Zangwill LM, Weinreb RN, Bowd C, Vizzeri G, Sample PA, et al. Agreement for Detecting Glaucoma Progression with the GDx Guided Progression Analysis, Automated Perimetry, and Optic Disc Photography. Ophthalmology. 2009.
9. Alexandrescu C, Dascalu AM, Panca A, Sescioreanu A, Mitulescu C, Ciuluvica R, et al. Confocal scanning laser ophthalmoscopy in glaucoma diagnosis and management. J Med Life. 2010;3(3):229–34. [PubMed: 20945812]
10. Alluwimi MS, Swanson WH, King BJ. Identifying Glaucomatous Damage to the Macula. Optom Vis Sci. 2018;95(2):96–105. [PubMed: 29370025]
11. Alluwimi MS, Swanson WH, Malinovsky VE. Between-subject variability in asymmetry analysis of macular thickness. Optom Vis Sci. 2014;91(5):484–90. [PubMed: 24727826]
12. Altemir I, Oros D, Elía N, Polo V, Larrosa JM, Pueyo V. Retinal asymmetry in children measured with optical coherence tomography. Am J Ophthalmol. 2013;156(6):1238–43.e1. [PubMed: 24075424]
13. Amini N, Nowroozizadeh S, Cirineo N, Henry S, Chang T, Chou T, et al. Influence of the disc-fovea angle on limits of RNFL variability and glaucoma discrimination. Invest Ophthalmol Vis Sci. 2014;55(11):7332–42. [PubMed: 25301880]
14. Anctil JL, Anderson DR. Early foveal involvement and generalized depression of the visual field in glaucoma. Arch Ophthalmol. 1984;102(3):363–70. [PubMed: 6703983]

15. Andreou PA, Wickremasinghe SS, Asaria RH, Tay E, Franks WA. A comparison of HRT II and GDx imaging for glaucoma detection in a primary care eye clinic setting. Eye (Lond). 2007;21(8):1050–5. [PubMed: 16691256]
16. Anraku A, Enomoto N, Takeyama A, Ito H, Tomita G. Baseline thickness of macular ganglion cell complex predicts progression of visual field loss. Graefes Arch Clin Exp Ophthalmol. 2014;252(1):109–15. [PubMed: 24253499]
17. Araie M Test-retest variability in structural parameters measured with glaucoma imaging devices. Jpn J Ophthalmol. 2013;57(1):1–24. [PubMed: 23138681]
18. Araie M, Murata H, Iwase A, Hangai M, Sugiyama K, Yoshimura N. Differences in Relationship Between Macular Inner Retinal Layer Thickness and Retinal Sensitivity in Eyes With Early and Progressed Glaucoma. Invest Ophthalmol Vis Sci. 2016;57(4):1588–94. [PubMed: 27046122]
19. Arden GB HC. Clinical and experimental evidence that the pattern electroretinogram (PERG) is generated in more proximal retinal layers than the focal electroretinogram (FERG). Ann N Y Acad Sci. 1982 6;388(1):580–601. [PubMed: 6953889]
20. Aref AA, Sayyad FE, Mwanza JC, Feuer WJ, Budenz DL. Diagnostic specificities of retinal nerve fiber layer, optic nerve head, and macular ganglion cell-inner plexiform layer measurements in myopic eyes. J Glaucoma. 2014;23(8):487–93. [PubMed: 23221911]
21. Arintawati P, Sone T, Akita T, Tanaka J, Kiuchi Y. The applicability of ganglion cell complex parameters determined from SD-OCT images to detect glaucomatous eyes. J Glaucoma. 2013;22(9):713–8. [PubMed: 22668975]
22. Asaoka R, Murata H, Hirasawa K, Fujino Y, Matsuura M, Miki A, et al. Using Deep Learning and Transfer Learning to Accurately Diagnose Early-Onset Glaucoma From Macular Optical Coherence Tomography Images. Am J Ophthalmol. 2019;198:136–45. [PubMed: 30316669]
23. Asaoka R, Russell RA, Malik R, Crabb DP, Garway-Heath DF. A novel distribution of visual field test points to improve the correlation between structure-function measurements. Invest Ophthalmol Vis Sci. 2012;53(13):8396–404. [PubMed: 23154456]
24. Asefzadeh B, Cavallerano AA, Fisch BM. Racial differences in macular thickness in healthy eyes. Optom Vis Sci. 2007;84(10):941–5. [PubMed: 18049358]
25. Asrani S, Rosdahl JA, Allingham RR. Novel software strategy for glaucoma diagnosis: asymmetry analysis of retinal thickness. Arch Ophthalmol. 2011;129(9):1205–11. [PubMed: 21911669]
26. Avery RA, Cnaan A, Schuman JS, Chen CL, Glaug NC, Packer RJ, et al. Intra- and inter-visit reproducibility of ganglion cell-inner plexiform layer measurements using handheld optical coherence tomography in children with optic pathway gliomas. Am J Ophthalmol. 2014;158(5):916–23. [PubMed: 25068639]
27. Awadalla MS, Fitzgerald J, Andrew NH, Zhou T, Marshall H, Qassim A, et al. Prevalence and type of artefact with spectral domain optical coherence tomography macular ganglion cell imaging in glaucoma surveillance. PLoS One. 2018;13(12):e0206684. [PubMed: 30517101]
28. Badala F, Nouri-Mahdavi K, Raoof DA, Leeprechanon N, Law SK, Caprioli J. Optic disk and nerve fiber layer imaging to detect glaucoma. Am J Ophthalmol. 2007;144(5):724–32. [PubMed: 17868631]
29. Bagga H, Greenfield DS. Quantitative assessment of structural damage in eyes with localized visual field abnormalities. Am J Ophthalmol. 2004;137(5):797–805. [PubMed: 15126142]
30. Bagga H, Greenfield DS, Knighton RW. Macular symmetry testing for glaucoma detection. J Glaucoma. 2005;14(5):358–63. [PubMed: 16148583]
31. Bambo MP, Cameo B, Hernandez R, Fuentemilla E, Guerri N, Ferrandez B, et al. Diagnostic ability of inner macular layers to discriminate early glaucomatous eyes using vertical and horizontal B-scan posterior pole protocols. PLoS One. 2018;13(6):e0198397. [PubMed: 29879152]
32. Bambo MP, Garcia-Martin E, Otin S, Sancho E, Fuertes I, Herrero R, et al. Influence of cataract surgery on repeatability and measurements of spectral domain optical coherence tomography. Br J Ophthalmol. 2014;98(1):52–8. [PubMed: 24174613]
33. Bambo MP, Guerri N, Ferrandez B, Cameo B, Fuertes I, Polo V, et al. Evaluation of the Macular Ganglion Cell-Inner Plexiform Layer and the Circumpapillary Retinal Nerve Fiber Layer in Early

to Severe Stages of Glaucoma: Correlation with Central Visual Function and Visual Field Indexes. Ophthalmic Res. 2017.

34. Barboni P, Carelli V, Savini G, Carbonelli M, La Morgia C, Sadun AA. Microcystic macular degeneration from optic neuropathy: not inflammatory, not trans-synaptic degeneration. Brain. 2013;136(Pt 7):e239. [PubMed: 23396580]
35. Bedggood P, Nguyen B, Lakkis G, Turpin A, McKendrick AM. Orientation of the Temporal Nerve Fiber Raphe in Healthy and in Glaucomatous Eyes. Invest Ophthalmol Vis Sci. 2017;58(10):4211–7. [PubMed: 28837723]
36. Bedggood P, Tanabe F, McKendrick AM, Turpin A. Automatic identification of the temporal retinal nerve fiber raphe from macular cube data. Biomed Opt Express. 2016;7(10):4043–53. [PubMed: 27867714]
37. Begum VU, Addepalli UK, Yadav RK, Shankar K, Senthil S, Garudadri CS, et al. Ganglion cell-inner plexiform layer thickness of high definition optical coherence tomography in perimetric and preperimetric glaucoma. Invest Ophthalmol Vis Sci. 2014;55(8):4768–75. [PubMed: 25015361]
38. Belghith A, Balasubramanian M, Bowd C, Weinreb RN, Zangwill LM. A unified framework for glaucoma progression detection using Heidelberg Retina Tomograph images. Comput Med Imaging Graph. 2014;38(5):411–20. [PubMed: 24709053]
39. Belghith A, Medeiros FA, Bowd C, Liebmann JM, Girkin CA, Weinreb RN, et al. Structural Change Can Be Detected in Advanced-Glaucoma Eyes. Invest Ophthalmol Vis Sci. 2016;57(9):Oct511–8. [PubMed: 27454660]
40. Besada E, Frauens BJ, Makhlouf R, Shechtman D, Rodman J, Demeritt M, et al. More sensitive correlation of afferent pupillary defect with ganglion cell complex. J Optom. 2018;11(2):75–85. [PubMed: 28676353]
41. Bhargava P, Calabresi PA. The expanding spectrum of aetiologies causing retinal microcystic macular change. Brain. 2013;136(Pt 11):3212–4. [PubMed: 24131594]
42. Blanks JC, Torigoe Y, Hinton DR, Blanks RH. Retinal pathology in Alzheimer's disease. I. Ganglion cell loss in foveal/parafoveal retina. Neurobiol Aging. 1996;17(3):377–84. [PubMed: 8725899]
43. Blumberg DM, Dale E, Pensec N, Cioffi GA, Radcliffe N, Pham M, et al. Discrimination of Glaucoma Patients From Healthy Individuals Using Combined Parameters From Spectral-domain Optical Coherence Tomography in an African American Population. J Glaucoma. 2016;25(3):e196–203. [PubMed: 26066503]
44. Blumenthal EZ, Sample PA, Berry CC, Lee AC, Girkin CA, Zangwill L, et al. Evaluating several sources of variability for standard and SWAP visual fields in glaucoma patients, suspects, and normals. Ophthalmology. 2003;110(10):1895–902. [PubMed: 14522760]
45. Blumenthal EZ, Sapir-Pichhadze R. Misleading statistical calculations in far-advanced glaucomatous visual field loss. Ophthalmology. 2003;110(1):196–200. [PubMed: 12511366]
46. Blumenthal EZ, Williams JM, Weinreb RN, Girkin CA, Berry CC, Zangwill LM. Reproducibility of nerve fiber layer thickness measurements by use of optical coherence tomography. Ophthalmology. 2000;107(12):2278–82. [PubMed: 11097610]
47. Bogunović H, Kwon YH, Rashid A, Lee K, Critser DB, Garvin MK, et al. Relationships of retinal structure and humphrey 24–2 visual field thresholds in patients with glaucoma. Invest Ophthalmol Vis Sci. 2015;56(1):259–71.
48. Bowd C, Zangwill LM, Berry CC, Blumenthal EZ, Vasile C, Sanchez-Galeana C, et al. Detecting early glaucoma by assessment of retinal nerve fiber layer thickness and visual function. Invest Ophthalmol Vis Sci. 2001;42(9):1993–2003. [PubMed: 11481263]
49. Bowd C, Zangwill LM, Weinreb RN, Medeiros FA, Belghith A. Estimating Optical Coherence Tomography Structural Measurement Floors to Improve Detection of Progression in Advanced Glaucoma. Am J Ophthalmol. 2017;175:37–44. [PubMed: 27914978]
50. Brazerol J, Iliev ME, Hohn R, Frankl S, Grabe H, Abegg M. Retrograde Maculopathy in Patients With Glaucoma. J Glaucoma. 2017;26(5):423–9. [PubMed: 28169924]
51. Burggraaff MC, Trieu J, de Vries-Knoppert WA, Balk L, Petzold A. The clinical spectrum of microcystic macular edema. Invest Ophthalmol Vis Sci. 2014;55(2):952–61. [PubMed: 24398089]

52. Caprioli J The importance of rates in glaucoma. Am J Ophthalmol. 2008;145(2):191–2. [PubMed: 18222187]
53. Caprioli J, Coleman AL. Intraocular pressure fluctuation a risk factor for visual field progression at low intraocular pressures in the advanced glaucoma intervention study. Ophthalmology. 2008;115(7):1123–9 e3. [PubMed: 18082889]
54. Carbonelli M, La Morgia C, Savini G, Cascavilla ML, Borrelli E, Chicani F, et al. Macular Microcysts in Mitochondrial Optic Neuropathies: Prevalence and Retinal Layer Thickness Measurements. PLoS One. 2015;10(6):e0127906. [PubMed: 26047507]
55. Cartwright MJ, Anderson DR. Correlation of asymmetric damage with asymmetric intraocular pressure in normal-tension glaucoma (low-tension glaucoma). Arch Ophthalmol. 1988;106(7):898–900. [PubMed: 3390051]
56. Cense BNN, Chen TC, Pierce MC, Yun SH, Park BH, Bouma BE, Tearney GJ, De Boer JF. Ultrahigh-resolution high-speed retinal imaging using spectral-domain optical coherence tomography. Opt Express. 2004 5 31;12(11):2435–47. [PubMed: 19475080]
57. Charalel RA, Lin HS, Singh K. Glaucoma screening using relative afferent pupillary defect. J Glaucoma. 2014;23(3):169–73. [PubMed: 23296370]
58. Chauhan BC, Sharpe GP, Hutchison DM. Imaging of the Temporal Raphe with Optical Coherence Tomography. Ophthalmology. 2014.
59. Chauhan BC, Vianna JR, Sharpe GP, Demirel S, Girkin CA, Mardin CY, et al. Differential Effects of Aging in the Macular Retinal Layers, Neuroretinal Rim, and Peripapillary Retinal Nerve Fiber Layer. Ophthalmology. 2019.
60. Chen MJ, Chang YF, Kuo YS, Hsu CC, Ko YC, Liu CJ. Macular ganglion cell-inner plexiform vs retinal nerve fiber layer measurement to detect early glaucoma with superior or inferior hemifield defects. J Chin Med Assoc. 2019;82(4):335–9. [PubMed: 30946212]
61. Chen MJ, Yang HY, Chang YF, Hsu CC, Ko YC, Liu CJ. Diagnostic ability of macular ganglion cell asymmetry in Preperimetric Glaucoma. BMC Ophthalmol. 2019;19(1):12. [PubMed: 30621639]
62. Chen S, McKendrick AM, Turpin A. Choosing two points to add to the 24–2 pattern to better describe macular visual field damage due to glaucoma. Br J Ophthalmol. 2015;99(9):1236–9. [PubMed: 25802251]
63. Chen TC, Hoguet A, Junk AK, Nouri-Mahdavi K, Radhakrishnan S, Takusagawa HL, et al. Spectral-Domain OCT: Helping the Clinician Diagnose Glaucoma: A Report by the American Academy of Ophthalmology. Ophthalmology. 2018;125(11):1817–27. [PubMed: 30322450]
64. Chew SS, Cunnningham WJ, Gamble GD, Danesh-Meyer HV. Retinal nerve fiber layer loss in glaucoma patients with a relative afferent pupillary defect. Invest Ophthalmol Vis Sci. 2010;51(10):5049–53. [PubMed: 20445112]
65. Chien JL, Ghassibi MP, Patthanathamrongkasem T, Abumasmah R, Rosman MS, Skaat A, et al. Glaucoma Diagnostic Capability of Global and Regional Measurements of Isolated Ganglion Cell Layer and Inner Plexiform Layer. J Glaucoma. 2017;26(3):208–15. [PubMed: 27811573]
66. Choi YJ, Jeoung JW, Park KH, Kim DM. Glaucoma detection ability of ganglion cell-inner plexiform layer thickness by spectral-domain optical coherence tomography in high myopia. Invest Ophthalmol Vis Sci. 2013;54(3):2296–304. [PubMed: 23462754]
67. Choi YJ, Jeoung JW, Park KH, Kim DM. Clinical Use of an Optical Coherence Tomography Linear Discriminant Function for Differentiating Glaucoma From Normal Eyes. J Glaucoma. 2016;25(3):e162–9. [PubMed: 25580887]
68. Cifuentes-Canorea P, Ruiz-Medrano J, Gutierrez-Bonet R, Peña-Garcia P, Saenz-Frances F, Garcia-Feijoo J, et al. Analysis of inner and outer retinal layers using spectral domain optical coherence tomography automated segmentation software in ocular hypertensive and glaucoma patients. PLoS One. 2018;13(4):e0196112. [PubMed: 29672563]
69. Coleman AL. Glaucoma. The Lancet. 1999;354(9192):1803–10.
70. Curcio CA, Allen KA. Topography of ganglion cells in human retina. J Comp Neurol. 1990;300(1):5–25. [PubMed: 2229487]

71. Dagdelen K, Dirican E. The assessment of structural changes on optic nerve head and macula in primary open angle glaucoma and ocular hypertension. Int J Ophthalmol. 2018;11(10):1631–7. [PubMed: 30364206]
72. Dalgliesh JD, Tariq YM, Burlutsky G, Mitchell P. Symmetry of retinal parameters measured by spectral-domain OCT in normal young adults. J Glaucoma. 2015;24(1):20–4. [PubMed: 23459201]
73. Daneshvar R, Yarmohammadi A, Alizadeh R, Henry S, Law SK, Caprioli J, et al. Prediction of Glaucoma Progression with Structural Parameters: Comparison of Optical Coherence Tomography and Clinical Disc Parameters. Am J Ophthalmol. 2019.
74. Dascalu AM, Cherecheanu AP, Stana D, Voinea L, Ciuluvica R, Savlovschi C, et al. Stereometric parameters change vs. Topographic Change Analysis (TCA) agreement in Heidelberg Retina Tomography III (HRT-3) early detection of clinical significant glaucoma progression. J Med Life. 2014;7(4):555–7. [PubMed: 25713621]
75. Dave P, Jethani J, Shah J. Asymmetry of Retinal Nerve Fiber Layer and Posterior Pole Asymmetry Analysis Parameters of Spectral Domain Optical Coherence Tomography in Children. Semin Ophthalmol. 2016:0.
76. Dave P, Shah J. Diagnostic accuracy of posterior pole asymmetry analysis parameters of spectralis optical coherence tomography in detecting early unilateral glaucoma. Indian J Ophthalmol. 2015;63(11):837–42. [PubMed: 26669335]
77. De Boer JF CB, Park BH, Pierce MC, Tearney GJ, Bouma BE. Improved signal-to-noise ratio in spectral-domain compared with time-domain optical coherence tomography. Optics letters. 2003 11 1;28(21):2067–9. [PubMed: 14587817]
78. De Moraes CG, Hood DC, Thenappan A, Girkin CA, Medeiros FA, Weinreb RN, et al. 24–2 Visual Fields Miss Central Defects Shown on 10–2 Tests in Glaucoma Suspects, Ocular Hypertensives, and Early Glaucoma. Ophthalmology. 2017;124(10):1449–56. [PubMed: 28551166]
79. De Moraes CG, Juthani VJ, Liebmann JM, Teng CC, Tello C, Susanna R Jr., et al. Risk factors for visual field progression in treated glaucoma. Arch Ophthalmol. 2011;129(5):562–8. [PubMed: 21555607]
80. De Moraes CG, Muhammad H, Kaur K, Wang D, Ritch R, Hood DC. Interindividual Variations in Foveal Anatomy and Artifacts Seen on Inner Retinal Probability Maps from Spectral Domain OCT Scans of the Macula. Transl Vis Sci Technol. 2018;7(2):4.
81. DeBuc DC, Somfai GM, Ranganathan S, Tatrai E, Ferencz M, Puliafito CA. Reliability and reproducibility of macular segmentation using a custom-built optical coherence tomography retinal image analysis software. J Biomed Opt. 2009;14(6):064023. [PubMed: 20059261]
82. Demirkaya N, van Dijk HW, van Schuppen SM, Abramoff MD, Garvin MK, Sonka M, et al. Effect of age on individual retinal layer thickness in normal eyes as measured with spectral-domain optical coherence tomography. Invest Ophthalmol Vis Sci. 2013;54(7):4934–40. [PubMed: 23761080]
83. Denniss J, Turpin A, McKendrick AM. Relating optical coherence tomography to visual fields in glaucoma: structure-function mapping, limitations and future applications. Clin Exp Optom. 2018.
84. Desatnik H, Quigley HA, Glovinsky Y. Study of central retinal ganglion cell loss in experimental glaucoma in monkey eyes. J Glaucoma. 1996;5(1):46–53. [PubMed: 8795733]
85. Distante P, Lombardo S, Verticchio Vercellin AC, Raimondi M, Rolando M, Tinelli C, et al. Structure/Function relationship and retinal ganglion cells counts to discriminate glaucomatous damages. BMC Ophthalmol. 2015;15:185. [PubMed: 26711893]
86. Dong ZM, Wollstein G, Schuman JS. Clinical Utility of Optical Coherence Tomography in Glaucoma. Invest Ophthalmol Vis Sci. 2016;57(9):OCT556–67. [PubMed: 27537415]
87. Drasdo N, Millican CL, Katholi CR, Curcio CA. The length of Henle fibers in the human retina and a model of ganglion receptive field density in the visual field. Vision Res. 2007;47(22):2901–11. [PubMed: 17320143]
88. Drexler W, Fujimoto JG. State-of-the-art retinal optical coherence tomography. Prog Retin Eye Res. 2008;27(1):45–88. [PubMed: 18036865]

89. Duan XR, Liang YB, Friedman DS, Sun LP, Wong TY, Tao QS, et al. Normal macular thickness measurements using optical coherence tomography in healthy eyes of adult Chinese persons: the Handan Eye Study. Ophthalmology. 2010;117(8):1585–94. [PubMed: 20472290]

90. Edlinger FSM, Schrems-Hoesl LM, Mardin CY, Laemmer R, Kruse FE, Schrems WA. Structural changes of macular inner retinal layers in early normal-tension and high-tension glaucoma by spectral-domain optical coherence tomography. Graefes Arch Clin Exp Ophthalmol. 2018;256(7):1245–56. [PubMed: 29523993]

91. Ehrlich AC, Raza AS, Ritch R, Hood DC. Modifying the conventional visual field test pattern to improve the detection of early glaucomatous defects in the central 10°. Transl Vis Sci Technol. 2014;3(6):6.

92. Esmaeelpour M, Povazay B, Hermann B, Hofer B, Kajic V, Kapoor K, et al. Three-dimensional 1060-nm OCT: choroidal thickness maps in normal subjects and improved posterior segment visualization in cataract patients. Invest Ophthalmol Vis Sci. 2010;51(10):5260–6. [PubMed: 20445110]

93. Fatehi N, Nowroozizadeh S, Henry S, Coleman AL, Caprioli J, Nouri-Mahdavi K. Association of Structural and Functional Measures With Contrast Sensitivity in Glaucoma. Am J Ophthalmol. 2017;178:129–39. [PubMed: 28342719]

94. Fishman RS. Optic disc asymmetry. A sign of ocular hypertension. Arch Ophthalmol. 1970;84(5):590–4. [PubMed: 5478884]

95. Fortune B and Pulling Tugging on the Retina: Mechanical Impact of Glaucoma Beyond the Optic Nerve Head. Invest Ophthalmol Vis Sci. 2019;60(1):26–35. [PubMed: 30601928]

96. Francoz M, Fenolland JR, Giraud JM, El Chehab H, Sendon D, May F, et al. Reproducibility of macular ganglion cell-inner plexiform layer thickness measurement with cirrus HD-OCT in normal, hypertensive and glaucomatous eyes. Br J Ophthalmol. 2014;98(3):322–8. [PubMed: 24307717]

97. Frishman LJ, Shen FF, Du L, Robson JG, Harwerth RS, Smith E, et al. The scotopic electroretinogram of macaque after retinal ganglion cell loss from experimental glaucoma. Invest Ophthalmol Vis Sci. 1996;37(1):125–41. [PubMed: 8550316]

98. Garas A, Vargha P, Hollo G. Reproducibility of retinal nerve fiber layer and macular thickness measurement with the RTVue-100 optical coherence tomograph. Ophthalmology. 2010;117(4):738–46. [PubMed: 20079538]

99. Garcia-Martin E, Fernandez J, Gil-Arribas L, Polo V, Larrosa JM, Otin S, et al. Effect of cataract surgery on optical coherence tomography measurements and repeatability in patients with non-insulin-dependent diabetes mellitus. Invest Ophthalmol Vis Sci. 2013;54(8):5303–12. [PubMed: 23860762]

100. Gardiner SK, Johnson CA, Demirel S. Factors predicting the rate of functional progression in early and suspected glaucoma. Invest Ophthalmol Vis Sci. 2012;53(7):3598–604. [PubMed: 22570353]

101. Garg A, Hood DC, Pensec N, Liebmann JM, Blumberg DM. Macular Damage, as Determined by Structure-Function Staging, Is Associated With Worse Vision-related Quality of Life in Early Glaucoma. Am J Ophthalmol. 2018;194:88–94. [PubMed: 30053467]

102. Garway-Heath DF, Caprioli J, Fitzke FW, Hitchings RA. Scaling the hill of vision: the physiological relationship between light sensitivity and ganglion cell numbers. Invest Ophthalmol Vis Sci. 2000;41(7):1774–82. [PubMed: 10845598]

103. Garway-Heath DF, Holder GE, Fitzke FW, Hitchings RA. Relationship between electrophysiological, psychophysical, and anatomical measurements in glaucoma. Invest Ophthalmol Vis Sci. 2002;43(7):2213–20. [PubMed: 12091419]

104. Garway-Heath DF, Poinoosawmy D, Fitzke FW, Hitchings RA. Mapping the visual field to the optic disc in normal tension glaucoma eyes. Ophthalmology. 2000;107(10):1809–15. [PubMed: 11013178]

105. Garway–Heath DF, Caprioli J, Fitzke FW, Hitchings RA. Scaling the Hill of Vision: The Physiological Relationship between Light Sensitivity and Ganglion Cell Numbers. Invest Ophthalmol Vis Sci. 2000;41(7):1774–82. [PubMed: 10845598]

106. GE H Significance of abnormal pattern electroretinography in anterior visual pathway dysfunction. Br J Ophthalmol. 1987 3 1;71(3):166–71. [PubMed: 3828269]

107. Ge L, Yuan Y, Shen M, Tao A, Wang J, Lu F. The role of axial resolution of optical coherence tomography on the measurement of corneal and epithelial thicknesses. Invest Ophthalmol Vis Sci. 2013;54(1):746–55. [PubMed: 23139281]

108. Gelfand JM, Nolan R, Schwartz DM, Graves J, Green AJ. Microcystic macular oedema in multiple sclerosis is associated with disease severity. Brain. 2012;135(Pt 6):1786–93. [PubMed: 22539259]

109. Ghasia FF, El-Dairi M, Freedman SF, Rajani A, Asrani S. Reproducibility of spectral-domain optical coherence tomography measurements in adult and pediatric glaucoma. J Glaucoma. 2015;24(1):55–63. [PubMed: 23722865]

110. Ghassabi Z, Nguyen AH, Amini N, Henry S, Caprioli J, Nouri-Mahdavi K. The Fovea-BMO Axis Angle and Macular Thickness Vertical Asymmetry Across The Temporal Raphe. J Glaucoma. 2018;27(11):993–8. [PubMed: 30180019]

111. Gills JP Jr WJ. Degeneration of the inner nuclear layer of the retina following lesions of the optic nerve. . Trans Am Ophthalmol Soc. 1966:64:6.

112. Giovannini A, Amato G, Mariotti C. The macular thickness and volume in glaucoma: an analysis in normal and glaucomatous eyes using OCT. Acta Ophthalmol Scand Suppl. 2002;236:34–6. [PubMed: 12390129]

113. Girkin CA, Liebmann J, Fingeret M, Greenfield DS, Medeiros F. The effects of race, optic disc area, age, and disease severity on the diagnostic performance of spectral-domain optical coherence tomography. Invest Ophthalmol Vis Sci. 2011;52(9):6148–53. [PubMed: 21421879]

114. Girkin CA, McGwin G Jr., Sinai MJ, Sekhar GC, Fingeret M, Wollstein G, et al. Variation in optic nerve and macular structure with age and race with spectral-domain optical coherence tomography. Ophthalmology. 2011;118(12):2403–8. [PubMed: 21907415]

115. Glovinsky Y, Quigley HA, Pease ME. Foveal ganglion cell loss is size dependent in experimental glaucoma. Invest Ophthalmol Vis Sci. 1993;34(2):395–400. [PubMed: 8440594]

116. Gonzalez-Garcia AO, Vizzeri G, Bowd C, Medeiros FA, Zangwill LM, Weinreb RN. Reproducibility of RTVue retinal nerve fiber layer thickness and optic disc measurements and agreement with Stratus optical coherence tomography measurements. Am J Ophthalmol. 2009;147(6):1067–74, 74 e1. [PubMed: 19268891]

117. Gonzalez-Hernandez M, Pablo LE, Armas-Dominguez K, de la Vega RR, Ferreras A, de la Rosa MG. Structure-function relationship depends on glaucoma severity. Br J Ophthalmol. 2009;93(9):1195–9. [PubMed: 19493858]

118. Govetto A, Su D, Farajzadeh M, Megerdichian A, Platner E, Ducournau Y, et al. Microcystoid Macular Changes in Association With Idiopathic Epiretinal Membranes in Eyes With and Without Glaucoma: Clinical Insights. Am J Ophthalmol. 2017;181:156–65. [PubMed: 28673749]

119. Greaney MJ, Hoffman DC, Garway-Heath DF, Nakla M, Coleman AL, Caprioli J. Comparison of optic nerve imaging methods to distinguish normal eyes from those with glaucoma. Invest Ophthalmol Vis Sci. 2002;43(1):140–5. [PubMed: 11773024]

120. Greenfield DS, Bagga H, Knighton RW. Macular thickness changes in glaucomatous optic neuropathy detected using optical coherence tomography. Arch Ophthalmol. 2003;121(1):41–6. [PubMed: 12523883]

121. Greenfield DS WR. Role of optic nerve imaging in glaucoma clinical practice and clinical trials. Am J Ophthalmol. 2008 4 1;145(4):598–603. [PubMed: 18295183]

122. Grewal DS, Tanna AP. Diagnosis of glaucoma and detection of glaucoma progression using spectral domain optical coherence tomography. Curr Opin Ophthalmol. 2013;24(2):150–61. [PubMed: 23328662]

123. Grover S, Murthy RK, Brar VS, Chalam KV. Normative data for macular thickness by high-definition spectral-domain optical coherence tomography (spectralis). Am J Ophthalmol. 2009;148(2):266–71. [PubMed: 19427616]

124. Guedes V, Schuman JS, Hertzmark E, Wollstein G, Correnti A, Mancini R, et al. Optical coherence tomography measurement of macular and nerve fiber layer thickness in normal and glaucomatous human eyes. Ophthalmology. 2003;110(1):177–89. [PubMed: 12511364]

125. Gupta D, Asrani S. Macular thickness analysis for glaucoma diagnosis and management. Taiwan J Ophthalmol. 2016;6(1):3–7. [PubMed: 29018702]
126. Gürses-Özden RTC, Vessani R, Zafar S, Liebmann JM, Ritch R. Macular and retinal nerve fiber layer thickness measurement reproducibility using optical coherence tomography (OCT-3). J Glaucoma. 2004 6 1;13(3):238–44. [PubMed: 15118470]
127. Haleem MS, Han L, Hemert J, Fleming A, Pasquale LR, Silva PS, et al. Regional Image Features Model for Automatic Classification between Normal and Glaucoma in Fundus and Scanning Laser Ophthalmoscopy (SLO) Images. J Med Syst. 2016;40(6):132. [PubMed: 27086033]
128. Hammel N, Belghith A, Weinreb RN, Medeiros FA, Mendoza N, Zangwill LM. Comparing the Rates of Retinal Nerve Fiber Layer and Ganglion Cell-Inner Plexiform Layer Loss in Healthy Eyes and in Glaucoma Eyes. Am J Ophthalmol. 2017;178:38–50. [PubMed: 28315655]
129. Hanumunthadu D, Ilginis T, Restori M, Sagoo MS, Tufail A, Balaggan KS, et al. Repeatability of swept-source optical coherence tomography retinal and choroidal thickness measurements in neovascular age-related macular degeneration. Br J Ophthalmol. 2017;101(5):603–8. [PubMed: 27491359]
130. Harman A, Abrahams B, Moore S, Hoskins R. Neuronal density in the human retinal ganglion cell layer from 16–77 years. Anat Rec. 2000;260(2):124–31. [PubMed: 10993949]
131. Harwerth RS, Carter-Dawson L, Shen F, Smith EL 3rd, Crawford ML. Ganglion cell losses underlying visual field defects from experimental glaucoma. Invest Ophthalmol Vis Sci. 1999;40(10):2242–50. [PubMed: 10476789]
132. Harwerth RS, Carter-Dawson L, Smith EL, Barnes G, Holt WF, Crawford ML. Neural losses correlated with visual losses in clinical perimetry. Invest Ophthalmol Vis Sci. 2004;45(9):3152–60. [PubMed: 15326134]
133. Harwerth RS, Vilupuru AS, Rangaswamy NV, Smith EL. The relationship between nerve fiber layer and perimetry measurements. Invest Ophthalmol Vis Sci. 2007;48(2):763–73. [PubMed: 17251476]
134. Harwerth RS, Wheat JL. Modeling the effects of aging on retinal ganglion cell density and nerve fiber layer thickness. Graefes Arch Clin Exp Ophthalmol. 2008;246(2):305–14. [PubMed: 17934750]
135. Harwerth RS, Wheat JL, Fredette MJ, Anderson DR. Linking structure and function in glaucoma. Prog Retin Eye Res. 2010;29(4):249–71. [PubMed: 20226873]
136. Harwerth RS, Wheat JL, Rangaswamy NV. Age-related losses of retinal ganglion cells and axons. Invest Ophthalmol Vis Sci. 2008;49(10):4437–43. [PubMed: 18539947]
137. Hasegawa T, Akagi T, Yoshikawa M, Suda K, Yamada H, Kimura Y, et al. Microcystic Inner Nuclear Layer Changes and Retinal Nerve Fiber Layer Defects in Eyes with Glaucoma. PLoS One. 2015;10(6):e0130175. [PubMed: 26066021]
138. Heijl A, Lindgren A, Lindgren G. Test-retest variability in glaucomatous visual fields. Am J Ophthalmol. 1989;108(2):130–5. [PubMed: 2757094]
139. Heijl A, Patella VM, Chong LX, Iwase A, Leung CK, Tuulonen A, et al. A New SITA Perimetric Threshold Testing Algorithm: Construction and a Multicenter Clinical Study. Am J Ophthalmol. 2019;198:154–65. [PubMed: 30336129]
140. Hernandez R, Burr JM, Vale L, Azuara-Blanco A, Cook JA, Banister K, et al. Monitoring ocular hypertension, how much and how often? A cost-effectiveness perspective. Br J Ophthalmol. 2016;100(9):1263–8. [PubMed: 26659710]
141. Hess DB, Asrani SG, Bhide MG, Enyedi LB, Stinnett SS, Freedman SF. Macular and retinal nerve fiber layer analysis of normal and glaucomatous eyes in children using optical coherence tomography. Am J Ophthalmol. 2005;139(3):509–17. [PubMed: 15767062]
142. Higashide T, Ohkubo S, Hangai M, Ito Y, Shimada N, Ohno-Matsui K, et al. Influence of Clinical Factors and Magnification Correction on Normal Thickness Profiles of Macular Retinal Layers Using Optical Coherence Tomography. PLoS One. 2016;11(1):e0147782. [PubMed: 26814541]
143. Hirasawa H, Araie M, Tomidokoro A, Saito H, Iwase A, Ohkubo S, et al. Reproducibility of thickness measurements of macular inner retinal layers using SD-OCT with or without correction of ocular rotation. Invest Ophthalmol Vis Sci. 2013;54(4):2562–70. [PubMed: 23493298]

144. Hollo G, Naghizadeh F. Influence of a new software version of the RTVue-100 optical coherence tomograph on the detection of glaucomatous structural progression. Eur J Ophthalmol. 2015;25(5):410–5. [PubMed: 25684156]

145. Hollo G, Naghizadeh F, Vargha P. Accuracy of macular ganglion-cell complex thickness to total retina thickness ratio to detect glaucoma in white Europeans. J Glaucoma. 2014;23(8):e132–7. [PubMed: 24247997]

146. Hollo G, Zhou Q. Evaluation of Retinal Nerve Fiber Layer Thickness and Ganglion Cell Complex Progression Rates in Healthy, Ocular Hypertensive, and Glaucoma Eyes With the Avanti RTVue-XR Optical Coherence Tomograph Based on 5-Year Follow-up. J Glaucoma. 2016;25(10):e905–e9. [PubMed: 26950575]

147. Hong EH, Shin YU, Kang MH, Cho H, Seong M. Wide scan imaging with swept-source optical coherent tomography for glaucoma diagnosis. PLoS One. 2018;13(4):e0195040. [PubMed: 29621263]

148. Hood DC. Relating retinal nerve fiber thickness to behavioral sensitivity in patients with glaucoma: application of a linear model. J Opt Soc Am A Opt Image Sci Vis. 2007;24(5):1426–30. [PubMed: 17429489]

149. Hood DC. Improving our understanding, and detection, of glaucomatous damage: An approach based upon optical coherence tomography (OCT). Prog Retin Eye Res. 2017;57:46–75. [PubMed: 28012881]

150. Hood DC, Anderson SC, Wall M, Kardon RH. Structure versus function in glaucoma: an application of a linear model. Invest Ophthalmol Vis Sci. 2007;48(8):3662–8. [PubMed: 17652736]

151. Hood DC, Cho J, Raza AS, Dale EA, Wang M. Reliability of a computer-aided manual procedure for segmenting optical coherence tomography scans. Optom Vis Sci. 2011;88(1):113–23. [PubMed: 21076358]

152. Hood DC, De Cuir N, Blumberg DM, Liebmann JM, Jarukasetphon R, Ritch R, et al. A Single Wide-Field OCT Protocol Can Provide Compelling Information for the Diagnosis of Early Glaucoma. Transl Vis Sci Technol. 2016;5(6):4.

153. Hood DC, De Moraes CG. Four Questions for Every Clinician Diagnosing and Monitoring Glaucoma. J Glaucoma. 2018;27(8):657–64. [PubMed: 29917000]

154. Hood DC, Kardon RH. A framework for comparing structural and functional measures of glaucomatous damage. Prog Retin Eye Res. 2007;26(6):688–710. [PubMed: 17889587]

155. Hood DC, Nguyen M, Ehrlich AC, Raza AS, Sliesoraityte I, De Moraes CG, et al. A Test of a Model of Glaucomatous Damage of the Macula With High-Density Perimetry: Implications for the Locations of Visual Field Test Points. Transl Vis Sci Technol. 2014;3(3):5.

156. Hood DC RA. Method for comparing visual field defects to local RNFL and RGC damage seen on frequency domain OCT in patients with glaucoma. Biomedical optics express. 2011 5 1;2(5):1097–105. [PubMed: 21559122]

157. Hood DC, Raza AS, de Moraes CG, Johnson CA, Liebmann JM, Ritch R. The Nature of Macular Damage in Glaucoma as Revealed by Averaging Optical Coherence Tomography Data. Transl Vis Sci Technol. 2012;1(1):3.

158. Hood DC, Raza AS, de Moraes CG, Liebmann JM, Ritch R. Glaucomatous damage of the macula. Prog Retin Eye Res. 2013;32:1–21. [PubMed: 22995953]

159. Hood DC, Raza AS, de Moraes CG, Odel JG, Greenstein VC, Liebmann JM, et al. Initial arcuate defects within the central 10 degrees in glaucoma. Invest Ophthalmol Vis Sci. 2011;52(2):940–6. [PubMed: 20881293]

160. Hood DC, Slobodnick A, Raza AS, de Moraes CG, Teng CC, Ritch R. Early glaucoma involves both deep local, and shallow widespread, retinal nerve fiber damage of the macular region. Invest Ophthalmol Vis Sci. 2014;55(2):632–49. [PubMed: 24370831]

161. Hood DC XL, Thienprasiddhi P, Greenstein VC, Odel JG, Grippo TM, Liebmann JM, Ritch R. The pattern electroretinogram in glaucoma patients with confirmed visual field deficits. Invest Ophthalmol Vis Sci. 2005 7 1;46(7):2411–8. [PubMed: 15980229]

162. Hou HW, Lin C, Leung CK. Integrating Macular Ganglion Cell Inner Plexiform Layer and Parapapillary Retinal Nerve Fiber Layer Measurements to Detect Glaucoma Progression. Ophthalmology. 2018;125(6):822–31. [PubMed: 29433852]
163. Hua R, Gangwani R, Guo L, McGhee S, Ma X, Li J, et al. Detection of preperimetric glaucoma using Bruch membrane opening, neural canal and posterior pole asymmetry analysis of optical coherence tomography. Sci Rep. 2016;6:21743. [PubMed: 26883374]
164. Huang G, Gast TJ, Burns SA. In-vivo Adaptive Optics imaging of the temporal raphe and its relationship to the optic disc and fovea in the human retina. Invest Ophthalmol Vis Sci. 2014.
165. Huang JY, Pekmezci M, Mesiwala N, Kao A, Lin S. Diagnostic power of optic disc morphology, peripapillary retinal nerve fiber layer thickness, and macular inner retinal layer thickness in glaucoma diagnosis with fourier-domain optical coherence tomography. J Glaucoma. 2011;20(2):87–94. [PubMed: 20577117]
166. Hung KC, Wu PC, Poon YC, Chang HW, Lai IC, Tsai JC, et al. Macular Diagnostic Ability in OCT for Assessing Glaucoma in High Myopia. Optom Vis Sci. 2016;93(2):126–35. [PubMed: 26704143]
167. Huo YJ, Guo Y, Li L, Wang HZ, Wang YX, Thomas R, et al. Age-related changes in and determinants of macular ganglion cell-inner plexiform layer thickness in normal Chinese adults. Clin Exp Ophthalmol. 2018;46(4):400–6. [PubMed: 28898515]
168. Hwang YH, Ahn SI, Ko SJ. Diagnostic ability of macular ganglion cell asymmetry for glaucoma. Clin Exp Ophthalmol. 2015;43(8):720–6. [PubMed: 25939316]
169. Hwang YH, Jeong YC, Kim HK, Sohn YH. Macular ganglion cell analysis for early detection of glaucoma. Ophthalmology. 2014;121(8):1508–15. [PubMed: 24702756]
170. Iester M, Telani S, Frezzotti P, Manni G, Uva M, Figus M, et al. Differences in central corneal thickness between the paired eyes and the severity of the glaucomatous damage. Eye (Lond). 2012;26(11):1424–30. [PubMed: 22975658]
171. Inkley D Bootstrap Methods and Their Applications Cambridge Series in Statistical and Probabilistic Mathematics. Cambridge University Press, Cambridge; 1997.
172. Inuzuka H, Kawase K, Sawada A, Aoyama Y, Yamamoto T. Macular retinal thickness in glaucoma with superior or inferior visual hemifield defects. J Glaucoma. 2013;22(1):60–4. [PubMed: 21878820]
173. Ishikawa H, Stein DM, Wollstein G, Beaton S, Fujimoto JG, Schuman JS. Macular segmentation with optical coherence tomography. Invest Ophthalmol Vis Sci. 2005;46(6):2012–7. [PubMed: 15914617]
174. Jacobsen AG, Bendtsen MD, Vorum H, Bogsted M, Hargitai J. Normal Value Ranges for Central Retinal Thickness Asymmetry in Healthy Caucasian Adults Measured by SPECTRALIS SD-OCT Posterior Pole Asymmetry Analysis. Invest Ophthalmol Vis Sci. 2015;56(6):3875–82. [PubMed: 26070059]
175. Jaffe GJ, Caprioli J. Optical coherence tomography to detect and manage retinal disease and glaucoma. Am J Ophthalmol. 2004;137(1):156–69. [PubMed: 14700659]
176. Jampel HD, Singh K, Lin SC, Chen TC, Francis BA, Hodapp E, et al. Assessment of visual function in glaucoma: a report by the American Academy of Ophthalmology. Ophthalmology. 2011;118(5):986–1002. [PubMed: 21539982]
177. Jang JW, Lee MW, Cho KJ. Comparative analysis of mean retinal thickness measured using SD-OCT in normal young or old age and glaucomatous eyes. Int Ophthalmol. 2018;38(6):2417–26. [PubMed: 29027057]
178. Jaumandreu L, Munoz-Negrete FJ, Oblanca N, Rebolleda G. Mapping the Structure-Function Relationship in Glaucoma and Healthy Patients Measured with Spectralis OCT and Humphrey Perimetry. J Ophthalmol. 2018;2018:1345409. [PubMed: 29850196]
179. Jeoung JW, Choi YJ, Park KH, Kim DM. Macular ganglion cell imaging study: glaucoma diagnostic accuracy of spectral-domain optical coherence tomography. Invest Ophthalmol Vis Sci. 2013;54(7):4422–9. [PubMed: 23722389]
180. Jiang X, Varma R, Wu S, Torres M, Azen SP, Francis BA, et al. Baseline risk factors that predict the development of open-angle glaucoma in a population: the Los Angeles Latino Eye Study. Ophthalmology. 2012;119(11):2245–53. [PubMed: 22796305]

181. Jung KI, Kang MK, Choi JA, Shin HY, Park CK. Structure-Function Relationship in Glaucoma Patients With Parafoveal Versus Peripheral Nasal Scotoma. Invest Ophthalmol Vis Sci. 2016;57(2):420–8. [PubMed: 26848881]
182. Kanadani FN, Hood DC, Grippo TM, Wangsupadilok B, Harizman N, Greenstein VC, et al. Structural and functional assessment of the macular region in patients with glaucoma. Br J Ophthalmol. 2006;90(11):1393–7. [PubMed: 16899526]
183. Kanamori A, Nakamura M, Escano MFT, Seya R, Maeda H, Negi A. Evaluation of the glaucomatous damage on retinal nerve fiber layer thickness measured by optical coherence tomography. Am J Ophthalmol. 2003;135(4):513–20. [PubMed: 12654369]
184. Kansal V, Armstrong JJ, Pintwala R, Hutnik C. Optical coherence tomography for glaucoma diagnosis: An evidence based meta-analysis. PLoS One. 2018;13(1):e0190621. [PubMed: 29300765]
185. Kashani AH, Zimmer-Galler IE, Shah SM, Dustin L, Do DV, Eliott D, et al. Retinal thickness analysis by race, gender, and age using Stratus OCT. Am J Ophthalmol. 2010;149(3):496–502.e1. [PubMed: 20042179]
186. Kawaguchi C, Nakatani Y, Ohkubo S, Higashide T, Kawaguchi I, Sugiyama K. Structural and functional assessment by hemispheric asymmetry testing of the macular region in preperimetric glaucoma. Jpn J Ophthalmol. 2014;58(2):197–204. [PubMed: 24318011]
187. Kelty PJ, Payne JF, Trivedi RH, Kelty J, Bowie EM, Burger BM. Macular thickness assessment in healthy eyes based on ethnicity using Stratus OCT optical coherence tomography. Invest Ophthalmol Vis Sci. 2008;49(6):2668–72. [PubMed: 18515595]
188. Kendell KR, Quigley HA, Kerrigan LA, Pease ME, Quigley EN. Primary open-angle glaucoma is not associated with photoreceptor loss. Invest Ophthalmol Vis Sci. 1995;36(1):200–5. [PubMed: 7822147]
189. Kerrigan-Baumrind LA, Quigley HA, Pease ME, Kerrigan DF, Mitchell RS. Number of ganglion cells in glaucoma eyes compared with threshold visual field tests in the same persons. Invest Ophthalmol Vis Sci. 2000;41(3):741–8. [PubMed: 10711689]
190. Kessel L, Hamann S, Wegener M, Tong J, Fraser CL. Microcystic macular oedema in optic neuropathy: case series and literature review. Clin Exp Ophthalmol. 2018;46(9):1075–86. [PubMed: 29799159]
191. Khanal S, Davey PG, Racette L, Thapa M. Intraeye retinal nerve fiber layer and macular thickness asymmetry measurements for the discrimination of primary open-angle glaucoma and normal tension glaucoma. J Optom. 2016;9(2):118–25. [PubMed: 26652244]
192. Kim HJ, Lee SY, Park KH, Kim DM, Jeoung JW. Glaucoma Diagnostic Ability of Layer-by-Layer Segmented Ganglion Cell Complex by Spectral-Domain Optical Coherence Tomography. Invest Ophthalmol Vis Sci. 2016;57(11):4799–805. [PubMed: 27654408]
193. Kim JH, Lee HS, Kim NR, Seong GJ, Kim CY. Relationship between visual acuity and retinal structures measured by spectral domain optical coherence tomography in patients with open-angle glaucoma. Invest Ophthalmol Vis Sci. 2014;55(8):4801–11. [PubMed: 25034596]
194. Kim KE, Park KH. Macular imaging by optical coherence tomography in the diagnosis and management of glaucoma. Br J Ophthalmol. 2017.
195. Kim KE, Park KH, Jeoung JW, Kim SH, Kim DM. Severity-dependent association between ganglion cell inner plexiform layer thickness and macular mean sensitivity in open-angle glaucoma. Acta Ophthalmol. 2014;92(8):e650–6. [PubMed: 24836437]
196. Kim KE, Yoo BW, Jeoung JW, Park KH. Long-Term Reproducibility of Macular Ganglion Cell Analysis in Clinically Stable Glaucoma Patients. Invest Ophthalmol Vis Sci. 2015;56(8):4857–64. [PubMed: 25829417]
197. Kim MJ, Jeoung JW, Park KH, Choi YJ, Kim DM. Topographic profiles of retinal nerve fiber layer defects affect the diagnostic performance of macular scans in preperimetric glaucoma. Invest Ophthalmol Vis Sci. 2014;55(4):2079–87. [PubMed: 24576877]
198. Kim NR, Kim JH, Lee J, Lee ES, Seong GJ, Kim CY. Determinants of perimacular inner retinal layer thickness in normal eyes measured by Fourier-domain optical coherence tomography. Invest Ophthalmol Vis Sci. 2011;52(6):3413–8. [PubMed: 21357406]

199. Kim NR, Lee ES, Seong GJ, Kang SY, Kim JH, Hong S, et al. Comparing the ganglion cell complex and retinal nerve fibre layer measurements by Fourier domain OCT to detect glaucoma in high myopia. Br J Ophthalmol. 2011;95(8):1115–21. [PubMed: 20805125]

200. Kim NR, Lee ES, Seong GJ, Kim JH, An HG, Kim CY. Structure-function relationship and diagnostic value of macular ganglion cell complex measurement using Fourier-domain OCT in glaucoma. Invest Ophthalmol Vis Sci. 2010;51(9):4646–51. [PubMed: 20435603]

201. Kim S, Lee JY, Kim SO, Kook MS. Macular structure-function relationship at various spatial locations in glaucoma. Br J Ophthalmol. 2015;99(10):1412–8. [PubMed: 25829487]

202. Kim YK, Ha A, Na KI, Kim HJ, Jeoung JW, Park KH. Temporal Relation between Macular Ganglion Cell-Inner Plexiform Layer Loss and Peripapillary Retinal Nerve Fiber Layer Loss in Glaucoma. Ophthalmology. 2017;124(7):1056–64. [PubMed: 28408038]

203. Kim YK, Jeoung JW, Park KH. Inferior Macular Damage in Glaucoma: Its Relationship to Retinal Nerve Fiber Layer Defect in Macular Vulnerability Zone. J Glaucoma. 2016.

204. Kim YK, Yoo BW, Kim HC, Park KH. Automated Detection of Hemifield Difference across Horizontal Raphe on Ganglion Cell--Inner Plexiform Layer Thickness Map. Ophthalmology. 2015;122(11):2252–60. [PubMed: 26278860]

205. Kita Y, Kita R, Takeyama A, Takagi S, Nishimura C, Tomita G. Ability of optical coherence tomography-determined ganglion cell complex thickness to total retinal thickness ratio to diagnose glaucoma. J Glaucoma. 2013;22(9):757–62. [PubMed: 22668980]

206. Kochendörfer L, Bauer P, Funk J, Töteberg-Harms M. Posterior pole asymmetry analysis with optical coherence tomography. Klin Monbl Augenheilkd. 2014;231(4):368–73. [PubMed: 24771169]

207. Koh V, Tham YC, Cheung CY, Mani B, Wong TY, Aung T, et al. Diagnostic accuracy of macular ganglion cell-inner plexiform layer thickness for glaucoma detection in a population-based study: Comparison with optic nerve head imaging parameters. PLoS One. 2018;13(6):e0199134. [PubMed: 29944673]

208. Koh VT, Tham Y-C, Cheung CY, Wong W-L, Baskaran M, Saw S-M, et al. Determinants of Ganglion Cell–Inner Plexiform Layer Thickness Measured by High-Definition Optical Coherence TomographyDeterminants of GC-IPL Thickness. Invest Ophthalmol Vis Sci. 2012;53(9):5853–9. [PubMed: 22836772]

209. Koo HC, Rhim WI, Lee EK. Morphologic and functional association of retinal layers beneath the epiretinal membrane with spectral-domain optical coherence tomography in eyes without photoreceptor abnormality. Graefes Arch Clin Exp Ophthalmol. 2012;250(4):491–8. [PubMed: 22086759]

210. Kotera Y, Hangai M, Hirose F, Mori S, Yoshimura N. Three-dimensional imaging of macular inner structures in glaucoma by using spectral-domain optical coherence tomography. Invest Ophthalmol Vis Sci. 2011;52(3):1412–21. [PubMed: 21087959]

211. Kreuz AC, de Moraes CG, Hatanaka M, Oyamada MK, Monteiro MLR. Macular and Multifocal PERG and FD-OCT in Preperimetric and Hemifield Loss Glaucoma. J Glaucoma. 2018;27(2):121–32. [PubMed: 29329137]

212. La Morgia C, Carelli V, Carbonelli M. Melanopsin Retinal Ganglion Cells and Pupil: Clinical Implications for Neuro-Ophthalmology. Front Neurol. 2018;9:1047. [PubMed: 30581410]

213. Lam DS, Leung KS, Mohamed S, Chan WM, Palanivelu MS, Cheung CY, et al. Regional variations in the relationship between macular thickness measurements and myopia. Invest Ophthalmol Vis Sci. 2007;48(1):376–82. [PubMed: 17197557]

214. Larrosa JM, Moreno-Montanes J, Martinez-de-la-Casa JM, Polo V, Velazquez-Villoria A, Berrozpe C, et al. A Diagnostic Calculator for Detecting Glaucoma on the Basis of Retinal Nerve Fiber Layer, Optic Disc, and Retinal Ganglion Cell Analysis by Optical Coherence Tomography. Invest Ophthalmol Vis Sci. 2015;56(11):6788–95. [PubMed: 26567791]

215. Lavinsky F, Wu M, Schuman JS, Lucy KA, Liu M, Song Y, et al. Can Macula and Optic Nerve Head Parameters Detect Glaucoma Progression in Eyes with Advanced Circumpapillary Retinal Nerve Fiber Layer Damage? Ophthalmology. 2018.

216. Le PV, Tan O, Chopra V, Francis BA, Ragab O, Varma R, et al. Regional correlation among ganglion cell complex, nerve fiber layer, and visual field loss in glaucoma. Invest Ophthalmol Vis Sci. 2013;54(6):4287–95. [PubMed: 23716631]
217. Lederer DE, Schuman JS, Hertzmark E, Heltzer J, Velazques LJ, Fujimoto JG, et al. Analysis of macular volume in normal and glaucomatous eyes using optical coherence tomography. Am J Ophthalmol. 2003;135(6):838–43. [PubMed: 12788124]
218. Ledolter J, Kardon RH. Assessing Trends in Functional and Structural Characteristics: A Survey of Statistical Methods With an Example From Ophthalmology. Transl Vis Sci Technol. 2018;7(5):34.
219. Lee HM, Lee WH, Kim KN, Jo YJ, Kim JY. Changes in thickness of central macula and retinal nerve fibre layer in severe hypertensive retinopathy: a 1-year longitudinal study. Acta Ophthalmol. 2018;96(3):e386–e92. [PubMed: 28975766]
220. Lee J, Kim YK, Ha A, Kim YW, Baek SU, Kim JS, et al. Temporal Raphe Sign for Discrimination of Glaucoma from Optic Neuropathy in Eyes with Macular Ganglion Cell-Inner Plexiform Layer Thinning. Ophthalmology. 2019;126(8):1131–9. [PubMed: 30576683]
221. Lee JW, Morales E, Sharifipour F, Amini N, Yu F, Afifi AA, et al. The relationship between central visual field sensitivity and macular ganglion cell/inner plexiform layer thickness in glaucoma. Br J Ophthalmol. 2017;101(8):1052–8. [PubMed: 28077369]
222. Lee KS, Lee JR, Na JH, Kook MS. Usefulness of macular thickness derived from spectral-domain optical coherence tomography in the detection of glaucoma progression. Invest Ophthalmol Vis Sci. 2013;54(3):1941–9. [PubMed: 23422822]
223. Lee MW, Park KS, Lim HB, Jo YJ, Kim JY. Long-term reproducibility of GC-IPL thickness measurements using spectral domain optical coherence tomography in eyes with high myopia. Sci Rep. 2018;8(1):11037. [PubMed: 30038425]
224. Lee SW, Jeong HW, Kim BM, Ahn YC, Jung W, Chen Z. Optimization for Axial Resolution, Depth Range, and Sensitivity of Spectral Domain Optical Coherence Tomography at 1.3 microm. J Korean Phys Soc. 2009;55(6):2354–60. [PubMed: 23239900]
225. Lee SY, Bae HW, Kwon HJ, Seong GJ, Kim CY. Repeatability and Agreement of Swept Source and Spectral Domain Optical Coherence Tomography Evaluations of Thickness Sectors in Normal Eyes. J Glaucoma. 2017;26(2):e46–e53. [PubMed: 27599180]
226. Lee SY, Jeoung JW, Park KH, Kim DM. Macular ganglion cell imaging study: interocular symmetry of ganglion cell-inner plexiform layer thickness in normal healthy eyes. Am J Ophthalmol. 2015;159(2):315–23.e2. [PubMed: 25447118]
227. Lee SY, Lee EK, Park KH, Kim DM, Jeoung JW. Asymmetry Analysis of Macular Inner Retinal Layers for Glaucoma Diagnosis: Swept-Source Optical Coherence Tomography Study. PLoS One. 2016;11(10):e0164866. [PubMed: 27764166]
228. Lee WJ, Baek SU, Kim YK, Park KH, Jeoung JW. Rates of Ganglion Cell-Inner Plexiform Layer Thinning in Normal, Open-Angle Glaucoma and Pseudoexfoliation Glaucoma Eyes: A Trend-Based Analysis. Invest Ophthalmol Vis Sci. 2019;60(2):599–604. [PubMed: 30721926]
229. Lee WJ, Kim TJ, Kim YK, Jeoung JW, Park KH. Serial Combined Wide-Field Optical Coherence Tomography Maps for Detection of Early Glaucomatous Structural Progression. JAMA Ophthalmol. 2018.
230. Lee WJ, Kim YK, Park KH, Jeoung JW. Trend-based Analysis of Ganglion Cell-Inner Plexiform Layer Thickness Changes on Optical Coherence Tomography in Glaucoma Progression. Ophthalmology. 2017;124(9):1383–91. [PubMed: 28412067]
231. Lee WJ, Na KI, Ha A, Kim YK, Jeoung JW, Park KH. Combined Use of Retinal Nerve Fiber Layer and Ganglion Cell-Inner Plexiform Layer Event-based Progression Analysis. Am J Ophthalmol. 2018;196:65–71. [PubMed: 30099036]
232. Lee WJ, Na KI, Kim YK, Jeoung JW, Park KH. Diagnostic Ability of Wide-field Retinal Nerve Fiber Layer Maps Using Swept-Source Optical Coherence Tomography for Detection of Preperimetric and Early Perimetric Glaucoma. J Glaucoma. 2017;26(6):577–85. [PubMed: 28368998]

233. Lee WJ, Oh S, Kim YK, Jeoung JW, Park KH. Comparison of glaucoma-diagnostic ability between wide-field swept-source OCT retinal nerve fiber layer maps and spectral-domain OCT. Eye (Lond). 2018.
234. Leitgeb RA SL, Drexler W, Fercher AF, Zawadzki RJ, Bajraszewski T. Real-time assessment of retinal blood flow with ultrafast acquisition by color Doppler Fourier domain optical coherence tomography. Opt Express. 2003 11 17;11(23):3116–21. [PubMed: 19471434]
235. Leske MC, Heijl A, Hussein M, Bengtsson B, Hyman L, Komaroff E. Factors for glaucoma progression and the effect of treatment: the early manifest glaucoma trial. Arch Ophthalmol. 2003;121(1):48–56. [PubMed: 12523884]
236. Leske MC, Heijl A, Hyman L, Bengtsson B, Dong L, Yang Z, et al. Predictors of long-term progression in the early manifest glaucoma trial. Ophthalmology. 2007;114(11):1965–72. [PubMed: 17628686]
237. Leung C, Chan W, Yung W, Ng A, Woo J, Tsang M, et al. Comparison of macular and peripapillary measurements for the detection of glaucomaAn Optical Coherence Tomography study. Ophthalmology. 2005;112(3):391–400. [PubMed: 15745764]
238. Leung CK. Diagnosing glaucoma progression with optical coherence tomography. Curr Opin Ophthalmol. 2014;25(2):104–11. [PubMed: 24370973]
239. Leung CK, Cheung CY, Weinreb RN, Qiu Q, Liu S, Li H, et al. Retinal nerve fiber layer imaging with spectral-domain optical coherence tomography: a variability and diagnostic performance study. Ophthalmology. 2009;116(7):1257–63, 63 e1–2. [PubMed: 19464061]
240. Leung CK, Ye C, Weinreb RN, Yu M, Lai G, Lam DS. Impact of age-related change of retinal nerve fiber layer and macular thicknesses on evaluation of glaucoma progression. Ophthalmology. 2013;120(12):2485–92. [PubMed: 23993360]
241. Lewis RA, Johnson CA, Adams AJ. Automated perimetry and short wavelength sensitivity in patients with asymmetric intraocular pressures. Graefes Arch Clin Exp Ophthalmol. 1993;231(5):274–8. [PubMed: 8319917]
242. Lim MC, Hoh ST, Foster PJ, Lim TH, Chew SJ, Seah SK, et al. Use of optical coherence tomography to assess variations in macular retinal thickness in myopia. Invest Ophthalmol Vis Sci. 2005;46(3):974–8. [PubMed: 15728555]
243. Lin JP, Lin PW, Lai IC, Tsai JC. Segmental inner macular layer analysis with spectral-domain optical coherence tomography for early detection of normal tension glaucoma. PLoS One. 2019;14(1):e0210215. [PubMed: 30629663]
244. Lin SC, Singh K, Jampel HD, Hodapp EA, Smith SD, Francis BA, et al. Optic nerve head and retinal nerve fiber layer analysis: a report by the American Academy of Ophthalmology. Ophthalmology. 2007;114(10):1937–49. [PubMed: 17908595]
245. Lisboa R, Paranhos A Jr., Weinreb RN, Zangwill LM, Leite MT, Medeiros FA. Comparison of different spectral domain OCT scanning protocols for diagnosing preperimetric glaucoma. Invest Ophthalmol Vis Sci. 2013;54(5):3417–25. [PubMed: 23532529]
246. Liu T, Hu AY, Kaines A, Yu F, Schwartz SD, Hubschman JP. A pilot study of normative data for macular thickness and volume measurements using cirrus high-definition optical coherence tomography. Retina. 2011;31(9):1944–50. [PubMed: 21499190]
247. Liu X, Shen M, Huang S, Leng L, Zhu D, Lu F. Repeatability and reproducibility of eight macular intra-retinal layer thicknesses determined by an automated segmentation algorithm using two SD-OCT instruments. PLoS One. 2014;9(2):e87996. [PubMed: 24505345]
248. Loewen NA, Zhang X, Tan O, Francis BA, Greenfield DS, Schuman JS, et al. Combining measurements from three anatomical areas for glaucoma diagnosis using Fourier-domain optical coherence tomography. Br J Ophthalmol. 2015;99(9):1224–9. [PubMed: 25795917]
249. Luo HD, Gazzard G, Fong A, Aung T, Hoh ST, Loon SC, et al. Myopia, axial length, and OCT characteristics of the macula in Singaporean children. Invest Ophthalmol Vis Sci. 2006;47(7):2773–81. [PubMed: 16799013]
250. Luo X, Patel NB, Rajagopalan LP, Harwerth RS, Frishman LJ. Relation between macular retinal ganglion cell/inner plexiform layer thickness and multifocal electroretinogram measures in experimental glaucoma. Invest Ophthalmol Vis Sci. 2014;55(7):4512–24. [PubMed: 24970256]

251. Malihi M, Moura Filho ER, Hodge DO, Sit AJ. Long-term trends in glaucoma-related blindness in Olmsted County, Minnesota. Ophthalmology. 2014;121(1):134–41. [PubMed: 24823760]
252. Malik R, Swanson WH, Garway-Heath DF. 'Structure-function relationship' in glaucoma: past thinking and current concepts. Clin Exp Ophthalmol. 2012;40(4):369–80. [PubMed: 22339936]
253. Martucci A, Toschi N, Cesareo M, Giannini C, Pocobelli G, Garaci F, et al. Spectral Domain Optical Coherence Tomography Assessment of Macular and Optic Nerve Alterations in Patients with Glaucoma and Correlation with Visual Field Index. J Ophthalmol. 2018;2018:6581846. [PubMed: 30402278]
254. Maslin JS, Mansouri K, Dorairaj SK. HRT for the Diagnosis and Detection of Glaucoma Progression. Open Ophthalmol J. 2015;9:58–67. [PubMed: 26069518]
255. Mauschitz MM, Holz FG, Finger RP, Breteler MMB. Determinants of Macular Layers and Optic Disc Characteristics on SD-OCT: The Rhineland Study. Transl Vis Sci Technol. 2019;8(3):34.
256. Mayama C, Saito H, Hirasawa H, Tomidokoro A, Araie M, Iwase A, et al. Diagnosis of Early-Stage Glaucoma by Grid-Wise Macular Inner Retinal Layer Thickness Measurement and Effect of Compensation of Disc-Fovea Inclination. Invest Ophthalmol Vis Sci. 2015;56(9):5681–90. [PubMed: 26313303]
257. McCann P, Hogg RE, Wright DM, McGuinness B, Young IS, Kee F, et al. Diagnostic Accuracy of Spectral-Domain OCT Circumpapillary, Optic Nerve Head, and Macular Parameters in the Detection of Perimetric Glaucoma. Ophthalmology Glaucoma. 2019;2(5):336–45. [PubMed: 32672676]
258. Medeiros F Corneal thickness measurements and frequency doubling technology perimetry abnormalities in ocular hypertensive eyes. Ophthalmology. 2003;110(10):1903–8. [PubMed: 14522761]
259. Medeiros FA, Lisboa R, Weinreb RN, Liebmann JM, Girkin C, Zangwill LM. Retinal ganglion cell count estimates associated with early development of visual field defects in glaucoma. Ophthalmology. 2013;120(4):736–44. [PubMed: 23246120]
260. Medeiros FA, Sample PA, Weinreb RN. Corneal thickness measurements and frequency doubling technology perimetry abnormalities in ocular hypertensive eyes. Ophthalmology. 2003;110(10):1903–8. [PubMed: 14522761]
261. Medeiros FA, Zangwill LM, Bowd C, Vessani RM, Susanna R Jr., Weinreb RN. Evaluation of retinal nerve fiber layer, optic nerve head, and macular thickness measurements for glaucoma detection using optical coherence tomography. Am J Ophthalmol. 2005;139(1):44–55. [PubMed: 15652827]
262. Medeiros FA, Zangwill LM, Girkin CA, Liebmann JM, Weinreb RN. Combining structural and functional measurements to improve estimates of rates of glaucomatous progression. Am J Ophthalmol. 2012;153(6):1197–205 e1. [PubMed: 22317914]
263. Menke MN, Dabov S, Knecht P, Sturm V. Reproducibility of retinal thickness measurements in healthy subjects using spectralis optical coherence tomography. Am J Ophthalmol. 2009;147(3):467–72. [PubMed: 19026403]
264. Menke MN, Knecht P, Sturm V, Dabov S, Funk J. Reproducibility of nerve fiber layer thickness measurements using 3D fourier-domain OCT. Invest Ophthalmol Vis Sci. 2008;49(12):5386–91. [PubMed: 18676630]
265. Michelessi M, Riva I, Martini E, Figus M, Frezzotti P, Agnifili L, et al. Macular versus nerve fibre layer versus optic nerve head imaging for diagnosing glaucoma at different stages of the disease: Multicenter Italian Glaucoma Imaging Study. Acta Ophthalmol. 2018.
266. Miraftabi A, Amini N, Gornbein J, Henry S, Romero P, Coleman AL, et al. Local Variability of Macular Thickness Measurements With SD-OCT and Influencing Factors. Transl Vis Sci Technol. 2016;5(4):5.
267. Miraftabi A, Amini N, Morales E, Henry S, Yu F, Afifi A, et al. Macular SD-OCT Outcome Measures: Comparison of Local Structure-Function Relationships and Dynamic Range. Invest Ophthalmol Vis Sci. 2016;57(11):4815–23. [PubMed: 27623336]
268. Mittal D, Dubey S, Gandhi M, Pegu J, Bhoot M, Gupta YP. Discriminating ability of Cirrus and RTVue optical coherence tomography in different stages of glaucoma. Indian J Ophthalmol. 2018;66(5):675–80. [PubMed: 29676314]

269. Mohammadzadeh V, Rabiolo A, Fu Q, Morales E, Coleman AL, Law SK, et al. Longitudinal Macular Structure-Function Relationships in Glaucoma. Ophthalmology.
270. Montesano G, Rossetti LM, Allegrini D, Romano MR, Crabb DP. Improving Visual Field Examination of the Macula Using Structural Information. Transl Vis Sci Technol. 2018;7(6).
271. Moon H, Lee JY, Sung KR, Lee JE. Macular Ganglion Cell Layer Assessment to Detect Glaucomatous Central Visual Field Progression. Korean J Ophthalmol. 2016;30(6):451–8. [PubMed: 27980364]
272. Morales-Fernandez L, Jimenez-Santos M, Martinez-de-la-Casa JM, Sanchez-Jean R, Nieves M, Saenz-Frances F, et al. Diagnostic capacity of SD-OCT segmented ganglion cell complex versus retinal nerve fiber layer analysis for congenital glaucoma. Eye (Lond). 2018;32(8):1338–44. [PubMed: 29643463]
273. Moreno PA, Konno B, Lima VC, Castro DP, Castro LC, Leite MT, et al. Spectral-domain optical coherence tomography for early glaucoma assessment: analysis of macular ganglion cell complex versus peripapillary retinal nerve fiber layer. Can J Ophthalmol. 2011;46(6):543–7. [PubMed: 22153644]
274. Murata N, Togano T, Miyamoto D, Ochiai S, Fukuchi T. Clinical evaluation of microcystic macular edema in patients with glaucoma. Eye (Lond). 2016;30(11):1502–8. [PubMed: 27518548]
275. Mwanza J-C, Durbin MK, Budenz DL, Girkin CA, Leung CK, Liebmann JM, et al. Profile and predictors of normal ganglion cell–inner plexiform layer thickness measured with frequency-domain optical coherence tomography. Invest Ophthalmol Vis Sci. 2011;52(11):7872–9. [PubMed: 21873658]
276. Mwanza JC, Budenz DL, Godfrey DG, Neelakantan A, Sayyad FE, Chang RT, et al. Diagnostic performance of optical coherence tomography ganglion cell--inner plexiform layer thickness measurements in early glaucoma. Ophthalmology. 2014;121(4):849–54. [PubMed: 24393348]
277. Mwanza JC, Durbin MK, Budenz DL, Girkin CA, Leung CK, Liebmann JM, et al. Profile and predictors of normal ganglion cell-inner plexiform layer thickness measured with frequency-domain optical coherence tomography. Invest Ophthalmol Vis Sci. 2011;52(11):7872–9. [PubMed: 21873658]
278. Mwanza JC, Durbin MK, Budenz DL, Girkin CA, Leung CK, Liebmann JM, et al. Profile and predictors of normal ganglion cell-inner plexiform layer thickness measured with frequency-domain optical coherence tomography. Invest Ophthalmol Vis Sci. 2011;52(11):7872–9. [PubMed: 21873658]
279. Mwanza JC, Durbin MK, Budenz DL, Sayyad FE, Chang RT, Neelakantan A, et al. Glaucoma diagnostic accuracy of ganglion cell-inner plexiform layer thickness: comparison with nerve fiber layer and optic nerve head. Ophthalmology. 2012;119(6):1151–8. [PubMed: 22365056]
280. Mwanza JC, Lee G, Budenz DL. Effect of Adjusting Retinal Nerve Fiber Layer Profile to Fovea-Disc Angle Axis on the Thickness and Glaucoma Diagnostic Performance. Am J Ophthalmol. 2016;161:12–21.e1–2. [PubMed: 26387935]
281. Mwanza JC, Lee G, Budenz DL, Warren JL, Wall M, Artes PH, et al. Validation of the UNC OCT Index for the Diagnosis of Early Glaucoma. Transl Vis Sci Technol. 2018;7(2):16.
282. Mwanza JC, Oakley JD, Budenz DL, Chang RT, Knight OJ, Feuer WJ. Macular ganglion cell-inner plexiform layer: automated detection and thickness reproducibility with spectral domain-optical coherence tomography in glaucoma. Invest Ophthalmol Vis Sci. 2011;52(11):8323–9. [PubMed: 21917932]
283. Mwanza JC, Warren JL, Budenz DL. Combining spectral domain optical coherence tomography structural parameters for the diagnosis of glaucoma with early visual field loss. Invest Ophthalmol Vis Sci. 2013;54(13):8393–400. [PubMed: 24282232]
284. Mylonas G, Ahlers C, Malamos P, Golbaz I, Deak G, Schuetze C, et al. Comparison of retinal thickness measurements and segmentation performance of four different spectral and time domain OCT devices in neovascular age-related macular degeneration. Br J Ophthalmol. 2009;93(11):1453–60. [PubMed: 19520692]

285. Na JH, Kook MS, Lee Y, Baek S. Structure-function relationship of the macular visual field sensitivity and the ganglion cell complex thickness in glaucoma. Invest Ophthalmol Vis Sci. 2012;53(8):5044–51. [PubMed: 22700706]

286. Na JH, Lee KS, Lee JR, Lee Y, Kook MS. The glaucoma detection capability of spectral-domain OCT and GDx-VCC deviation maps in early glaucoma patients with localized visual field defects. Graefes Arch Clin Exp Ophthalmol. 2013;251(10):2371–82. [PubMed: 23818227]

287. Na JH, Sung KR, Baek S, Sun JH, Lee Y. Macular and retinal nerve fiber layer thickness: which is more helpful in the diagnosis of glaucoma? Invest Ophthalmol Vis Sci. 2011;52(11):8094–101. [PubMed: 21911590]

288. Na JH, Sung KR, Lee Y. Factors associated with the signal strengths obtained by spectral domain optical coherence tomography. Korean J Ophthalmol. 2012;26(3):169–73. [PubMed: 22670072]

289. Naghizadeh F, Garas A, Vargha P, Hollo G. Detection of early glaucomatous progression with different parameters of the RTVue optical coherence tomograph. J Glaucoma. 2014;23(4):195–8. [PubMed: 22922666]

290. Nakano N, Hangai M, Nakanishi H, Mori S, Nukada M, Kotera Y, et al. Macular ganglion cell layer imaging in preperimetric glaucoma with speckle noise-reduced spectral domain optical coherence tomography. Ophthalmology. 2011;118(12):2414–26. [PubMed: 21924499]

291. Nakano N, Hangai M, Noma H, Nukada M, Mori S, Morooka S, et al. Macular imaging in highly myopic eyes with and without glaucoma. Am J Ophthalmol. 2013;156(3):511–23.e6. [PubMed: 23777978]

292. Nakatani Y, Higashide T, Ohkubo S, Takeda H, Sugiyama K. Evaluation of macular thickness and peripapillary retinal nerve fiber layer thickness for detection of early glaucoma using spectral domain optical coherence tomography. J Glaucoma. 2011;20(4):252–9. [PubMed: 20520570]

293. Nassif NA CB, Park BH, Pierce MC, Yun SH, Bouma BE, Tearney GJ, Chen TC, De Boer JF. In vivo high-resolution video-rate spectral-domain optical coherence tomography of the human retina and optic nerve. Opt Express. 2004 2 9;12(3):367–76. [PubMed: 19474832]

294. Nicholas SP, Werner EB. Location of early glaucomatous visual field defects. Can J Ophthalmol. 1980;15(3):131–3. [PubMed: 7437940]

295. Nieves-Moreno M, Martinez-de-la-Casa JM, Bambo MP, Morales-Fernandez L, Van Keer K, Vandewalle E, et al. New Normative Database of Inner Macular Layer Thickness Measured by Spectralis OCT Used as Reference Standard for Glaucoma Detection. Transl Vis Sci Technol. 2018;7(1):20.

296. Nieves-Moreno M, Martinez-de-la-Casa JM, Cifuentes-Canorea P, Sastre-Ibanez M, Santos-Bueso E, Saenz-Frances F, et al. Normative database for separate inner retinal layers thickness using spectral domain optical coherence tomography in Caucasian population. PLoS One. 2017;12(7):e0180450. [PubMed: 28678834]

297. Nouri-Mahdavi K Usefulness of Macular Temporal Vertical Asymmetry for Differentiating Optic Neuropathies from Glaucoma. Ophthalmology. 2019;126(8):1140. [PubMed: 31327379]

298. Nouri-Mahdavi K, Fatehi N, Caprioli J. Longitudinal Macular Structure-Function Relationships in Glaucoma and Their Sources of Variability. Am J Ophthalmol. 2019.

299. Nouri-Mahdavi K, Hoffman D, Coleman AL, Liu G, Li G, Gaasterland D, et al. Predictive factors for glaucomatous visual field progression in the Advanced Glaucoma Intervention Study. Ophthalmology. 2004;111(9):1627–35. [PubMed: 15350314]

300. Nouri-Mahdavi K, Nowroozizadeh S, Nassiri N, Cirineo N, Knipping S, Giaconi J, et al. Macular ganglion cell/inner plexiform layer measurements by spectral domain optical coherence tomography for detection of early glaucoma and comparison to retinal nerve fiber layer measurements. Am J Ophthalmol. 2013;156(6):1297–307.e2. [PubMed: 24075422]

301. Ohkubo S, Higashide T, Udagawa S, Sugiyama K, Hangai M, Yoshimura N, et al. Focal relationship between structure and function within the central 10 degrees in glaucoma. Invest Ophthalmol Vis Sci. 2014;55(8):5269–77. [PubMed: 25082882]

302. Ojima T, Tanabe T, Hangai M, Yu S, Morishita S, Yoshimura N. Measurement of retinal nerve fiber layer thickness and macular volume for glaucoma detection using optical coherence tomography. Jpn J Ophthalmol. 2007;51(3):197–203. [PubMed: 17554482]

303. Ooto S, Hangai M, Tomidokoro A, Saito H, Araie M, Otani T, et al. Effects of age, sex, and axial length on the three-dimensional profile of normal macular layer structures. Invest Ophthalmol Vis Sci. 2011;52(12):8769–79. [PubMed: 21989721]

304. Park JW, Jung HH, Heo H, Park SW. Validity of the temporal-to-nasal macular ganglion cell-inner plexiform layer thickness ratio as a diagnostic parameter in early glaucoma. Acta Ophthalmol. 2015;93(5):e356–65. [PubMed: 25619801]

305. Park K, Kim J, Lee J. Measurement of macular structure-function relationships using spectral domain-optical coherence tomography (SD-OCT) and pattern electroretinograms (PERG). PLoS One. 2017;12(5):e0178004. [PubMed: 28545121]

306. Park K, Kim J, Lee J. Macular Vessel Density and Ganglion Cell/Inner Plexiform Layer Thickness and Their Combinational Index Using Artificial Intelligence. J Glaucoma. 2018.

307. Park SC, De Moraes CG, Teng CC, Tello C, Liebmann JM, Ritch R. Initial parafoveal versus peripheral scotomas in glaucoma: risk factors and visual field characteristics. Ophthalmology. 2011;118(9):1782–9. [PubMed: 21665283]

308. Park SC, Kung Y, Su D, Simonson JL, Furlanetto RL, Liebmann JM, et al. Parafoveal scotoma progression in glaucoma: humphrey 10–2 versus 24–2 visual field analysis. Ophthalmology. 2013;120(8):1546–50. [PubMed: 23697959]

309. Pazos M, Dyrda AA, Biarnes M, Gomez A, Martin C, Mora C, et al. Diagnostic Accuracy of Spectralis SD OCT Automated Macular Layers Segmentation to Discriminate Normal from Early Glaucomatous Eyes. Ophthalmology. 2017;124(8):1218–28. [PubMed: 28461015]

310. Pearce JG, Maddess T. Inter-visit Test-Retest Variability of OCT in Glaucoma. Optom Vis Sci. 2017;94(3):404–10. [PubMed: 27870778]

311. Pekel G, Acer S, Yagci R, Kaya H, Ozbakis F, Bahar A, et al. Posterior pole asymmetry analysis and retinal thickness measurements in young relatives of glaucoma patients. Kaohsiung J Med Sci. 2015;31(8):420–5. [PubMed: 26228281]

312. Pollet-Villard F, Chiquet C, Romanet JP, Noel C, Aptel F. Structure-function relationships with spectral-domain optical coherence tomography retinal nerve fiber layer and optic nerve head measurements. Invest Ophthalmol Vis Sci. 2014;55(5):2953–62. [PubMed: 24692125]

313. Polo V, Garcia-Martin E, Bambo MP, Pinilla J, Larrosa JM, Satue M, et al. Reliability and validity of Cirrus and Spectralis optical coherence tomography for detecting retinal atrophy in Alzheimer's disease. Eye (Lond). 2014;28(6):680–90. [PubMed: 24625377]

314. Prager AJ, Hood DC, Liebmann JM, De Moraes CG, Al-Aswad LA, Yu Q, et al. Association of Glaucoma-Related, Optical Coherence Tomography-Measured Macular Damage With Vision-Related Quality of Life. JAMA Ophthalmol. 2017;135(7):783–8. [PubMed: 28594977]

315. Qiu K, Chen B, Yang J, Zheng C, Chen H, Zhang M, et al. Effect of optic disc-fovea distance on the normative classifications of macular inner retinal layers as assessed with OCT in healthy subjects. Br J Ophthalmol. 2019;103(6):821–5. [PubMed: 30100556]

316. Quigley HA, Broman AT. The number of people with glaucoma worldwide in 2010 and 2020. Br J Ophthalmol. 2006;90(3):262–7. [PubMed: 16488940]

317. Quigley HA, Dunkelberger GR, Green WR. Retinal ganglion cell atrophy correlated with automated perimetry in human eyes with glaucoma. Am J Ophthalmol. 1989;107(5):453–64. [PubMed: 2712129]

318. Quigley HA, Katz J, Derick RJ, Gilbert D, Sommer A. An evaluation of optic disc and nerve fiber layer examinations in monitoring progression of early glaucoma damage. Ophthalmology. 1992;99(1):19–28. [PubMed: 1741133]

319. Quigley HA, Nickells RW, Kerrigan LA, Pease ME, Thibault DJ, Zack DJ. Retinal ganglion cell death in experimental glaucoma and after axotomy occurs by apoptosis. Invest Ophthalmol Vis Sci. 1995;36(5):774–86. [PubMed: 7706025]

320. Racette LFM, Bebie H, Holló G, Johnson CA, Matsumoto C. Visual field digest A guide to perimetry and the Ocotpus perimeter. 8th Edition Haag-Streit AG, Koniz, Switzerland 2019.

321. Rao HL, Addepalli UK, Chaudhary S, Kumbar T, Senthil S, Choudhari NS, et al. Ability of different scanning protocols of spectral domain optical coherence tomography to diagnose preperimetric glaucoma. Invest Ophthalmol Vis Sci. 2013;54(12):7252–7. [PubMed: 24114539]

322. Rao HL, Hussain RS, Januwada M, Pillutla LN, Begum VU, Chaitanya A, et al. Structural and functional assessment of macula to diagnose glaucoma. Eye (Lond). 2016.
323. Rao HL, Januwada M, Hussain RS, Pillutla LN, Begum VU, Chaitanya A, et al. Comparing the Structure-Function Relationship at the Macula With Standard Automated Perimetry and Microperimetry. Invest Ophthalmol Vis Sci. 2015;56(13):8063–8. [PubMed: 26720457]
324. Rao HL, Kumar AU, Babu JG, Kumar A, Senthil S, Garudadri CS. Predictors of normal optic nerve head, retinal nerve fiber layer, and macular parameters measured by spectral domain optical coherence tomography. Invest Ophthalmol Vis Sci. 2011;52(2):1103–10. [PubMed: 21087966]
325. Rao HL, Qasim M, Hussain RS, Januwada M, Pillutla LN, Begum VU, et al. Structure-Function Relationship in Glaucoma Using Ganglion Cell-Inner Plexiform Layer Thickness Measurements. Invest Ophthalmol Vis Sci. 2015;56(6):3883–8. [PubMed: 26070060]
326. Rao HL, Zangwill LM, Weinreb RN, Sample PA, Alencar LM, Medeiros FA. Comparison of different spectral domain optical coherence tomography scanning areas for glaucoma diagnosis. Ophthalmology. 2010;117(9):1692–9, 9.e1. [PubMed: 20493529]
327. Raza AS, Cho J, de Moraes CG, Wang M, Zhang X, Kardon RH, et al. Retinal ganglion cell layer thickness and local visual field sensitivity in glaucoma. Arch Ophthalmol. 2011;129(12):1529–36. [PubMed: 22159673]
328. Raza AS, Cho J, de Moraes CG, Wang M, Zhang X, Kardon RH, et al. Retinal ganglion cell layer thickness and local visual field sensitivity in glaucoma. Arch Ophthalmol. 2011;129(12):1529–36. [PubMed: 22159673]
329. Raza AS, Hood DC. Evaluation of the Structure-Function Relationship in Glaucoma Using a Novel Method for Estimating the Number of Retinal Ganglion Cells in the Human Retina. Invest Ophthalmol Vis Sci. 2015;56(9):5548–56. [PubMed: 26305526]
330. Reichenbach A, Wurm A, Pannicke T, Iandiev I, Wiedemann P, Bringmann A. Muller cells as players in retinal degeneration and edema. Graefes Arch Clin Exp Ophthalmol. 2007;245(5):627–36. [PubMed: 17219109]
331. Reus NJ, Lemij HG, Garway-Heath DF, Airaksinen PJ, Anton A, Bron AM, et al. Clinical assessment of stereoscopic optic disc photographs for glaucoma: the European Optic Disc Assessment Trial. Ophthalmology. 2010;117(4):717–23. [PubMed: 20045571]
332. Rolle T, Briamonte C, Curto D, Grignolo FM. Ganglion cell complex and retinal nerve fiber layer measured by fourier-domain optical coherence tomography for early detection of structural damage in patients with preperimetric glaucoma. Clin Ophthalmol. 2011;5:961–9. [PubMed: 21792286]
333. Rolle T, Manerba L, Lanzafame P, Grignolo FM. Diagnostic Power of Macular Retinal Thickness Analysis and Structure-Function Relationship in Glaucoma Diagnosis Using SPECTRALIS OCT. Curr Eye Res. 2015:1–9.
334. Russell RA, Malik R, Chauhan BC, Crabb DP, Garway-Heath DF. Improved estimates of visual field progression using bayesian linear regression to integrate structural information in patients with ocular hypertension. Invest Ophthalmol Vis Sci. 2012;53(6):2760–9. [PubMed: 22467579]
335. Salgarello T, Colotto A, Valente P, Petrocelli G, Galan ME, Scullica L, et al. Posterior pole retinal thickness in ocular hypertension and glaucoma: early changes detected by hemispheric asymmetries. J Glaucoma. 2005;14(5):375–83. [PubMed: 16148586]
336. Sato S, Hirooka K, Baba T, Tenkumo K, Nitta E, Shiraga F. Correlation between the ganglion cell-inner plexiform layer thickness measured with cirrus HD-OCT and macular visual field sensitivity measured with microperimetry. Invest Ophthalmol Vis Sci. 2013;54(4):3046–51. [PubMed: 23580483]
337. Schiefer U, Dietzsch J, Dietz K, Wilhelm B, Bruckmann A, Wilhelm H, et al. Associating the magnitude of relative afferent pupillary defect (RAPD) with visual field indices in glaucoma patients. Br J Ophthalmol. 2012;96(5):629–33. [PubMed: 22328816]
338. Schmidt-Erfurth ULR, Michels S, Povazay B, Sacu S, Hermann B, Ahlers C, Sattmann H, Scholda C, Fercher AF, Drexler W. Three-dimensional ultrahigh-resolution optical coherence tomography of macular diseases. Invest Ophthalmol Vis Sci. 2005 9 1;46(9):3393–402. [PubMed: 16123444]

339. Schulze A, Lamparter J, Pfeiffer N, Berisha F, Schmidtmann I, Hoffmann EM. Diagnostic ability of retinal ganglion cell complex, retinal nerve fiber layer, and optic nerve head measurements by Fourier-domain optical coherence tomography. Graefes Arch Clin Exp Ophthalmol. 2011;249(7):1039–45. [PubMed: 21240522]

340. Schulze A, Lamparter J, Pfeiffer N, Berisha F, Schmidtmann I, Hoffmann EM. Comparison of Laser Scanning Diagnostic Devices for Early Glaucoma Detection. J Glaucoma. 2015;24(6):442–7. [PubMed: 24844535]

341. Schuman JS. Spectral domain optical coherence tomography for glaucoma (an AOS thesis). Trans Am Ophthalmol Soc. 2008;106:426–58. [PubMed: 19277249]

342. Schuman JS, Hee MR, Arya AV, Pedut-Kloizman T, Puliafito CA, Fujimoto JG, et al. Optical coherence tomography: a new tool for glaucoma diagnosis. Curr Opin Ophthalmol. 1995;6(2):89–95. [PubMed: 10150863]

343. Schuman JS, Pedut-Kloizman T, Hertzmark E, Hee MR, Wilkins JR, Coker JG, et al. Reproducibility of nerve fiber layer thickness measurements using optical coherence tomography. Ophthalmology. 1996;103(11):1889–98. [PubMed: 8942887]

344. Seo JH, Kim TW, Weinreb RN, Park KH, Kim SH, Kim DM. Detection of localized retinal nerve fiber layer defects with posterior pole asymmetry analysis of spectral domain optical coherence tomography. Invest Ophthalmol Vis Sci. 2012;53(8):4347–53. [PubMed: 22577076]

345. Seol BR, Jeoung JW, Park KH. Glaucoma Detection Ability of Macular Ganglion Cell-Inner Plexiform Layer Thickness in Myopic Preperimetric Glaucoma. Invest Ophthalmol Vis Sci. 2015;56(13):8306–13. [PubMed: 26720484]

346. Seong M, Sung KR, Choi EH, Kang SY, Cho JW, Um TW, et al. Macular and peripapillary retinal nerve fiber layer measurements by spectral domain optical coherence tomography in normal-tension glaucoma. Invest Ophthalmol Vis Sci. 2010;51(3):1446–52. [PubMed: 19834029]

347. Sepulveda JA, Turpin A, McKendrick AM. Individual Differences in Foveal Shape: Feasibility of Individual Maps Between Structure and Function Within the Macular Region. Invest Ophthalmol Vis Sci. 2016;57(11):4772–8. [PubMed: 27623333]

348. Sezgin Akcay BI, Gunay BO, Kardes E, Unlu C, Ergin A. Evaluation of the Ganglion Cell Complex and Retinal Nerve Fiber Layer in Low, Moderate, and High Myopia: A Study by RTVue Spectral Domain Optical Coherence Tomography. Semin Ophthalmol. 2017;32(6):682–8. [PubMed: 27404600]

349. Shah NN, Bowd C, Medeiros FA, Weinreb RN, Sample PA, Hoffmann EM, et al. Combining structural and functional testing for detection of glaucoma. Ophthalmology. 2006;113(9):1593–602. [PubMed: 16949444]

350. Sharifipour F, Morales E, Lee JW, Giaconi J, Afifi AA, Yu F, et al. Vertical Macular Asymmetry Measures Derived From SD-OCT for Detection of Early Glaucoma. Invest Ophthalmol Vis Sci. 2017;58(10):4310–7. [PubMed: 28800651]

351. Sharma P, Sample PA, Zangwill LM, Schuman JS. Diagnostic Tools for Glaucoma Detection and Management. Surv Ophthalmol. 2008;53(6, Supplement):S17–S32. [PubMed: 19038620]

352. Shin HY, Park HY, Jung KI, Park CK. Comparative study of macular ganglion cell-inner plexiform layer and peripapillary retinal nerve fiber layer measurement: structure-function analysis. Invest Ophthalmol Vis Sci. 2013;54(12):7344–53. [PubMed: 24130187]

353. Shin JW, Sung KR, Lee GC, Durbin MK, Cheng D. Ganglion Cell-Inner Plexiform Layer Change Detected by Optical Coherence Tomography Indicates Progression in Advanced Glaucoma. Ophthalmology. 2017;124(10):1466–74. [PubMed: 28549518]

354. Shin JW, Sung KR, Park SW. Patterns of Progressive Ganglion Cell-Inner Plexiform Layer Thinning in Glaucoma Detected by OCT. Ophthalmology. 2018.

355. Shoji T, Nagaoka Y, Sato H, Chihara E. Impact of high myopia on the performance of SD-OCT parameters to detect glaucoma. Graefes Arch Clin Exp Ophthalmol. 2012;250(12):1843–9. [PubMed: 22555896]

356. Shoji T, Sato H, Ishida M, Takeuchi M, Chihara E. Assessment of glaucomatous changes in subjects with high myopia using spectral domain optical coherence tomography. Invest Ophthalmol Vis Sci. 2011;52(2):1098–102. [PubMed: 21051712]

357. Sigler EJ. Microcysts in the inner nuclear layer, a nonspecific SD-OCT sign of cystoid macular edema. Invest Ophthalmol Vis Sci. 2014;55(5):3282–4. [PubMed: 24867911]
358. Sinai MJ. The Normative Database for the RTVue.Software version 4.0.
359. Sng CC, Cheung CY, Man RE, Wong W, Lavanya R, Mitchell P, et al. Influence of diabetes on macular thickness measured using optical coherence tomography: the Singapore Indian Eye Study. Eye (Lond). 2012;26(5):690–8. [PubMed: 22344185]
360. Sommer A, Duggan C, Auer C, Abbey H. Analytic approaches to the interpretation of automated threshold perimetric data for the diagnosis of early glaucoma. Trans Am Ophthalmol Soc. 1985;83:250–67. [PubMed: 3832529]
361. Sommer A, Katz J, Quigley HA, Miller NR, Robin AL, Richter RC, et al. Clinically detectable nerve fiber atrophy precedes the onset of glaucomatous field loss. Arch Ophthalmol. 1991;109(1):77–83. [PubMed: 1987954]
362. Song WK, Lee SC, Lee ES, Kim CY, Kim SS. Macular thickness variations with sex, age, and axial length in healthy subjects: a spectral domain-optical coherence tomography study. Invest Ophthalmol Vis Sci. 2010;51(8):3913–8. [PubMed: 20357206]
363. Stein JD, Talwar N, Laverne AM, Nan B, Lichter PR. Trends in use of ancillary glaucoma tests for patients with open-angle glaucoma from 2001 to 2009. Ophthalmology. 2012;119(4):748–58. [PubMed: 22218146]
364. Suda K, Hangai M, Akagi T, Noma H, Kimura Y, Hasegawa T, et al. Comparison of Longitudinal Changes in Functional and Structural Measures for Evaluating Progression of Glaucomatous Optic Neuropathy. Invest Ophthalmol Vis Sci. 2015;56(9):5477–84. [PubMed: 26284553]
365. Sullivan-Mee M, Gentry JM, Qualls C. Relationship between asymmetric central corneal thickness and glaucomatous visual field loss within the same patient. Optom Vis Sci. 2006;83(7):516–9. [PubMed: 16840876]
366. Sullivan-Mee M, Ruegg CC, Pensyl D, Halverson K, Qualls C. Diagnostic precision of retinal nerve fiber layer and macular thickness asymmetry parameters for identifying early primary open-angle glaucoma. Am J Ophthalmol. 2013;156(3):567–77.e1. [PubMed: 23810475]
367. Sung KR, Cho JW, Lee S, Yun SC, Choi J, Na JH, et al. Characteristics of visual field progression in medically treated normal-tension glaucoma patients with unstable ocular perfusion pressure. Invest Ophthalmol Vis Sci. 2011;52(2):737–43. [PubMed: 20861474]
368. Sung KR, Sun JH, Na JH, Lee JY, Lee Y. Progression detection capability of macular thickness in advanced glaucomatous eyes. Ophthalmology. 2012;119(2):308–13. [PubMed: 22182800]
369. Swanson WH, Felius J, Pan F. Perimetric defects and ganglion cell damage: interpreting linear relations using a two-stage neural model. Invest Ophthalmol Vis Sci. 2004;45(2):466–72. [PubMed: 14744886]
370. Takayama K, Hangai M, Durbin M, Nakano N, Morooka S, Akagi T, et al. A novel method to detect local ganglion cell loss in early glaucoma using spectral-domain optical coherence tomography. Invest Ophthalmol Vis Sci. 2012;53(11):6904–13. [PubMed: 22977136]
371. Takeyama A, Kita Y, Kita R, Tomita G. Influence of axial length on ganglion cell complex (GCC) thickness and on GCC thickness to retinal thickness ratios in young adults. Jpn J Ophthalmol. 2014;58(1):86–93. [PubMed: 24242185]
372. Takihara Y, Inatani M, Fukushima M, Iwao K, Iwao M, Tanihara H. Trabeculectomy with Mitomycin C for Neovascular Glaucoma: Prognostic Factors for Surgical Failure. Am J Ophthalmol. 2009;147(5):912–8.e1. [PubMed: 19195639]
373. Tan O, Chopra V, Lu AT, Schuman JS, Ishikawa H, Wollstein G, et al. Detection of macular ganglion cell loss in glaucoma by Fourier-domain optical coherence tomography. Ophthalmology. 2009;116(12):2305–14 e1–2. [PubMed: 19744726]
374. Tan O, Li G, Lu AT, Varma R, Huang D, Advanced Imaging for Glaucoma Study G. Mapping of macular substructures with optical coherence tomography for glaucoma diagnosis. Ophthalmology. 2008;115(6):949–56. [PubMed: 17981334]
375. Tatham AJ, Meira-Freitas D, Weinreb RN, Marvasti AH, Zangwill LM, Medeiros FA. Estimation of retinal ganglion cell loss in glaucomatous eyes with a relative afferent pupillary defect. Invest Ophthalmol Vis Sci. 2014;55(1):513–22. [PubMed: 24282221]

376. Tatsumi Y, Nakamura M, Fujioka M, Nakanishi Y, Kusuhara A, Maeda H, et al. Quantification of retinal nerve fiber layer thickness reduction associated with a relative afferent pupillary defect in asymmetric glaucoma. Br J Ophthalmol. 2007;91(5):633–7. [PubMed: 17050576]

377. Thompson AC, Jammal AA, Medeiros FA. Performance of the Rule of 5 for Detecting Glaucoma Progression between Visits with OCT. Ophthalmology Glaucoma. 2019;2(5):319–26. [PubMed: 32672674]

378. Tick S, Rossant F, Ghorbel I, Gaudric A, Sahel JA, Chaumet-Riffaud P, et al. Foveal shape and structure in a normal population. Invest Ophthalmol Vis Sci. 2011;52(8):5105–10. [PubMed: 21803966]

379. Topcon Medical Systems I. TOPCON 3D OCT Series Normative Database. 2011.

380. Toutouzas K, Karanasos A, Stefanadis C. Pitfalls of angiography in the assessment of atherosclerosis: the role of optical coherence tomography. J Invasive Cardiol. 2012;24(5):246–7. [PubMed: 22562923]

381. Traynis I, De Moraes CG, Raza AS, Liebmann JM, Ritch R, Hood DC. Prevalence and nature of early glaucomatous defects in the central 10 degrees of the visual field. JAMA Ophthalmol. 2014;132(3):291–7. [PubMed: 24407153]

382. Turpin A, Chen S, Sepulveda JA, McKendrick AM. Customizing Structure-Function Displacements in the Macula for Individual Differences. Invest Ophthalmol Vis Sci. 2015;56(10):5984–9. [PubMed: 26393464]

383. Turpin A, McKendrick AM, Johnson CA, Vingrys AJ. Properties of perimetric threshold estimates from full threshold, ZEST, and SITA-like strategies, as determined by computer simulation. Invest Ophthalmol Vis Sci. 2003;44(11):4787–95. [PubMed: 14578400]

384. Ueda K, Kanamori A, Akashi A, Kawaka Y, Yamada Y, Nakamura M. Difference in correspondence between visual field defect and inner macular layer thickness measured using three types of spectral-domain OCT instruments. Jpn J Ophthalmol. 2015;59(1):55–64. [PubMed: 25377494]

385. Ueda K, Kanamori A, Akashi A, Tomioka M, Kawaka Y, Nakamura M. Effects of Axial Length and Age on Circumpapillary Retinal Nerve Fiber Layer and Inner Macular Parameters Measured by 3 Types of SD-OCT Instruments. J Glaucoma. 2016;25(4):383–9. [PubMed: 25580890]

386. Um TW, Sung KR, Wollstein G, Yun SC, Na JH, Schuman JS. Asymmetry in hemifield macular thickness as an early indicator of glaucomatous change. Invest Ophthalmol Vis Sci. 2012;53(3):1139–44. [PubMed: 22247461]

387. Ustaoglu M, Solmaz N, Onder F. Discriminating performance of macular ganglion cell-inner plexiform layer thicknesses at different stages of glaucoma. Int J Ophthalmol. 2019;12(3):464–71. [PubMed: 30918817]

388. van Velthoven ME, van der Linden MH, de Smet MD, Faber DJ, Verbraak FD. Influence of cataract on optical coherence tomography image quality and retinal thickness. Br J Ophthalmol. 2006;90(10):1259–62. [PubMed: 16980644]

389. Verticchio Vercellin AC, Jassim F, Poon LY, Tsikata E, Braaf B, Shah S, et al. Diagnostic Capability of Three-Dimensional Macular Parameters for Glaucoma Using Optical Coherence Tomography Volume Scans. Invest Ophthalmol Vis Sci. 2018;59(12):4998–5010. [PubMed: 30326067]

390. Wadhwani M, Bali SJ, Satyapal R, Angmo D, Sharma R, Pandey V, et al. Test-retest variability of retinal nerve fiber layer thickness and macular ganglion cell-inner plexiform layer thickness measurements using spectral-domain optical coherence tomography. J Glaucoma. 2015;24(5):e109–15. [PubMed: 25517254]

391. Wagner-Schuman M, Dubis AM, Nordgren RN, Lei Y, Odell D, Chiao H, et al. Race-and sex-related differences in retinal thickness and foveal pit morphology. Invest Ophthalmol Vis Sci. 2011;52(1):625–34. [PubMed: 20861480]

392. Wan KH, Lam AKN, Leung CK. Optical Coherence Tomography Angiography Compared With Optical Coherence Tomography Macular Measurements for Detection of Glaucoma. JAMA Ophthalmol. 2018;136(8):866–74. [PubMed: 29852029]

393. Wang M, Hood DC, Cho JS, Ghadiali Q, De Moraes CG, Zhang X, et al. Measurement of local retinal ganglion cell layer thickness in patients with glaucoma using frequency-domain optical coherence tomography. Arch Ophthalmol. 2009;127(7):875–81. [PubMed: 19597108]

394. Wang M, Lu AT, Varma R, Schuman JS, Greenfield DS, Huang D. Combining information from 3 anatomic regions in the diagnosis of glaucoma with time-domain optical coherence tomography. J Glaucoma. 2014;23(3):129–35. [PubMed: 22828002]

395. Wang WW, Wang HZ, Liu JR, Zhang XF, Li M, Huo YJ, et al. Diagnostic ability of ganglion cell complex thickness to detect glaucoma in high myopia eyes by Fourier domain optical coherence tomography. Int J Ophthalmol. 2018;11(5):791–6. [PubMed: 29862177]

396. Wassle H, Grunert U, Rohrenbeck J, Boycott BB. Cortical magnification factor and the ganglion cell density of the primate retina. Nature. 1989;341(6243):643–6. [PubMed: 2797190]

397. Weber AJ, Kaufman PL, Hubbard WC. Morphology of single ganglion cells in the glaucomatous primate retina. Invest Ophthalmol Vis Sci. 1998;39(12):2304–20. [PubMed: 9804139]

398. Weinreb RN, Aung T, Medeiros FA. The pathophysiology and treatment of glaucoma: a review. JAMA. 2014;311(18):1901–11. [PubMed: 24825645]

399. Weinreb RN, Friedman DS, Fechtner RD, Cioffi GA, Coleman AL, Girkin CA, et al. Risk assessment in the management of patients with ocular hypertension. Am J Ophthalmol. 2004;138(3):458–67. [PubMed: 15364230]

400. Wen JC, Freedman SF, El-Dairi MA, Asrani S. Microcystic Macular Changes in Primary Open-angle Glaucoma. J Glaucoma. 2016;25(3):258–62. [PubMed: 25265005]

401. Wexler A, Sand T, Elsas TB. Macular thickness measurements in healthy Norwegian volunteers: an optical coherence tomography study. BMC Ophthalmol. 2010;10:13. [PubMed: 20465801]

402. Wilsey LJ, Reynaud J, Cull G, Burgoyne CF, Fortune B. Macular Structure and Function in Nonhuman Primate Experimental Glaucoma. Invest Ophthalmol Vis Sci. 2016;57(4):1892–900. [PubMed: 27082305]

403. Wojtkowski MBT, Targowski P, Kowalczyk A. Real-time in vivo imaging by high-speed spectral optical coherence tomography. Optics letters. 2003 10 1;28(19):1745–7. [PubMed: 14514087]

404. Wojtkowski MSV, Ko TH, Fujimoto JG, Kowalczyk A, Duker JS. Ultrahigh-resolution, high-speed, Fourier domain optical coherence tomography and methods for dispersion compensation. Opt Express. 2004 5 31;12(11):2404–22. [PubMed: 19475077]

405. Wolff BBC, Vasseur V, Mauget-Faÿsse M, Sahel JA, Vignal C. Retinal inner nuclear layer microcystic changes in optic nerve atrophy: a novel spectral-domain OCT finding. Retina. 2013 33(10):2133–8. [PubMed: 23644558]

406. Wollstein G, Ishikawa H, Wang J, Beaton SA, Schuman JS. Comparison of three optical coherence tomography scanning areas for detection of glaucomatous damage. Am J Ophthalmol. 2005;139(1):39–43. [PubMed: 15652826]

407. Wollstein G, Schuman JS, Price LL, Aydin A, Beaton SA, Stark PC, et al. Optical coherence tomography (OCT) macular and peripapillary retinal nerve fiber layer measurements and automated visual fields. Am J Ophthalmol. 2004;138(2):218–25. [PubMed: 15289130]

408. Wong AC, Chan CW, Hui SP. Relationship of gender, body mass index, and axial length with central retinal thickness using optical coherence tomography. Eye (Lond). 2005;19(3):292–7. [PubMed: 15258609]

409. Wong JJ, Chen TC, Shen LQ, Pasquale LR. Macular imaging for glaucoma using spectral-domain optical coherence tomography: a review. Semin Ophthalmol. 2012;27(5–6):160–6. [PubMed: 23163271]

410. Wu Z, Vazeen M, Varma R, Chopra V, Walsh AC, LaBree LD, et al. Factors associated with variability in retinal nerve fiber layer thickness measurements obtained by optical coherence tomography. Ophthalmology. 2007;114(8):1505–12. [PubMed: 17367862]

411. Wu Z, Weng DSD, Rajshekhar R, Ritch R, Hood DC. Effectiveness of a Qualitative Approach Toward Evaluating OCT Imaging for Detecting Glaucomatous Damage. Transl Vis Sci Technol. 2018;7(4):7.

412. Wu Z, Weng DSD, Thenappan A, Ritch R, Hood DC. Evaluation of a Region-of-Interest Approach for Detecting Progressive Glaucomatous Macular Damage on Optical Coherence Tomography. Transl Vis Sci Technol. 2018;7(2):14.

413. Wygnanski T, Desatnik H, Quigley HA, Glovinsky Y. Comparison of Ganglion Cell Loss and Cone Loss in Experimental Glaucoma. Am J Ophthalmol. 1995;120(2):184–9. [PubMed: 7639302]
414. Yamada H, Hangai M, Nakano N, Takayama K, Kimura Y, Miyake M, et al. Asymmetry analysis of macular inner retinal layers for glaucoma diagnosis. Am J Ophthalmol. 2014;158(6):1318–29.e3. [PubMed: 25194230]
415. Yamada H, Hangai M, Nakano N, Takayama K, Kimura Y, Miyake M, et al. Asymmetry analysis of macular inner retinal layers for glaucoma diagnosis. Am J Ophthalmol. 2014;158(6):1318–29 e3. [PubMed: 25194230]
416. Yamashita T, Sakamoto T, Kakiuchi N, Tanaka M, Kii Y, Nakao K. Posterior pole asymmetry analyses of retinal thickness of upper and lower sectors and their association with peak retinal nerve fiber layer thickness in healthy young eyes. Invest Ophthalmol Vis Sci. 2014;55(9):5673–8. [PubMed: 25118262]
417. Yamashita T, Tanaka M, Kii Y, Nakao K, Sakamoto T. Association between retinal thickness of 64 sectors in posterior pole determined by optical coherence tomography and axial length and body height. Invest Ophthalmol Vis Sci. 2013;54(12):7478–82. [PubMed: 24168996]
418. Yang HY, Chang YF, Hsu CC, Ko YC, Liu CJ, Chen MJ. Macular ganglion cell asymmetry for detecting paracentral scotoma in early glaucoma. Clin Ophthalmol. 2018;12:2253–60. [PubMed: 30464386]
419. Yang Q, Reisman CA, Wang Z, Fukuma Y, Hangai M, Yoshimura N, et al. Automated layer segmentation of macular OCT images using dual-scale gradient information. Opt Express. 2010;18(20):21293–307. [PubMed: 20941025]
420. Yang Z, Tatham AJ, Weinreb RN, Medeiros FA, Liu T, Zangwill LM. Diagnostic ability of macular ganglion cell inner plexiform layer measurements in glaucoma using swept source and spectral domain optical coherence tomography. PLoS One. 2015;10(5):e0125957. [PubMed: 25978420]
421. Yoshida T, Iwase A, Hirasawa H, Murata H, Mayama C, Araie M, et al. Discriminating between glaucoma and normal eyes using optical coherence tomography and the 'Random Forests' classifier. PLoS One. 2014;9(8):e106117. [PubMed: 25167053]
422. Yoshioka NZB, Phu J, Choi AY, Khuu SK, Masselos K, Hennessy MP, Kalloniatis M. Consistency of structure-function correlation between spatially scaled visual field stimuli and in vivo OCT ganglion cell counts. Invest Ophthalmol Vis Sci. 2018 4 1;59(5):1693–703. [PubMed: 29610852]
423. Younis AA, Eggenberger ER. Correlation of relative afferent pupillary defect and retinal nerve fiber layer loss in unilateral or asymmetric demyelinating optic neuropathy. Invest Ophthalmol Vis Sci. 2010;51(8):4013–6. [PubMed: 20207978]
424. Zangwill LM, Weinreb RN, Beiser JA, Berry CC, Cioffi GA, Coleman AL, et al. Baseline topographic optic disc measurements are associated with the development of primary open-angle glaucoma: the Confocal Scanning Laser Ophthalmoscopy Ancillary Study to the Ocular Hypertension Treatment Study. Arch Ophthalmol. 2005;123(9):1188–97. [PubMed: 16157798]
425. Zeimer R, Asrani S, Zou S, Quigley H, Jampel H. Quantitative detection of glaucomatous damage at the posterior pole by retinal thickness mapping. A pilot study. Ophthalmology. 1998;105(2):224–31. [PubMed: 9479279]
426. Zeimer R, Shahidi M, Mori M, Zou S, Asrani S. A new method for rapid mapping of the retinal thickness at the posterior pole. Invest Ophthalmol Vis Sci. 1996;37(10):1994–2001. [PubMed: 8814139]
427. Zha Y, Huang W, Zhuang J, Cai J. Posterior pole asymmetry analysis and retinal nerve fibre layer thickness measurements in primary angle-closure suspect patients. BMC Ophthalmol. 2019;19(1):36. [PubMed: 30691419]
428. Zhang C, Guo Y, Slater BJ, Miller NR, Bernstein SL. Axonal degeneration, regeneration and ganglion cell death in a rodent model of anterior ischemic optic neuropathy (rAION). Exp Eye Res. 2010;91(2):286–92. [PubMed: 20621651]

429. Zhang C, Tatham AJ, Weinreb RN, Zangwill LM, Yang Z, Zhang JZ, et al. Relationship between ganglion cell layer thickness and estimated retinal ganglion cell counts in the glaucomatous macula. Ophthalmology. 2014;121(12):2371–9. [PubMed: 25148790]

430. Zhang X, Bregman CJ, Raza AS, De Moraes G, Hood DC. Deriving visual field loss based upon OCT of inner retinal thicknesses of the macula. Biomed Opt Express. 2011;2(6):1734–42. [PubMed: 21698033]

431. Zhang X, Dastiridou A, Francis BA, Tan O, Varma R, Greenfield DS, et al. Baseline Fourier-Domain Optical Coherence Tomography Structural Risk Factors for Visual Field Progression in the Advanced Imaging for Glaucoma Study. Am J Ophthalmol. 2016;172:94–103. [PubMed: 27651070]

432. Zhang X, Francis BA, Dastiridou A, Chopra V, Tan O, Varma R, et al. Longitudinal and Cross-Sectional Analyses of Age Effects on Retinal Nerve Fiber Layer and Ganglion Cell Complex Thickness by Fourier-Domain OCT. Transl Vis Sci Technol. 2016;5(2):1.

433. Zhang X, Loewen N, Tan O, Greenfield DS, Schuman JS, Varma R, et al. Predicting Development of Glaucomatous Visual Field Conversion Using Baseline Fourier-Domain Optical Coherence Tomography. Am J Ophthalmol. 2016;163:29–37. [PubMed: 26627918]

434. Zhang Y, Li N, Chen J, Wei H, Jiang SM, Chen XM. A new strategy to interpret OCT posterior pole asymmetry analysis for glaucoma diagnosis. Int J Ophthalmol. 2017;10(12):1857–63. [PubMed: 29259904]

435. Zhang Y, Wen W, Sun X. Comparison of Several Parameters in Two Optical Coherence Tomography Systems for Detecting Glaucomatous Defects in High Myopia. Invest Ophthalmol Vis Sci. 2016;57(11):4910–5. [PubMed: 27654417]

436. Zhao Z, Jiang C. Effect of myopia on ganglion cell complex and peripapillary retinal nerve fibre layer measurements: a Fourier-domain optical coherence tomography study of young Chinese persons. Clin Exp Ophthalmol. 2013;41(6):561–6. [PubMed: 23231592]

437. Zivkovic M, Dayanir V, Zlatanovic M, Zlatanovic G, Jaksic V, Jovanovic P, et al. Ganglion Cell-Inner Plexiform Layer Thickness in Different Glaucoma Stages Measured by Optical Coherence Tomography. Ophthalmic Res. 2018;59(3):148–54. [PubMed: 28877522]

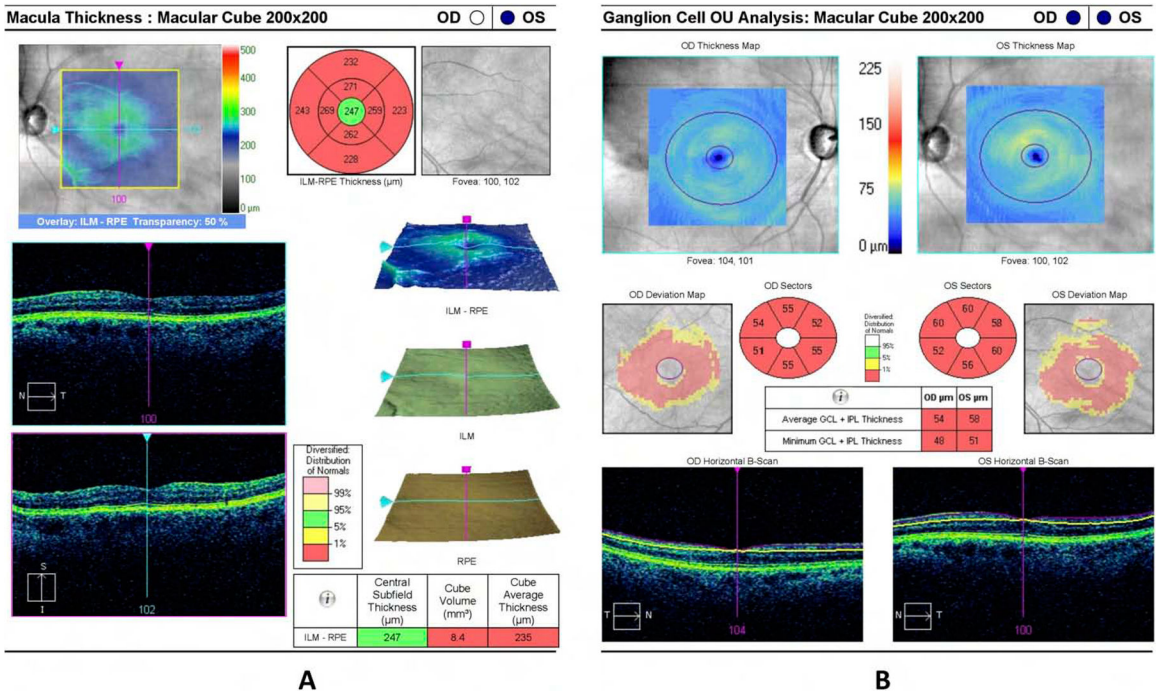

Figure 1.

A) A printout of Cirrus HD-OCT's macular OCT image displaying full macular thickness measurements presented in the Early Treatment of Diabetic Retinopathy Study (ETDRS) grid format. Top row, the thickness maps demonstrate a false color map of the central macular retinal thickness and full retinal thickness in ETDRS regions. Left middle and bottom panels provide raw OCT images. Right column images represent 3-D images of macula (top) and the top surfaces of the inner limiting membrane (middle) and the retinal pigment epithelium (bottom). The very bottom row on the right displays the central subfield thickness, macular cube volume, and macular cube average from left to right, respectively, with their corresponding color scheme for statistical significance. **B**) The Ganglion Cell Analysis printout provides the ganglion cell/inner plexiform (GCIPL) layer thickness measurements in an ellipse 4.8×4.0 mm in size excluding the central 1.2×1.0 mm (the central fovea). This elliptical region is divided into 6 wedge-shaped sectors where the GCIPL thickness is averaged. Top row, the thickness maps demonstrate a false color map of the GCIPL thickness; middle row, deviation maps and global, sectoral, and minimum GCIPL thickness measurements. The former show regions where the GCIPL thickness has fallen below the 5% limit based on the normative database with the yellow color representing measurements with p value <0.05 and >0.01 and the red superpixels representing superpixels where the GCIPL thickness has decreased to below the 1 percentile cutoff point in the normative database. Bottom row, raw OCT images provide the opportunity for the reviewer to inspect the quality of the layer segmentation.

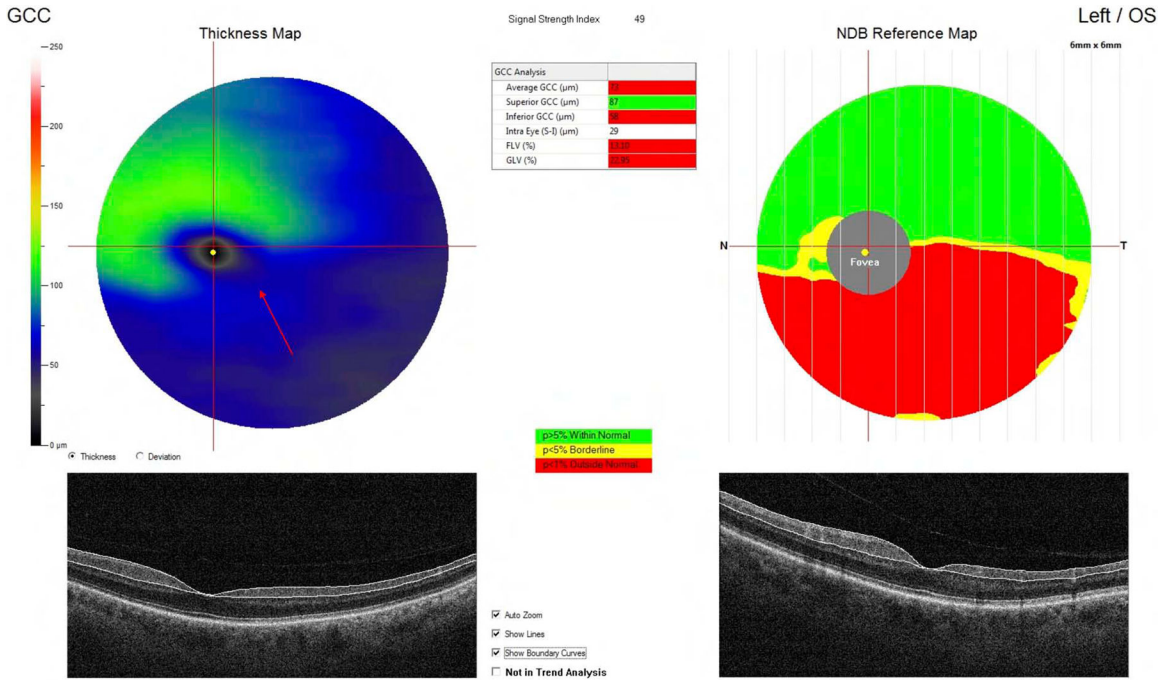

Figure 2.

The ganglion cell complex (GCC) printout of the left eye of a glaucoma patient with significant and extensive inferior macular GCC thinning acquired with the RTVue SD-OCT (OptoVue Inc., Fremont, CA, USA). The GCC thickness map is represented in the upper left; the inferior temporal macular region displayed in blue (red arrow) demonstrates a significant reduction in the GCC thickness. The upper right graph represents the significance map and is pseudocolor coded; GCC thickness in areas shown in green falls within the normal range (5%−95% prediction interval in the normative database). The yellow color indicates borderline abnormal GCC thickness, i.e., the thickness measurement falls between 1 and 5 percentile cutoff points in the normative database, and the red color displays areas where the GCC thickness measurements are outside normal limits (<1 percentile cutoff in the normative database). The central masked area shown in gray on the right upper image is explained by the lack of retinal ganglion cells in the center of the fovea. The table (middle on top) provides summary GCC parameters including average, superior, and inferior thickness, intra-eye superior-inferior asymmetry, focal loss volume (FLV) and global loss volume (GLV). High-resolution B-scans with GCC segmentation results are also provided in the lower section of the printout.

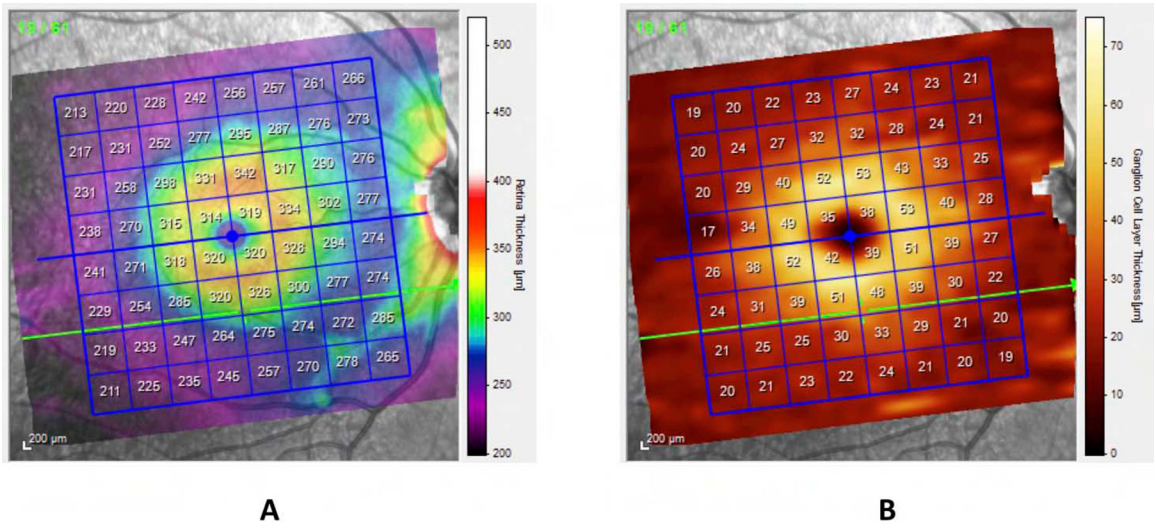

Figure 3.

Printouts of the posterior Pole Algorithm of the Spectralis OCT demonstrating a grid of 64 superpixels, 3°×3° in size, providing the full macular thickness (**A**) or the ganglion cell layer thickness (**B**) in a 24°×24° region of the macula centered on the fovea. Note that the pseudocolor scales used are different.

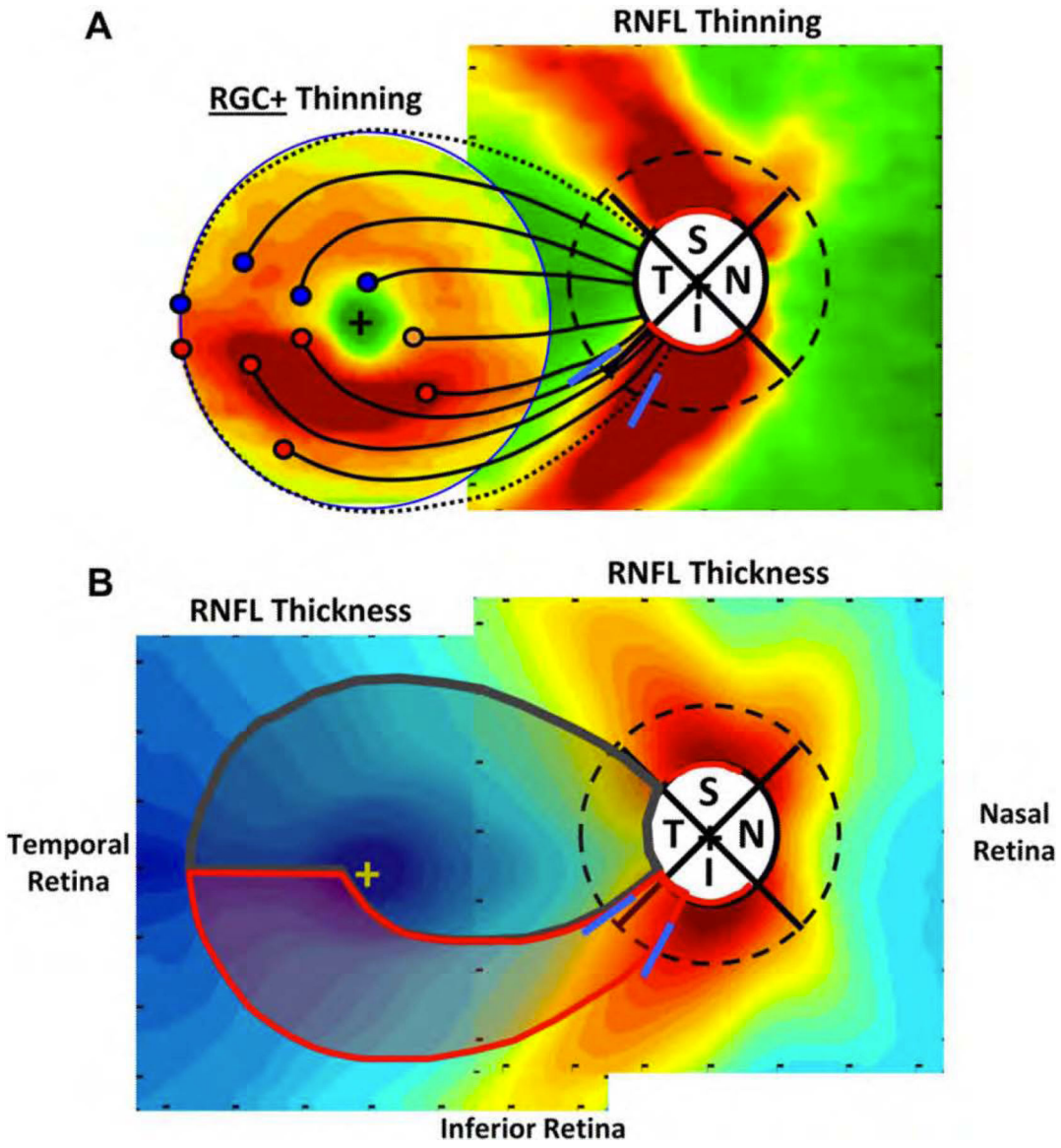

Figure 4.

A schematic model of superimposed retinal nerve fiber layer (RNFL) and macular thickness maps (ganglion cell/inner plexiform layer in A and RNFL in B).[158] **A**) Projection path of retinal ganglion cell (RGC) axons from the macular region to corrresponding areas of the optic disc. Blue lines in the inferotemproal region of the disc define the optic disc sector to which RGC axons from the macular zone of vulnerability (MZV) project. **B**) A representation of the MZV (region delineated in red) and its projection onto the optic disc (defined by blue lines. The temporal and superior region with a black boundary tend to be damaged later in glaucoma. (Figure published with permission from Hood et al.[158])

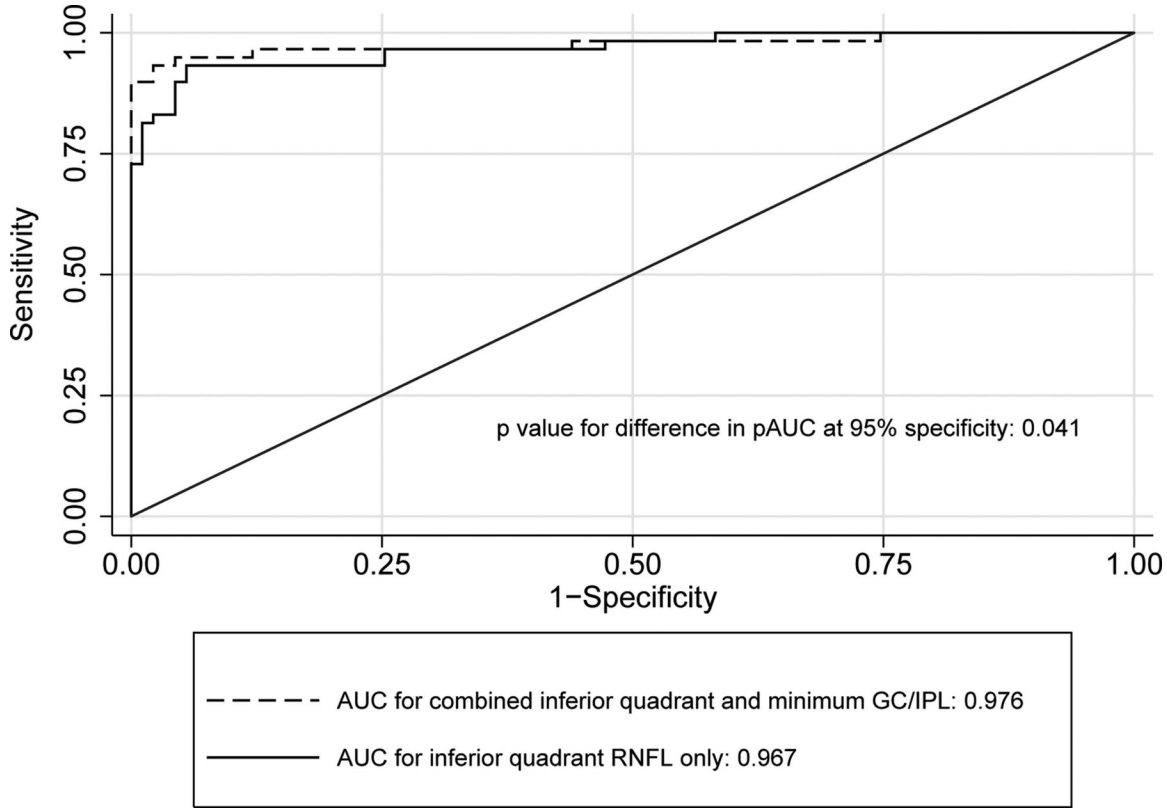

Figure 5.

A comparison of the area under the receiver operating characteristics curves (AUC) for detection of perimetric glaucoma between the inferior quadrant retinal nerve fiber layer thickness alone and the inferior RNFL combined with the minimum ganglion cell/inner plexiform layer (GCIPL) thickness (the best macular parameter in the study). The AUC was higher for the combined variable (p value =0.041 for comparison of the partial AUCs). (Figure with permission from Nouri-Mahdavi et al.[300])

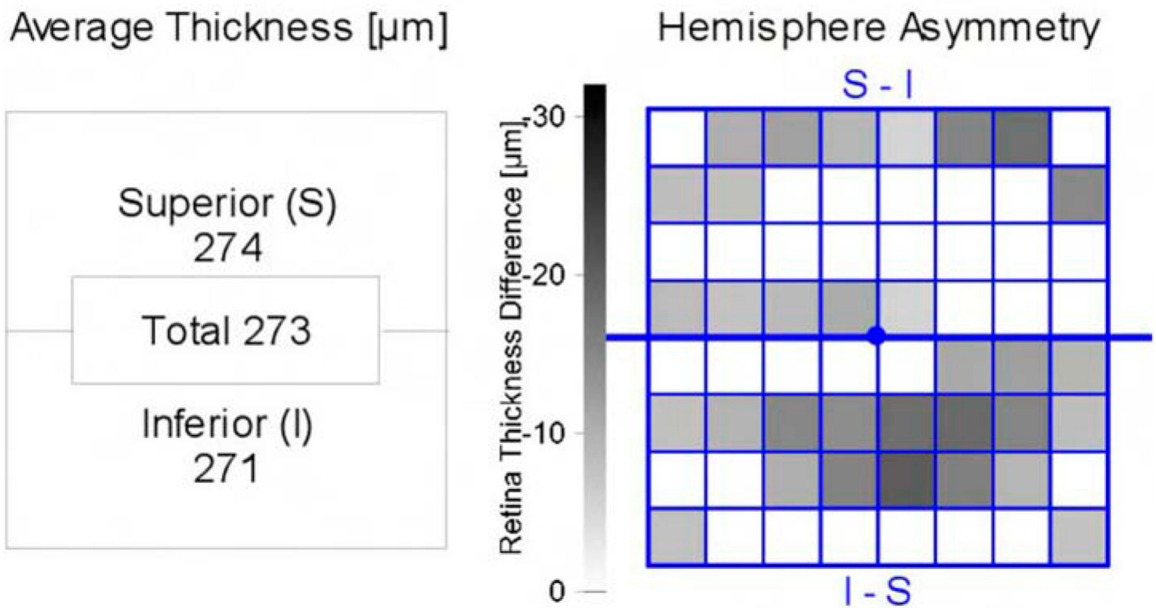

Figure 6.

Vertical full macular thickness asymmetry across the horizontal meridian on the Posterior Pole Algorithm of the Spectralis OCT as an early sign of glaucomatous damage in the right eye of a patient with early glaucoma. The inferior macula demonstrates a large number of superpixels flagged as various shades of gray indicating thinning compared to the superior macula.

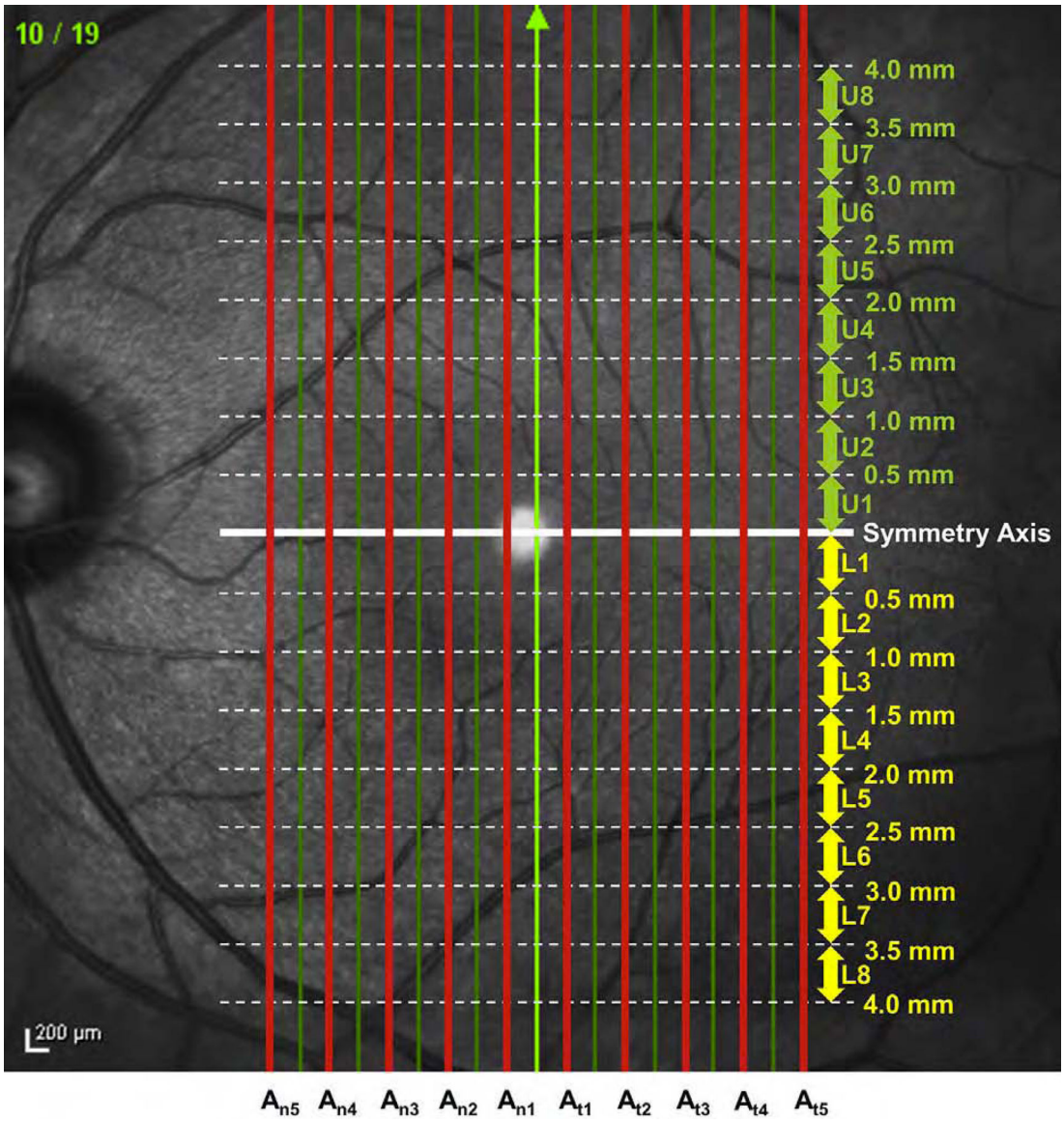

Figure 7.

Schematic representation of the vertical asymmetry algorithm developed by Yamada et al.[414] for Spectralis OCT. The minimum asymmetry unit was calculated as the absolute value of the logarithm of the ratio of the average upper (Ux) and lower thickness (Lx) measurements ($|\log_{10}(Ux/Lx)|$) for each of the 10 vertical scans (in red). The Asymmetry Index for each eye was then estimated by averaging the asymmetry values for the 10 vertical scans. (Printed with permission from Yamada et al.[414])

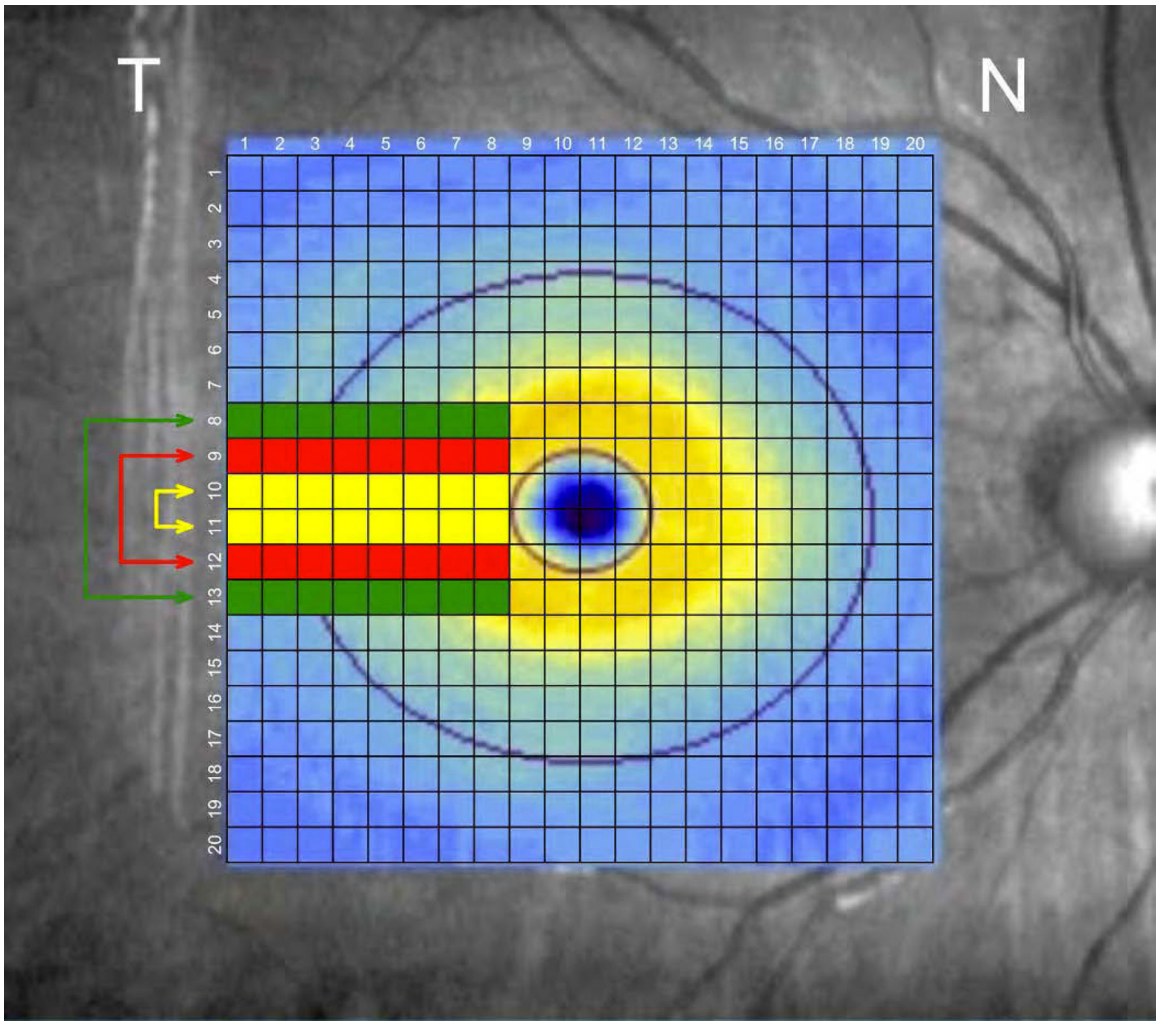

Figure 8.

Definition of the temporal vertical asymmetry on Cirrus HD-OCT according to Sharifipour et al..[350] The 200×200 macular cube of Cirrus SD-OCT was arranged as a 20×20 grid of superpixels. The best performing asymmetry index compared average thickness measurements of the 8 superpixels temporal to the fovea on the 3 rows above and below the temporal raphe. (Figure published with permission from Sharifipour F. et al.[350])

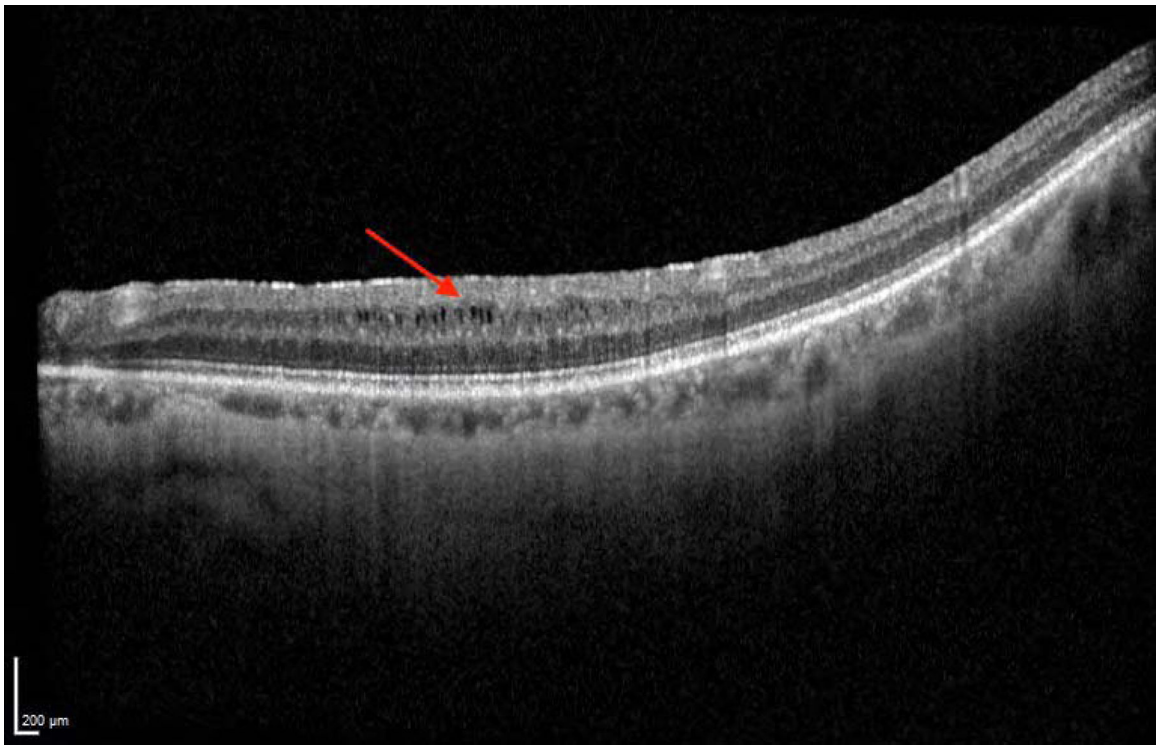

Figure 9.
Microcystic macular edema (MME) manifests as hyporeflective cystic and lacunar areas within the inner nuclear layer on OCT cross-sectional images (red arrow).

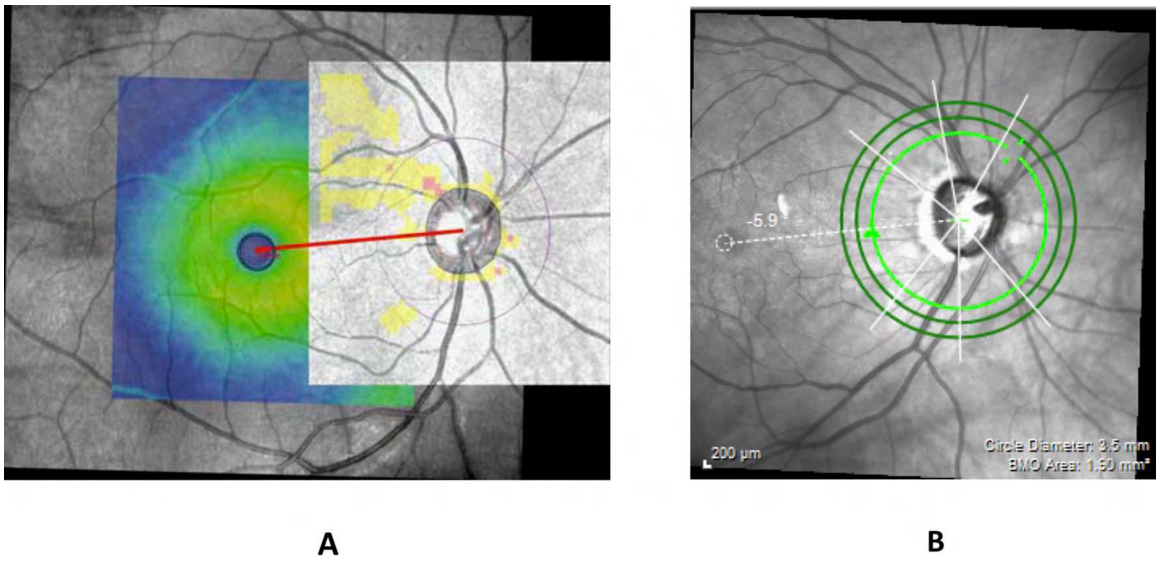

Figure 10.

A) The Fovea-Bruch membrane opening (FoBMO) angle as measured on co-registered images of the optic disc and macular cubes of Cirrus HD-OCT.[110] **B**) The Spectralis OCT automaticallay measures the FoBMO after delineating the BMO and the fovea. C) The ganglion cell/inner plexiform thickness asymmetry across the horizontal meridian is influenced by the FoBMO angle; a more (negatively) tilted FoBMO angle is associated with relatively thinner inferior GCIPL thickness along the horizontal raphe compared with the superior region. (Figure published with permission from Ghassabi et al.[110])

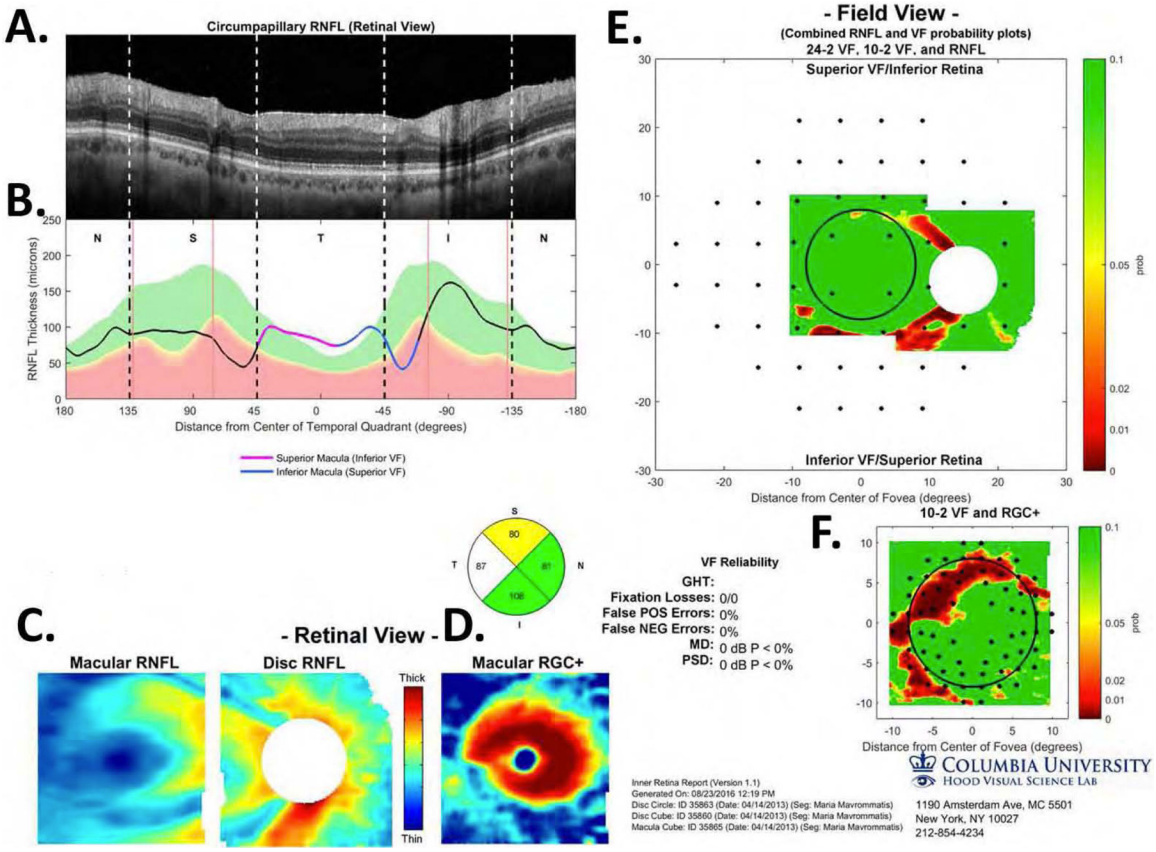

Figure 11.

A one-page OCT report providing an overlay of the retinal nerve fiber layer (RNFL) and ganglion cell/inner plexiform layer (GCIPL) OCT measurements and 24–2 and 10–2 visual field test locations.[149] **A**) The raw image of the circumpapillary scan displayed in the NSTIN format, i.e., starting from the nasal quadrant going counterclockwise in the right eye. **B**) The circumpapillary-RNFL thickness plot obtained from the disc cube scan from panel C, right; it corresponds to the raw image of the OCT scan in panel A and is displayed shown in NSTIN orientation. **C**) The RNFL thickness maps from the OCT cube scan of the macula (left) and the optic disc (right). **D**) The GCIPL thickness color map from the OCT cube scan of the macula. For both panels C and D, warmer colors represent thicker RNFL or GCIPL measurements. **E**) The RNFL probability map is shown in visual field view with the 24–2 locations overlaid. Warmer colors represent deeper defects. **F**) The GCIPL probability map based upon the thickness maps in panel D with superimposed 10–2 visual field locations. The black circles in panels E and F demonstrate the boundaries (±8°) of the macula; the color bars on the right provide the probability cutoffs for RNFL (E) and GCIPL (F) thickness measurements. (Figure published with permission from Hood et al.[149])

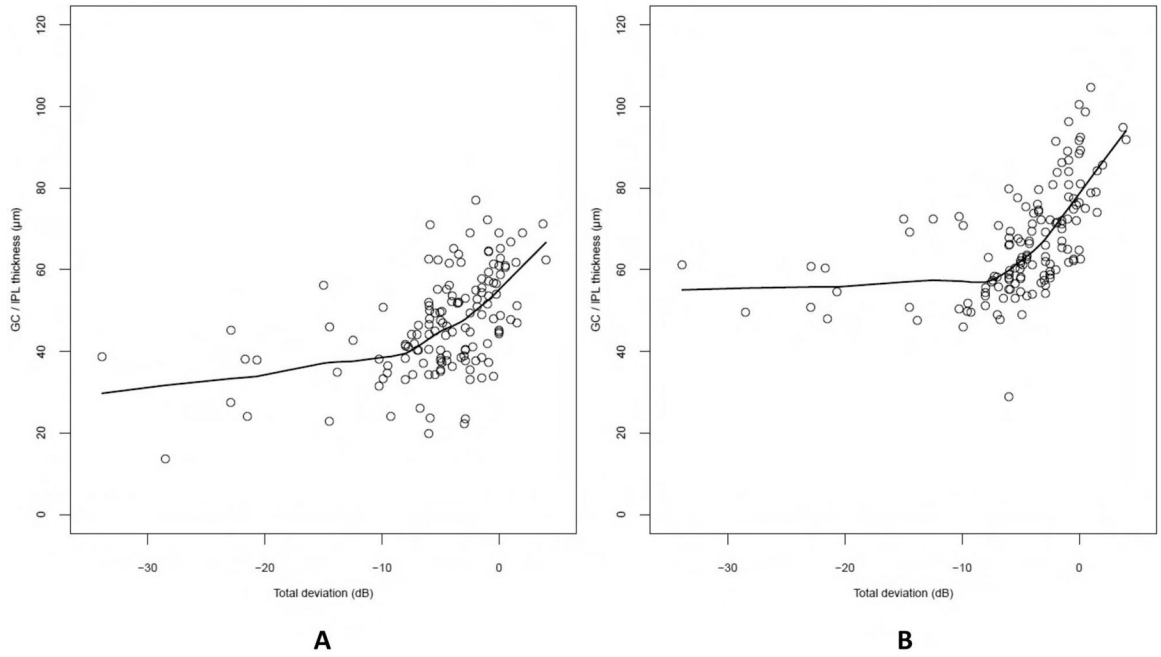

Figure 12.

The scatter plots demonstrate that the structure-function relationship between ganglion cell inner plexiform layer thickness and total deviation at central 10–2 visual field locations improves after adjustment for retinal ganglion cell displacement (**A**, before adjustment, **B**, after adjustment).

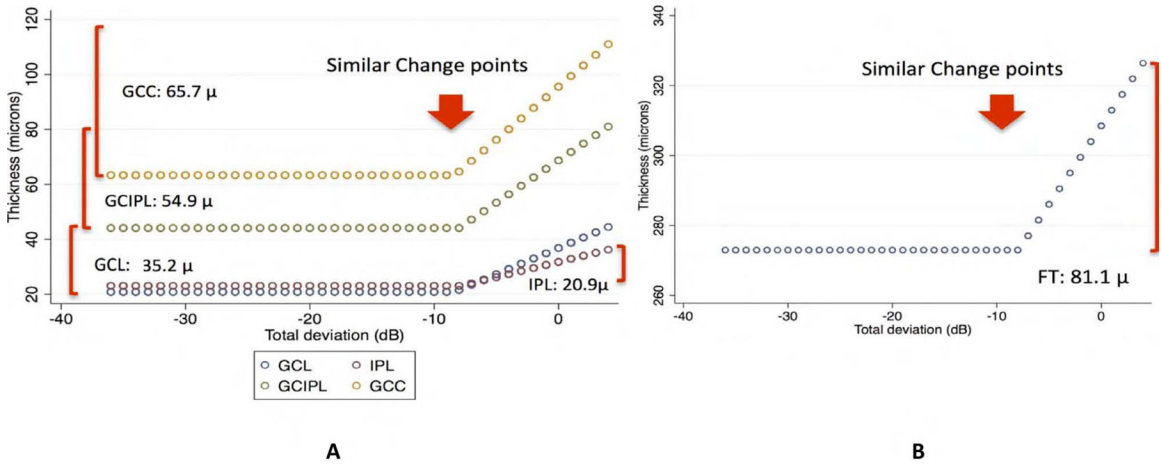

Figure 13.

A broken-stick model of cross-sectional structure-function relationships for 5 different macular variables (full macular thickness, ganglion cell complex, ganglion cell/inner plexiform layer, ganglion cell layer and inner plexiform layer). The Y-axis represents thickness measurements at 3°×3° superpixels measurements and the X-axis shows total deviation values at corresponding 10–2 visual field locations. The red brackets demonstrate the dynamic range for each macular parameter. (Figure published with permission from Miraftabi A et al.[267])

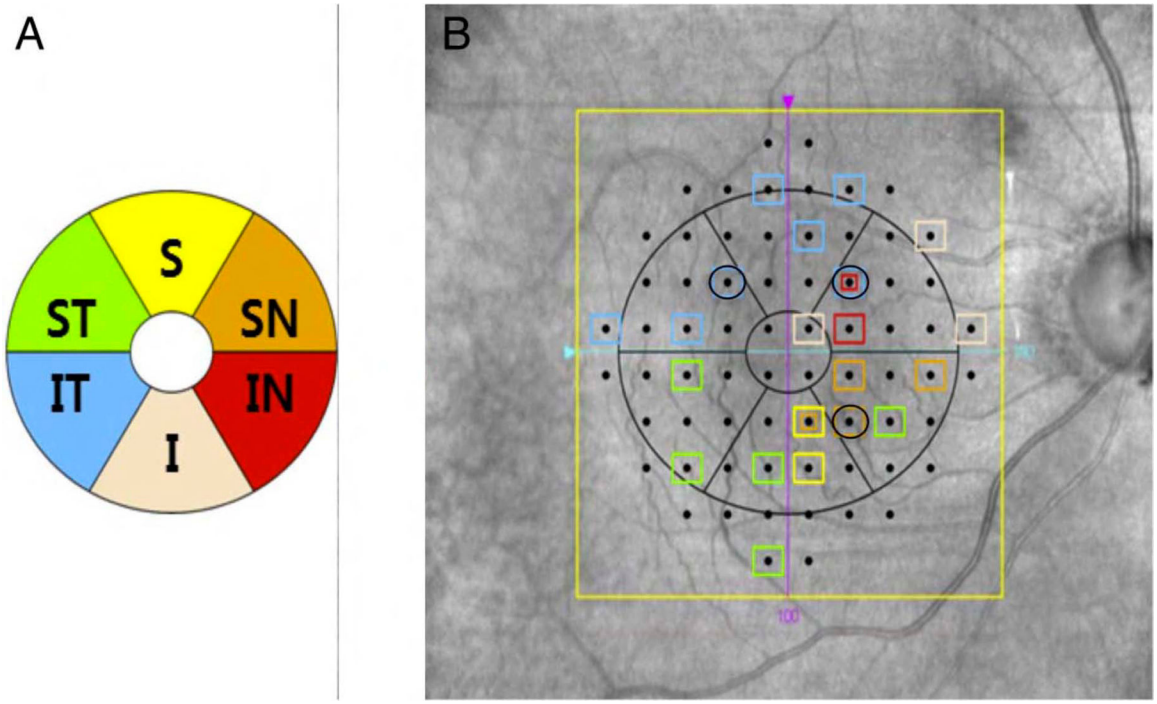

Figure 14.

A) The 6 sectors defined on the Cirrus HD-OCT printout: S = superior, ST = superior temporal, IT = inferior temporal, I = inferior, IN = inferior temporal, SN = superior nasal, SN = superior nasal. **B)** 10–2 visual field locations demonstrating the highest correlations with the ganglion cell/inner plexiform layer (GCIPL) thickness in various sectors; 21 out of 68 visual field locations were significantly correlated with sectoral GCIPL thickness measurements and are displayed by colored squares. Two locations superiorly and 1 inferior location marked by black circles are locations already tested with 24–2 pattern. (Figure published with permission from Lee JW et al.[221])

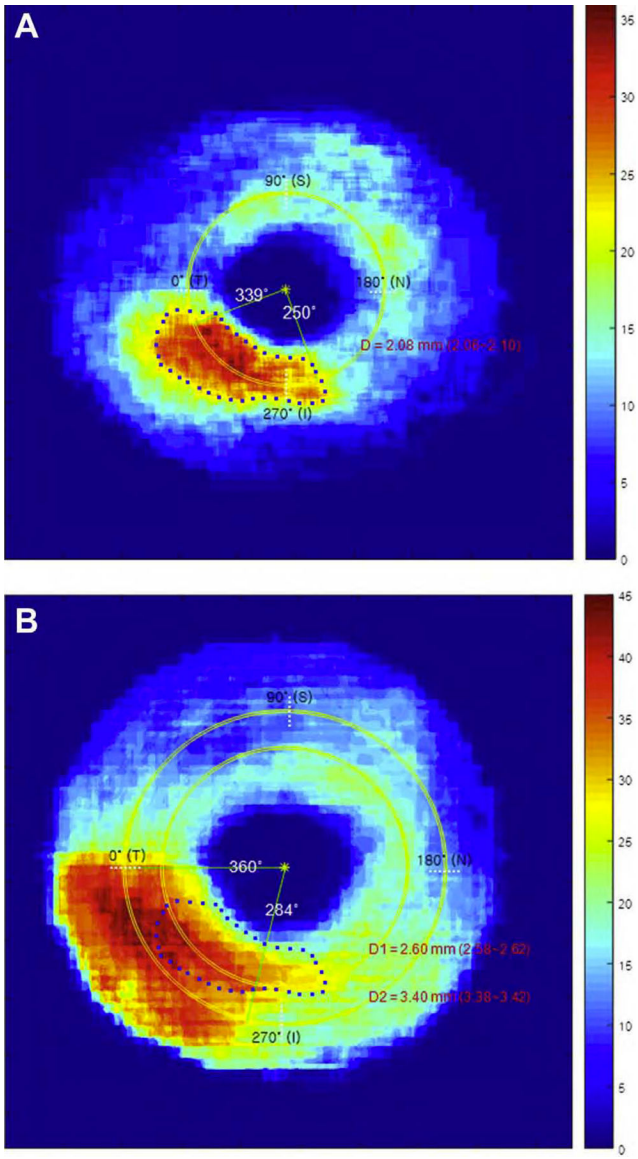

Figure 15.

A) Spatial distribution of progressive thinning of the ganglion cell/inner plexiform layer (GCIPL) in a study by Shin et al.; 292 glaucoma eyes were followed over an average of 6 years.[354] Warmer colors display more frequent occurrence of progressive thinning. **B**) Spatial distribution of ganglion cell/inner plexiform layer (GCIPL) thinning in the central macula at baseline created by overlaying the magnitude of thickness deviation from the normative database on the GCIPL thickness map. The inferotemporal region was the most frequently affected area in the central macula. The dotted region represents the area demonstrating the most prominent progressive changes. (Figure published with permission from Shin et al.[354])